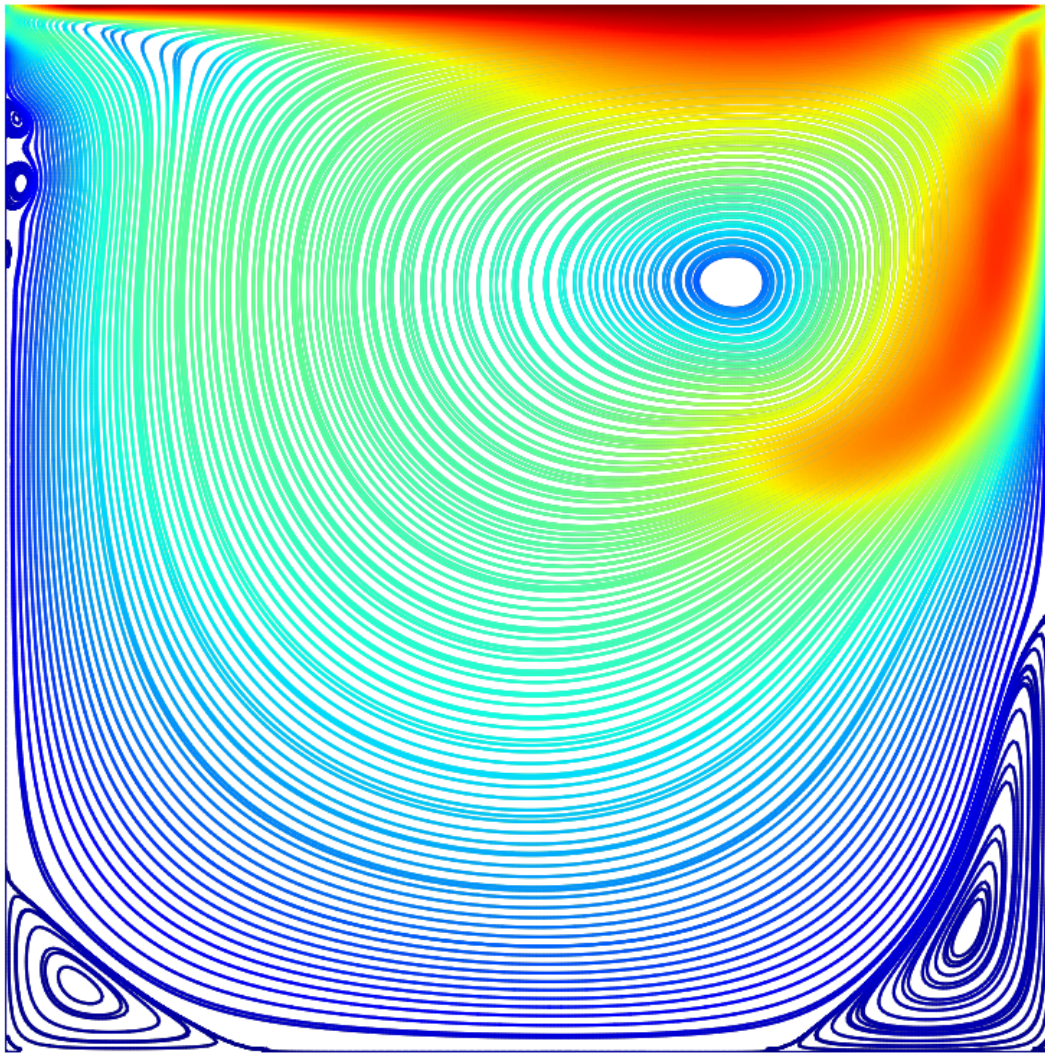


A mimetic dual-field discretization with exact conservation properties for the incompressible Navier-Stokes equations with periodic or Dirichlet boundary conditions



A mimetic dual-field discretization with exact conservation properties for the incompressible Navier-Stokes with periodic or Dirichlet boundary conditions

by

Wolf Nederpel

A thesis on behalf of the Delft Institute for Applied Mathematics
to obtain the degree of Master of Science in Applied Mathematics at
Delft University of Technology

To be publicly defended on the 11th of October at 14:00 in lecture hall Ampère

Faculty:	EEMCS	TU Delft
Specialization:	Computational Science and Engineering	
Project Duration:	December 5, 2022 - October 11, 2023	
Supervisors:	Dr. Deepesh Toshniwal	TU Delft
	Dr. Artur Palha	TU Delft
Thesis committee:	Prof.dr.ir. Kees Vuik	TU Delft
	Dr.ir. Wim van Horssen	TU Delft
	Dr. Deepesh Toshniwal	TU Delft
	Dr. Artur Palha	TU Delft
Student number:	4697146	

An electronic version of this thesis is available at <https://repository.tudelft.nl/>.

Abstract

The Navier-Stokes equations govern the flow of viscous fluids such as air or water. Since no general solution is known, computer simulations are used to obtain approximate solutions. As computers are unable to handle continuous representations of fields, finite-dimensional projection of fields is required, resulting in a loss of information. A difficulty in constructing these discrete solutions, is to obtain discrete solutions that have the same conservation properties as continuous solutions. Other challenges include the efficient handling of the nonlinear term in the equations.

In this thesis we aim to construct a numerical method whose solutions satisfy the conservation of mass, kinetic energy and helicity exactly. To achieve this, a structure preserving (mimetic) spectral element method is employed. Such methods aim to represent properties of the continuous problem exactly in the discrete problem. These methods have their theoretic roots in differential geometry, where there is a clear connection between fields and the geometric objects they are associated with. From this association we note that the fields in the Navier-Stokes equations show a dual nature, where each field can be associated to two types of geometric objects. In [1] this dual nature is used to construct a mass, kinetic energy and helicity conserving method that handles the nonlinear term efficiently by using a leapfrog scheme for problems on periodic domains. In this thesis this work is extended to handle Dirichlet boundary conditions.

When considering periodic boundary conditions, the constructed numerical method exhibits the same conservation properties of energy and helicity as the Navier-Stokes equations. When considering Dirichlet boundary conditions, some additional contributions to the dissipation rates of energy and helicity are noted in the cases of inflow into the domain and nonzero normal vorticity at the boundary respectively. These additional contributions cannot be meaningfully quantified within the employed approach, and are a result of strongly enforced boundary conditions on velocity. Furthermore, the numerical method constructs a pointwise divergence free velocity field at every other time step.

The mimetic spectral element method allows for high order spatial approximation of fields. Optimal spatial convergence orders are observed for all fields. Temporal integration was done via a combination of the trapezoidal and midpoint rule and the expected second order temporal convergence is observed.

Preface

Starting my master thesis, I set out to find a project somewhat out of my comfort zone, while still being related to a familiar field of study. The project at hand involves a finite element application inspired by the principles of differential geometry. Although I had a reasonable grasp of finite elements, my prior encounter with differential geometry could be classified as a low point in my academic journey. In this context, this project was what I was looking for. I am proud to say that I have overcome this challenge and I hope that the document at hand contains useful work.

This achievement was only possible because of the great supervision from Deepesh Toshniwal and Artur Palha. I would like to thank them for their patience in explaining concepts to me repeatedly as I worked to fully comprehend them, as well as for their detailed and comprehensive feedback on my work. Additionally, I would also like to thank my friends Christopher and Corn e. Our regular study sessions and discussions kept me motivated and sane throughout this project.

*Wolf Nederpel
Delft, October 2023*

Contents

1	Introduction	4
2	Continuous conservation properties	7
2.1	Vector calculus identities	8
2.2	Helicity conservation	8
2.3	Kinetic energy conservation	9
2.4	Enstrophy conservation	10
3	The fundamental theorems and the de Rham complex	13
3.1	Three dimensional setting	13
3.2	Two dimensional setting	15
4	Weak forms	18
4.1	Three dimensional weak forms	18
4.2	Three dimensional dual-field weak form	20
4.3	Two dimensional weak forms	20
4.4	Two dimensional dual-field weak form	22
5	Discrete function spaces	23
5.1	B-spline basis functions	23
5.2	One dimensional basis functions	25
5.3	Two dimensional basis functions	27
5.4	Three dimensional basis functions	32
5.5	Incidence matrices	32
6	Discrete problem	35
6.1	Spatial discretization	35
6.2	Temporal integration	35
6.3	Boundary conditions	37
6.4	Fully discrete problem as linear systems	40
6.5	Two dimensional linear systems	41
6.6	Conservation properties of the numerical method	42
7	Numerical results	56
7.1	Details on implementation	56
7.2	Convergence results	56
7.3	Conservation properties	60
7.4	Lid-driven cavity	65
8	Conclusions and future research	70

1 Introduction

The Navier-Stokes equations govern the flow of viscous fluids such as air or water. Since no general solution is known, computer simulations are used to obtain approximate solutions. As computers are unable to handle continuous representations of fields, finite-dimensional projection of fields is required, resulting in a loss of information. A difficulty in constructing these discrete solutions, is to obtain discrete solutions that have the same conservation properties as continuous solutions. Other challenges include the efficient handling of the nonlinear term in the equations.

The Navier-Stokes equations conserve mass, kinetic energy, helicity (in 3D) and enstrophy (in 2D). These conservation properties lead to specific characteristics of turbulent fluid flow. A corner stone of turbulent flows is the energy cascade from large to small scales, initially described by Kolmogorov in [2]. This cascade is a consequence of energy conservation. As a result of enstrophy conservation in two dimensions, an additional energy cascade from small to large scales is seen along side the usual large to small scale cascade [3]. The equations also conserve helicity [4], [5], which leads to a joint cascade of helicity and energy [6], [7]. For discrete solutions to produce the same cascades, it is important that these conservation properties of the Navier-Stokes equations also hold after discretization.

In this thesis we aim to construct a numerical method whose solutions satisfy the conservation of mass, kinetic energy and helicity exactly. To achieve this, a structure preserving (mimetic) spectral element method is employed. Such methods aim to represent properties of the continuous problem exactly in the discrete problem. These methods have their theoretic roots in differential geometry, where there is a clear connection between fields and the geometric objects they are associated with. From this association we note that the fields in the Navier-Stokes equations show a dual nature, where each field can be associated to two types of geometric objects. In [1] this dual nature is used to construct a mass, kinetic energy and helicity conserving method that handles the nonlinear term efficiently by using a leapfrog scheme for problems on periodic domains. In this thesis this work is extended to handle Dirichlet boundary conditions. Notably, enstrophy is not conserved by the methodology presented [1] nor in this work, and as such, the work is mainly relevant for 3D problems. For an approach that conserves enstrophy see [8].

As mentioned before, mimetic methods largely use differential geometry to describe the physics and the geometry of the field problem at hand. The application of differential geometry, and its discrete counterpart algebraic topology, to physical field problems was first described by Tonti in 1975 [9]. Burke further advocated for the use of differential geometry to describe physical theories in his book *Applied Differential Geometry* [10], and is also the author of the strongly titled "Div Grad Curl are Dead" draft. Hyman and Scovel then derived mimetic approximations to differential operators using algebraic topology in 1988 [11]. This was later extended by Bochev and Hyman in 2006 with, among others, discrete wedge products, codifferentials and inner products in [12]. Kreeft et al. further extended the methodology in 2011 with curvilinear elements in [13].

Matiussi highlights the importance of the mimetic ideas for numerical methods in [14], [15], noting that numerical methods benefit from identifying the inherently discrete topological equations and that incorrectly identifying the geometric objects associated to physical fields can cause poor performance. Applications of this geometric approach are plenty. See for example [16] for an application to Euler fluids and [17], [18] for electromagnetism. Vital to this thesis were the applications to Stokes flow in [19], [20], with a priori error analysis done in [21], and to the Navier-Stokes

equations in [1], [8]. The ideas are also applied to the 2.5D Hall MHD equations in [22].

A review of methods with discrete conservation properties can be found in [23], and a broad overview of the relevant theory for mimetic methods is given in [24], specifically Chapters 4 to 7.

In a mimetic spectral element method, basis functions are required to spatially discretize a field problem. Fields will then be approximated by linear combinations of these basis functions. B-spline basis functions may be used for this purpose, which allows for exact representation of a large class of physical domains. These methods are often filed under the name isogeometric analysis, and were first introduced by [25]. In [26]–[30] these ideas were analyzed further.

After discretization of the Navier-Stokes equations in a mimetic spectral element method, we will encounter saddle point problems. Broadly speaking, there are two types of methods for solving saddle point problems. Numerical methods can either avoid the Ladyzhenskaya–Babuska–Brezzi (LBB) condition, or satisfy it. Mimetic methods aim to satisfy it by having the discrete problem adhere to the de Rham complex. As such, the de Rham complex is crucial to obtaining a stable method. This de Rham complex highlights how different Sobolev spaces relate to each other via differential operators.

The structure encoded in the de Rham complex is also the structure that leads to the aforementioned conservation of kinetic energy, helicity (in 3D) and enstrophy (in 2D). By constructing a numerical method that adheres to a discrete de Rham complex, the door is opened for provable discrete conservation laws.

Energy conservation is property of many numerical methods for the Navier-Stokes equations, as it tends to produce to stable methods. Helicity conservation is a topic of more recent research. Work on developing methods with helicity conservation properties started with [31] for problems on periodic domains and with [32] for axisymmetric problems. The work of [31] is extended in [33] and [34], culminating in the work of [35]. Although these methods show promising conservation properties for both energy and helicity, they do not exactly conserve mass. In [29] isogeometric techniques are applied to the unsteady Navier-Stokes equations, which results in pointwise mass conservation. Furthermore, discrete balance laws are derived for, among other quantities, helicity on periodic domains. This helicity balance law does rely on theoretically obtained values for the vorticity however. Most recently, [1] presented a scheme utilizing mimetic discretizations which shows helicity conservation on periodic domains. Additionally, it also shows exact mass conservation and energy conservation, and efficiently handles the nonlinearity using a leapfrog scheme.

In this thesis, the work of [1] is extended to handle Dirichlet boundary conditions. Expressions are derived for the conservation properties of the method and numerical results on convergence and conservation properties are presented. We find that the method produces a pointwise divergence free velocity field, and allows for exact helicity and energy conservation.

For problems on periodic domains, the numerical method conserves kinetic energy and helicity when the Navier-Stokes equations do so too. When the Navier-Stokes equations allow for energy or helicity dissipation, the dissipation rates of the numerical mimic their continuous counterpart. For problems with Dirichlet boundary conditions, the same results are found with some notable additional assumptions on the problem at hand. When the problem allows for inflow into the domain, there is an additional term contributing to the energy dissipation. Similarly, when the problem allows for nonzero normal vorticity at the boundary, there is an additional term contributing to the

helicity dissipation.

In Section 2 the Navier-Stokes equations are presented and some of their conservation properties are highlighted. In Section 3 the de Rham complex is introduced and the connection between physical fields and geometric objects is addressed. Section 4 employs this de Rham complex to setup a dual field weak form of the Navier-Stokes equations, this weak form is consistent with the de Rham complex. Discrete function spaces and their basis functions to spatially discretize the weak form are introduced in 5. In the construction of the discrete spaces and their basis functions, it is ensured that they constitute a discrete de Rham complex, that mimics the continuous de Rham complex of Section 3. With all structures in place, Section 6 presents the fully discrete problem, and notably the handling of Dirichlet boundary conditions is discussed. Numerical results regarding temporal and spatial convergence orders and conservation properties obtained with this discrete problem are presented in Section 7. Finally, in Section 8 conclusions are drawn regarding the performance of the numerical method.

2 Continuous conservation properties

Viscous incompressible fluid flow is governed by the Navier-Stokes equations, a set of conservation laws for mass and momentum involving velocity \vec{u} and pressure p and a source function \vec{f} . We consider the equations for a fluid with constant density. As a basis for the numerical scheme, we use the equations in rotational and dimensionless form. Here we employ and introduce a vorticity field $\vec{\omega}$. Given a domain Ω , initial condition $\vec{u}|_{t=0} = \vec{u}_0$ and suitable boundary conditions on $\partial\Omega$, the equations are given by

$$\begin{cases} \vec{\omega} - \text{curl } \vec{u} = 0, & (2.1a) \\ \frac{\partial \vec{u}}{\partial t} + \vec{\omega} \times \vec{u} + \nu \text{curl } \vec{\omega} + \text{grad } p = \vec{f}, & (2.1b) \\ \text{div } \vec{u} = 0. & (2.1c) \end{cases}$$

At this stage, we will not specify a concrete domain, initial conditions or source function, to make the presentation general. Where necessary, we will specify the conditions under which a result is valid.

Some notable quantities of interest are mass, helicity \mathcal{H} , kinetic energy \mathcal{K} and enstrophy \mathcal{E} , given by

$$\mathcal{H} := (\vec{u}, \vec{\omega}), \quad (2.2)$$

$$\mathcal{K} := \frac{1}{2}(\vec{u}, \vec{u}), \quad (2.3)$$

$$\mathcal{E} := \frac{1}{2}(\vec{\omega}, \vec{\omega}), \quad (2.4)$$

where (\cdot, \cdot) indicates the L^2 inner product over Ω :

$$(\vec{a}, \vec{b}) := \int_{\Omega} \vec{a} \cdot \vec{b} \, d\Omega. \quad (2.5)$$

In the inviscid limit ($\nu \rightarrow 0$), with a conservative source function ($\vec{f} = \text{grad } \phi$) and in the absence of boundary contributions, such as on a periodic domain or on an infinite domain with vanishing velocities, the Navier-Stokes equations conserve mass, kinetic energy, helicity and enstrophy (in 2D). As mentioned in the introduction, the conservation of these quantities lead to energy and helicity cascades crucial to turbulence modeling [2]–[7].

The mass conservation for a fluid with constant density is immediate from the divergence free constraint. We will derive the expressions for the time rate of change of helicity, kinetic energy and enstrophy, and we will show that these quantities are conserved in the inviscid limit ($\nu \rightarrow 0$), for conservative source function ($\vec{f} = \text{grad } \phi$) and in the absence of boundary contributions. The absence of boundary contributions can be a result of for example considering a periodic domain or of assuming all relevant fields and their derivatives go to zero at the boundary. To this end let us first present the key mathematical structures that lead to these conservation properties. In the discretization of the equations, we aim to satisfy these key structures. This allows the numerical method we will construct to exhibit some of the same conservation properties as the Navier-Stokes equations.

2.1 Vector calculus identities

Two vector calculus properties will be key in the derivation below. First the triple product, for any vector fields \vec{a} , \vec{b} , \vec{c} , it holds that

$$(\vec{a} \times \vec{b}, \vec{c}) = (\vec{c} \times \vec{a}, \vec{b}) = (\vec{b} \times \vec{c}, \vec{a}). \quad (2.6)$$

When $a = c$, we know $a \times c = a \times a = 0$, and so we arrive at the orthogonality identity:

$$(\vec{a} \times \vec{b}, \vec{a}) = 0. \quad (2.7)$$

Second, we make use of the derivative identities, for any scalar field a and vector field \vec{b} , we have

$$\text{curl grad } a = 0 \quad \text{and} \quad \text{div curl } \vec{b} = 0. \quad (2.8)$$

These identities will be captured by the exact de Rham complex that is introduced in Section 3. The discrete setting that will be introduced afterwards must allow for the same identities such conservation properties can be proven for the discrete problem as well.

2.2 Helicity conservation

First, we write out the time derivative of the inner product:

$$\frac{d\mathcal{H}}{dt} = \frac{d}{dt}(\vec{u}, \vec{\omega}) \quad (2.9a)$$

$$= \left(\frac{\partial \vec{u}}{\partial t}, \vec{\omega}\right) + \left(\vec{u}, \frac{\partial \vec{\omega}}{\partial t}\right). \quad (2.9b)$$

Using the definition of vorticity $\vec{\omega} = \text{curl } \vec{u}$, (2.1a), this is equal to

$$\frac{d\mathcal{H}}{dt} = \left(\frac{\partial \vec{u}}{\partial t}, \vec{\omega}\right) + \left(\vec{u}, \text{curl } \frac{\partial \vec{u}}{\partial t}\right). \quad (2.9c)$$

Now we can use the evolution equation (2.1b) to expand $\frac{\partial \vec{u}}{\partial t}$ to find

$$\frac{d\mathcal{H}}{dt} = \left(\frac{\partial \vec{u}}{\partial t}, \vec{\omega}\right) + \left(\vec{u}, \text{curl } \frac{\partial \vec{u}}{\partial t}\right) \quad (2.9d)$$

$$= -(\vec{\omega} \times \vec{u}, \vec{\omega}) - \nu(\text{curl } \vec{\omega}, \vec{\omega}) - (\text{grad } p, \vec{\omega}) + (\vec{f}, \vec{\omega}) \\ - (\vec{u}, \text{curl } (\vec{\omega} \times \vec{u})) - \nu(\vec{u}, \text{curl curl } \vec{\omega}) - (\vec{u}, \text{curl grad } p) + (\vec{u}, \text{curl } \vec{f}). \quad (2.9e)$$

Using (2.7) allows us to cancel $(\vec{\omega} \times \vec{u}, \vec{\omega})$, and (2.8) allows us to cancel $(\vec{u}, \text{curl grad } p)$, giving

$$\frac{d\mathcal{H}}{dt} = -\nu \left((\text{curl } \vec{\omega}, \vec{\omega}) + (\vec{u}, \text{curl curl } \vec{\omega}) \right) \quad (2.9f)$$

$$- (\text{grad } p, \vec{\omega}) + (\vec{f}, \vec{\omega}) - (\vec{u}, \text{curl } (\vec{\omega} \times \vec{u})) + (\vec{u}, \text{curl } \vec{f}).$$

Integration by parts on $(\text{grad } p, \vec{\omega})$ and $(\vec{u}, \text{curl } (\vec{\omega} \times \vec{u}))$ results in

$$\frac{d\mathcal{H}}{dt} = -\nu \left((\text{curl } \vec{\omega}, \vec{\omega}) + (\vec{u}, \text{curl curl } \vec{\omega}) \right) \\ + (p, \text{div } \vec{\omega}) + (\vec{f}, \vec{\omega}) - (\text{curl } \vec{u}, \vec{\omega} \times \vec{u}) + (\vec{u}, \text{curl } \vec{f}) \quad (2.9g)$$

$$+ \int_{\partial\Omega} \vec{u} \times (\vec{\omega} \times \vec{u}) \cdot d\partial\Omega - \int_{\partial\Omega} p(\vec{\omega} \cdot n) d\partial\Omega.$$

Now we can use the definition of vorticity $\vec{\omega} = \text{curl } \vec{u}$, combined with (2.7) and (2.8) to cancel $(\text{curl } \vec{u}, \vec{\omega} \times \vec{u})$ and $(p, \text{div } \vec{\omega}) = (p, \text{div } \text{curl } \vec{\omega})$, giving

$$\begin{aligned} \frac{d\mathcal{H}}{dt} &= -\nu \left((\text{curl } \vec{\omega}, \vec{\omega}) + (\vec{u}, \text{curl } \text{curl } \vec{\omega}) \right) + (\vec{f}, \vec{\omega}) + (\vec{u}, \text{curl } \vec{f}) \\ &\quad + \int_{\partial\Omega} \vec{u} \times (\vec{\omega} \times \vec{u}) \cdot d\partial\Omega - \int_{\partial\Omega} p(\vec{\omega} \cdot \vec{n}) d\partial\Omega. \end{aligned} \quad (2.9h)$$

Finally, we will use integration by parts on $(\vec{f}, \vec{\omega}) = (\vec{f}, \text{curl } \vec{u})$ to obtain

$$\begin{aligned} \frac{d\mathcal{H}}{dt} &= -\nu \left((\text{curl } \vec{\omega}, \vec{\omega}) + (\vec{u}, \text{curl } \text{curl } \vec{\omega}) \right) + 2(\vec{u}, \text{curl } \vec{f}) - \int_{\partial\Omega} \vec{f} \times \vec{u} \cdot d\partial\Omega \\ &\quad + \int_{\partial\Omega} \vec{u} \times (\vec{\omega} \times \vec{u}) \cdot d\partial\Omega - \int_{\partial\Omega} p(\vec{\omega} \cdot \vec{n}) d\partial\Omega. \end{aligned} \quad (2.9i)$$

Consider this expression in the absence of boundary contributions and in the inviscid limit ($\nu \rightarrow 0$). Under these conditions it holds that

$$\frac{d\mathcal{H}}{dt} = 2(\vec{u}, \text{curl } \vec{f}). \quad (2.10)$$

When we additionally consider a conservative source function $\vec{f} = \text{grad } \phi$ we can conclude

$$\frac{d\mathcal{H}}{dt} = 2(\vec{u}, \text{curl } \text{grad } \phi) \stackrel{(2.8)}{=} 0. \quad (2.11)$$

Remark (Helicity conservation in 2D).

The two dimensional setting can be viewed as a reduction of the three dimensional setting with

$$\vec{u} = \begin{bmatrix} \vec{u}_1 \\ \vec{u}_2 \\ 0 \end{bmatrix} \quad \text{and} \quad \vec{\omega} = \begin{bmatrix} 0 \\ 0 \\ \vec{\omega}_3 \end{bmatrix}. \quad (2.12)$$

$$(2.13)$$

This way helicity is trivially zero as

$$\vec{u} \cdot \vec{\omega} = \begin{bmatrix} \vec{u}_1 \\ \vec{u}_2 \\ 0 \end{bmatrix} \cdot \begin{bmatrix} 0 \\ 0 \\ \vec{\omega}_3 \end{bmatrix} = 0. \quad (2.14)$$

2.3 Kinetic energy conservation

Expanding the time derivative in the inner product similarly to the helicity case we find

$$\frac{d\mathcal{K}}{dt} = \left(\frac{\partial \vec{u}}{\partial t}, \vec{u} \right) \quad (2.15a)$$

$$= -(\vec{\omega} \times \vec{u}, \vec{u}) - \nu (\text{curl } \vec{\omega}, \vec{u}) - (\text{grad } p, \vec{u}) + (\vec{f}, \vec{u}). \quad (2.15b)$$

Using (2.7) to cancel $(\vec{\omega} \times \vec{u}, \vec{u})$ and integration by parts on $(\text{grad } p, \vec{u})$ now gives

$$\frac{d\mathcal{K}}{dt} = -\nu (\text{curl } \vec{\omega}, \vec{u}) + (p, \text{div } \vec{u}) + (\vec{f}, \vec{u}) - \int_{\partial\Omega} p(\vec{u} \cdot \vec{n}) d\partial\Omega. \quad (2.15c)$$

As \vec{u} is divergence free by (2.1c) this becomes:

$$\frac{d\mathcal{K}}{dt} = -\nu (\text{curl } \vec{\omega}, \vec{u}) + (\vec{f}, \vec{u}) - \int_{\partial\Omega} p(\vec{u} \cdot \vec{n}) d\partial\Omega. \quad (2.15d)$$

In the inviscid limit and in the absence of boundary contributions terms this becomes

$$\frac{d\mathcal{K}}{dt} = (\vec{f}, \vec{u}). \quad (2.16)$$

With a conservative source function $\vec{f} = \text{grad } \phi$, we can identically use $\vec{f} \equiv 0$ and set $\tilde{p} = p - \phi$ and set $\vec{f} = 0$. With these requirements in place we can conclude

$$\frac{d\mathcal{K}}{dt} = 0. \quad (2.17)$$

It is also worth noting that, in the absence of boundary contributions with a conservative source functions \vec{f} , but for viscous flow, we find

$$\frac{d\mathcal{K}}{dt} = -\nu (\text{curl } \vec{\omega}, \vec{u}) \quad (2.18a)$$

$$= -\nu (\vec{\omega}, \vec{\omega}) \quad (2.18b)$$

$$= 2\nu\mathcal{E}. \quad (2.18c)$$

2.4 Enstrophy conservation

Enstrophy is only conserved by the two dimensional Navier-Stokes equations. In two dimensions, there are two types of curl operator. One applies to scalar fields, written as rot, and another applies to vector fields, written as curl. These operators are defined as

$$\text{rot } \vec{f}(x, y) := \frac{\partial f_2}{\partial x} - \frac{\partial f_1}{\partial y}, \quad (2.19)$$

and

$$\text{curl } f(x, y) := \left[\frac{\partial f}{\partial y}, -\frac{\partial f}{\partial x} \right]^\top. \quad (2.20)$$

Using these operators the two dimensional Navier-Stokes equations are given as

$$\left\{ \begin{array}{l} \omega - \text{rot } \vec{u} = 0, \end{array} \right. \quad (2.21a)$$

$$\left\{ \begin{array}{l} \frac{\partial \vec{u}}{\partial t} + \omega \times \vec{u} + \nu \text{curl } \omega + \text{grad } p = \vec{f}, \end{array} \right. \quad (2.21b)$$

$$\left\{ \begin{array}{l} \text{div } \vec{u} = 0. \end{array} \right. \quad (2.21c)$$

The derivative identities (2.8) also apply in two dimensions using the rot and curl operator. For any scalar field a and vector field b , we have

$$\text{curl grad } a = 0 \quad \text{and} \quad \text{div rot } \vec{b}. \quad (2.22)$$

Using the two dimensional Navier-Stokes equations and the derivative identities we will show enstrophy conservation in the absence of boundary contributions, in the inviscid limit and with conservative source function.

Again, writing out the time derivative of the inner product and using the definition of vorticity (2.21a) we find:

$$\frac{d\mathcal{E}}{dt} = \left(\frac{\partial w}{\partial t}, w \right) \quad (2.23a)$$

$$= \left(\text{rot} \frac{\partial \vec{u}}{\partial t}, w \right) \quad (2.23b)$$

$$= -\left(\text{rot} (w \times \vec{u}), w \right) - \nu \left(\text{rot curl } w, w \right) - \left(\text{rot grad } p, w \right) + \left(\text{rot } \vec{f}, w \right). \quad (2.23c)$$

Using (2.22) we can cancel $\left(\text{rot grad } p, w \right)$ to obtain

$$\frac{d\mathcal{E}}{dt} = -\left(\text{rot} (w \times \vec{u}), w \right) - \nu \left(\text{rot curl } w, w \right) + \left(\text{rot } \vec{f}, w \right). \quad (2.23d)$$

To derive an expression for $\left(\text{rot} (w \times \vec{u}), w \right)$, consider the following:

$$\text{rot} (w \times \vec{u}) = \text{rot} \begin{bmatrix} -w\vec{u}_2 \\ w\vec{u}_1 \end{bmatrix} \quad (2.24a)$$

$$= \frac{\partial w\vec{u}_1}{dx} + \frac{\partial w\vec{u}_2}{dy} \quad (2.24b)$$

$$= \text{div} (w\vec{u}) \quad (2.24c)$$

$$= \vec{u} \cdot \text{grad } w + w \text{div } \vec{u} \quad (2.24d)$$

$$\stackrel{(2.21c)}{=} \vec{u} \cdot \text{grad } w. \quad (2.24e)$$

Now we combine (2.24c) and (2.24e) to find

$$2 \text{rot} (w \times \vec{u}) = \vec{u} \cdot \text{grad } w + \text{div} (w\vec{u}). \quad (2.24f)$$

This expression can now be used in $\left(\text{rot} (w \times \vec{u}), w \right)$ to derive

$$\left(\text{rot} (w \times \vec{u}), w \right) = \frac{1}{2}(\vec{u} \cdot \text{grad } w, w) + \frac{1}{2}(\text{div}(w\vec{u}), w). \quad (2.25a)$$

Using the definition of the inner product (2.5), the fields in the first inner product can be reordered to find

$$\left(\text{rot} (w \times \vec{u}), w \right) = \frac{1}{2}(\text{grad } w, w\vec{u}) + \frac{1}{2}(\text{div} (w\vec{u}), w). \quad (2.25b)$$

Now integration by parts on the first term yields:

$$= -\frac{1}{2}(w, \text{div}(w\vec{u})) + \frac{1}{2}(\text{div} (w\vec{u}), w) + \int_{\partial\Omega} w^2 \vec{u} \cdot d\partial\Omega \quad (2.25c)$$

$$= \int_{\partial\Omega} w^2 \vec{u} \cdot d\partial\Omega. \quad (2.25d)$$

Using this result in (2.23d) gives:

$$\frac{d\mathcal{E}}{dt} = - \int_{\partial\Omega} w^2 \vec{u} \cdot d\partial\Omega - \nu (\text{rot curl } w, w) + (\text{rot } \vec{f}, w). \quad (2.26)$$

Again, we see that in the inviscid limit, in the absence of boundary contributions and with conservative source function this results in conservation of enstrophy i.e.

$$\frac{d\mathcal{E}}{dt} = 0. \quad (2.27)$$

It is worth noting that the derivation in (2.24) only holds in two dimensions, in three dimensions the Navier-Stokes equations do not conserve enstrophy. This result has large consequences for turbulent flows. In three dimensions there is one energy cascade from large to small scales, but in two dimensions there is also an inverse energy cascade from small to large scales possible as a result of enstrophy conservation [3].

3 The fundamental theorems and the de Rham complex

We aim to construct a numerical method for solving the incompressible Navier-Stokes equations that mimics the continuous problem in the sense that we have exact adherence to some of the continuous conservation properties. As noted in the previous section, the derivative identities (2.8) and (2.22) played a key role in deriving the continuous conservation properties. These identities are present when the function spaces used to represent the fields constitute an exact de Rham complex. Therefore, in this section we will introduce the function spaces used to represent the fields in the Navier-Stokes equation, and the introduce the de Rham complex in both two and three dimensions.

3.1 Three dimensional setting

In standard three dimensional vector calculus, there are three fundamental theorems linking integrals over geometric objects, to the integrals over the boundary of those geometric objects. These are the fundamental theorem of calculus, Stokes' theorem, and Gauss's divergence theorem. Given a path $\gamma : [a, b] \rightarrow \mathbb{R}^n$, surface \mathcal{S} and a volume \mathcal{V} , the theorems state

$$\int_{\gamma} \text{grad } p \cdot d\gamma = p(\gamma(b)) - p(\gamma(a)), \quad (3.1a)$$

$$\int_{\mathcal{S}} \text{curl } \vec{v} \times \vec{n} \cdot d\mathcal{S} = \int_{\partial\mathcal{S}} \vec{v} \cdot d\gamma, \quad (3.1b)$$

$$\int_{\mathcal{V}} \text{div } \vec{s} \cdot d\mathcal{V} = \int_{\partial\mathcal{V}} \vec{s} \cdot \vec{n} \cdot d\mathcal{S}. \quad (3.1c)$$

These theorems show that $\text{div } \vec{s}$ is related to volumes, \vec{s} and $\text{curl } \vec{v}$ are related to surfaces, \vec{v} and $\text{grad } p$ are related to lines, or paths, and p itself is related to points. These differences between fields, that is, the type of geometric objects they are to be integrated over, are not usually clear in vector calculus, only the difference between a vector field and a scalar field is directly apparent. However, In the same way one should not add a scalar to a vector, one should not add fields with a different geometrical association. This is particularly relevant at the discrete level, where members of different function spaces will have different types of basis functions.

The div , grad , and curl operators also relate certain Sobolev spaces that are of interest for constructing weak forms. These function spaces are the spaces where fields are defined, and certain differential operators applied to those fields, have a meaning:

$$L^2(\Omega) := \{f : \left(\int_{\Omega} f \cdot f \, d\Omega\right)^{1/2} < \infty\}, \quad (3.2a)$$

$$H(\text{div}, \Omega) := \{\vec{f} : \vec{f} \in L^2(\Omega) \wedge \text{div } \vec{f} \in L^2(\Omega)\}, \quad (3.2b)$$

$$H(\text{curl}, \Omega) := \{\vec{f} : \vec{f} \in L^2(\Omega) \wedge \text{curl } \vec{f} \in L^2(\Omega)\}, \quad (3.2c)$$

$$H^1(\Omega) := \{f : f \in L^2(\Omega) \wedge \text{grad } f \in L^2(\Omega)\}. \quad (3.2d)$$

Note how only a single differential operator is defined on each space, other differential operators do not have a sensible meaning.

It should be noted that many of the fields we will encounter in this thesis are time dependent, consider for example $\vec{u} : \Omega \times [0, t_{\text{end}}] \rightarrow \mathbb{R}^n$, when we write

$$\vec{u} \in H(\text{div}), \quad (3.3)$$

it is implied that

$$\vec{u}|_{t=z} \in H(\text{div}) \quad \text{for each } z \in [0, t_{\text{end}}]. \quad (3.4)$$

The domain Ω will be left out when referencing these function spaces, in this thesis we will always work with Lipschitz and simply connected domains. The de Rham complex is what highlights the relations between these function spaces. In a 3-dimensional setting it is given by

$$H^1 \xrightarrow{\text{grad}} H(\text{curl}) \xrightarrow{\text{curl}} H(\text{div}) \xrightarrow{\text{div}} L^2. \quad (3.5)$$

This complex describes how the div, grad, and curl operators relate the function spaces to each other. We write $\mathcal{N}(\cdot)$ for the null space of (\cdot) . The complex implies:

$$f \in H^1 \implies \text{grad } f \in \mathcal{N}(\text{curl}) \subset H(\text{curl}), \quad (3.6a)$$

$$\vec{f} \in H(\text{curl}) \implies \text{curl } \vec{f} \in \mathcal{N}(\text{div}) \subset H(\text{div}), \quad (3.6b)$$

$$\vec{f} \in H(\text{div}) \implies \text{div } \vec{f} \in L^2. \quad (3.6c)$$

By these implications, the complex encodes the identities (2.8). Recall how these identities, i.e. the exactness of the complex, were crucial to showing the conservation properties of the Navier-Stokes equations. The discrete function spaces we will construct should also constitute an exact de Rham complex if we aim to adhere to these conservation properties.

When constructing a weak form for the Navier-Stokes equations, it is not possible to choose spaces in such a way that each differential operator can be directly applied. In such cases we apply the operators weakly using integration by parts. The weakly applied, or adjoint, operators are defined by integration by parts as:

For $b \in L^2$

$$\begin{aligned} (\vec{a}, \text{grad}^* b) &:= \int_{\partial\Omega} b(\vec{a} \cdot n) \, d\partial\Omega - (\text{div } \vec{a}, b) & \forall \vec{a} \in H(\text{div}) \\ &=: B^{\text{grad}}(\vec{a}, b) & - (\text{div } \vec{a}, b), \end{aligned} \quad (3.7a)$$

for $\vec{b} \in H(\text{div})$

$$\begin{aligned} (\vec{a}, \text{curl}^* \vec{b}) &:= \int_{\partial\Omega} \vec{b} \times \vec{a} \cdot d\partial\Omega + (\text{curl } \vec{a}, \vec{b}) & \forall \vec{a} \in H(\text{curl}) \\ &=: B^{\text{curl}}(\vec{a}, \vec{b}) & + (\text{curl } \vec{a}, \vec{b}), \end{aligned} \quad (3.7b)$$

for $\vec{b} \in H(\text{curl})$

$$\begin{aligned} (a, \text{div}^* \vec{b}) &:= \int_{\partial\Omega} a(\vec{b} \cdot n) \, d\partial\Omega - (\text{grad } a, \vec{b}) & \forall a \in H^1 \\ &=: B^{\text{div}}(a, \vec{b}) & - (\text{grad } a, \vec{b}). \end{aligned} \quad (3.7c)$$

We will use the terms $B(\cdot, \cdot)$ over the boundary integrals for brevity. Observe how when div is an operator from $H(\text{div})$ to L^2 , grad^* is an operator from L^2 to $H(\text{div})$. Similarly, curl^* is an operator from $H(\text{div})$ to $H(\text{curl})$ and div^* is an operator from $H(\text{curl})$ to H^1 . As such, the adjoint operators can be included in the de Rham complex (3.5) as follows:

$$H^1 \begin{array}{c} \xrightarrow{\text{grad}} \\ \xleftarrow{\text{div}^*} \end{array} H(\text{curl}) \begin{array}{c} \xrightarrow{\text{curl}} \\ \xleftarrow{\text{curl}^*} \end{array} H(\text{div}) \begin{array}{c} \xrightarrow{\text{div}} \\ \xleftarrow{\text{grad}^*} \end{array} L^2 . \quad (3.8)$$

This complex will be used to construct weak forms that adhere to it, in the sense where each differential operator is defined on the space it acts on.

We will see that equations that can be formulated according to the de Rham complex without utilizing the weakly applied operators can be satisfied exactly. Weakly applied operators introduce a metric dependency, which will inevitably lead to approximation errors. In differential geometry, this is made apparent from the usage of the Hodge- \star operator in the adjoint differential operators. For more on the Hodge- \star see [36], [37], in [13] it is discussed within the context of mimetic methods, and in [19] it is discussed within the more specific context of a divergence free Stokes flow solution.

3.2 Two dimensional setting

In a 2-dimensional setting we do not have the usual Gauss's divergence theorem, but instead we have

$$\int_S \text{div } \vec{l} \cdot d\mathcal{S} = \int_{\partial S} \vec{l} \cdot n \, d\gamma, \quad (3.9)$$

Furthermore, as noted earlier, the role of the curl operator in three dimensions is split into two operators in two dimensions. This then gives two instances of Stokes' theorem. One with the rot operator, which is similar to (3.1b), given by:

$$\int_S \text{rot } \vec{l} \cdot d\mathcal{S} = \int_{\partial S} \vec{l} \cdot d\gamma, \quad (3.10)$$

and one with the curl operator, with $\gamma : [a, b] \rightarrow \mathbb{R}^2$, given by :

$$\int_{\gamma} \text{curl } p \cdot n \, d\gamma = \int_a^b \begin{bmatrix} \frac{\partial p(\gamma(t))}{\partial y} \\ -\frac{\partial p(\gamma(t))}{\partial x} \end{bmatrix} \cdot \begin{bmatrix} \frac{\partial \gamma(t)}{\partial y} \\ -\frac{\partial \gamma(t)}{\partial x} \end{bmatrix} d\gamma \quad (3.11a)$$

$$= \int_a^b \begin{bmatrix} \frac{\partial p(\gamma(t))}{\partial x} \\ \frac{\partial p(\gamma(t))}{\partial y} \end{bmatrix} \cdot \begin{bmatrix} \frac{\partial \gamma(t)}{\partial x} \\ \frac{\partial \gamma(t)}{\partial y} \end{bmatrix} d\gamma \quad (3.11b)$$

$$= \int_{\gamma} \text{grad } p \cdot d\gamma \quad (3.11c)$$

$$= p(\gamma(b)) - p(\gamma(a)). \quad (3.11d)$$

When we define

$$H(\text{rot}) := \{ \vec{f} : \vec{f} \in L^2(\Omega) \wedge \text{rot } \vec{f} \in L^2(\Omega) \}, \quad (3.12)$$

we can construct two exact exact Rham complexes in 2D, either

$$H^1 \xrightarrow{\text{curl}} H(\text{div}) \xrightarrow{\text{div}} L^2, \quad (3.13)$$

or

$$H^1 \xrightarrow{\text{grad}} H(\text{rot}) \xrightarrow{\text{rot}} L^2. \quad (3.14)$$

These complexes imply respectively

$$f \in H^1 \implies \text{curl } f \in \mathcal{N}(\text{div}) \subset H(\text{div}), \quad (3.15a)$$

$$\vec{f} \in H(\text{div}) \implies \text{div } \vec{f} \in L^2, \quad (3.15b)$$

and

$$f \in H^1 \implies \text{grad } f \in \mathcal{N}(\text{rot}) \subset H(\text{rot}), \quad (3.15c)$$

$$\vec{f} \in H(\text{rot}) \implies \text{rot } \vec{f} \in L^2. \quad (3.15d)$$

Again, we can extend these complexes with weakly applied, adjoint operators. In 2D these are defined by integration by parts as:

For $b \in L^2$

$$\begin{aligned} (\vec{a}, \text{grad}^* b) &:= \int_{\partial\Omega} b(\vec{a} \cdot n) \, d\partial\Omega - (\text{div } \vec{a}, b) & \forall \vec{a} \in H(\text{div}) \\ &=: B^{\text{grad}}(\vec{a}, b) & - (\text{div } \vec{a}, b), \end{aligned} \quad (3.16a)$$

for $\vec{b} \in H(\text{div})$

$$\begin{aligned} (a, \text{rot}^* \vec{b}) &:= \int_{\partial\Omega} \begin{bmatrix} \vec{b}_2 \\ -\vec{b}_1 \end{bmatrix} a \cdot d\partial\Omega + (\text{curl } a, \vec{b}) & \forall a \in H^1 \\ &=: B^{\text{rot}}(a, \vec{b}) & - (\text{curl } a, \vec{b}), \end{aligned} \quad (3.16b)$$

for $\vec{b} \in L^2$

$$\begin{aligned} (\vec{a}, \text{curl}^* b) &:= \int_{\partial\Omega} \begin{bmatrix} -\vec{a}_2 \\ \vec{a}_1 \end{bmatrix} b \cdot d\partial\Omega + (\text{rot } \vec{a}, b) & \forall \vec{a} \in H(\text{rot}) \\ &=: B^{\text{curl}}(\vec{a}, b) & - (\text{rot } \vec{a}, b), \end{aligned} \quad (3.16c)$$

for $\vec{b} \in H(\text{curl})$

$$\begin{aligned} (a, \text{div}^* \vec{b}) &:= \int_{\partial\Omega} a(\vec{b} \cdot n) \, d\partial\Omega - (\text{grad } a, \vec{b}) & \forall a \in H^1 \\ &=: B^{\text{div}}(a, \vec{b}) & - (\text{grad } a, \vec{b}). \end{aligned} \quad (3.16d)$$

Again, we will use the terms $B(\cdot, \cdot)$ over the boundary integrals for brevity. Using these adjoint operators, the complexes (3.13) and (3.14) respectively become

$$H^1 \begin{array}{c} \xrightarrow{\text{curl}} \\ \xleftarrow{\text{rot}^*} \end{array} H(\text{div}) \begin{array}{c} \xrightarrow{\text{div}} \\ \xleftarrow{\text{grad}^*} \end{array} L^2 , \quad (3.17)$$

and

$$H^1 \begin{array}{c} \xrightarrow{\text{grad}} \\ \xleftarrow{\text{div}^*} \end{array} H(\text{rot}) \begin{array}{c} \xrightarrow{\text{rot}} \\ \xleftarrow{\text{curl}^*} \end{array} L^2 . \quad (3.18)$$

Again, weak forms will be constructed that adhere to these complexes.

4 Weak forms

There are two separate ways in which to construct weak forms for the Navier-Stokes equations that adhere to the de Rham complexes. As in [1], these two weak forms will be combined to form a dual-field weak form, where each field in the strong form of the Navier-Stokes equations is sought after by two separate fields, in different function spaces, in the weak form. This will allow for efficient handling of the nonlinearity when combined with a leap-frog time stepping scheme, as well as allow for conservation of helicity.

4.1 Three dimensional weak forms

Recall that the three dimensional Navier-Stokes equations are given by

$$\begin{cases} \vec{\omega} - \text{curl } \vec{u} = 0, & (4.1a) \\ \frac{\partial \vec{u}}{\partial t} + \vec{\omega} \times \vec{u} + \nu \text{curl } \vec{\omega} + \text{grad } p = \vec{f}, & (4.1b) \\ \text{div } \vec{u} = 0, & (4.1c) \end{cases}$$

and that the three dimensional de Rham complex is given by

$$H^1 \begin{array}{c} \xrightarrow{\text{grad}} \\ \xleftarrow{\text{div}^*} \end{array} H(\text{curl}) \begin{array}{c} \xleftarrow{\text{curl}} \\ \xrightarrow{\text{curl}^*} \end{array} H(\text{div}) \begin{array}{c} \xleftarrow{\text{div}} \\ \xrightarrow{\text{grad}^*} \end{array} L^2 . \quad (4.2)$$

Consider first the divergence free constraint (4.1c) on its own. Note that we can either set $\vec{u} \in H(\text{div})$ and apply div strongly,

$$\text{div } \vec{u} = 0, \quad (4.3)$$

or we can chose to set $\vec{u} \in H(\text{curl})$ and apply div weakly.

$$\text{div}^* \vec{u} = 0. \quad (4.4)$$

The first option would lead to the weak form:

Find $\vec{u} \in H(\text{div})$ such that

$$(q, \text{div } \vec{u}) = 0 \quad \forall q \in L^2. \quad (4.5)$$

The second option would lead to the weak form:

Find $\vec{u} \in H(\text{curl})$ such that

$$(\text{grad } q, \vec{u}) = \int_{\partial\Omega} q(\vec{u} \cdot \vec{n}) \, d\partial\Omega \quad \forall q \in L^2. \quad (4.6)$$

Each choice will lead to a valid weak form. As mentioned earlier, these two weak forms will be combined later. For now let us continue with $\vec{u} \in H(\text{div})$. We will call this the divergence conforming weak form.

4.1.1 Divergence conforming weak form

Now that we have identified $\vec{u} \in H(\text{div})$, we can consider the vorticity defining equation (4.1a), where the curl operator is applied to \vec{u} . Now we see that we cannot apply curl directly to \vec{u} and expect a weakly finite result, as such we apply it weakly:

$$\vec{\omega} - \text{curl}^* \vec{u} = 0. \quad (4.7)$$

Since $\text{curl}^* : H(\text{div}) \rightarrow H(\text{curl})$, and we should not add fields of different function spaces, this gives $\vec{\omega} \in H(\text{curl})$.

Now, consider the evolution equation (4.1b). We find we can directly apply curl to $\vec{\omega}$ and so $\text{curl} \vec{\omega} \in H(\text{div})$. To avoid adding fields of different spaces this forces us to apply grad weakly as grad^* and to set $p \in L^2$.

For now, we leave open the space of the vorticity in the nonlinear term, this will be discussed later in Section 4.2. As defined in Section 3, given a differential operator $d \in \{\text{curl}, \text{grad div}\}$, we write the boundary integrals resulting from a weakly applied operator d^* as $B^d(\cdot, \cdot)$ to avoid clutter.

The divergence conforming weak form is now given by:

Find $\{\vec{\omega}_1 \in H(\text{curl}), \vec{u}_2 \in H(\text{div}), p_3 \in L^2\}^1$ such that

$$\left\{ \begin{array}{ll} (\vec{\tau}_1, \vec{\omega}_1) - (\text{curl} \vec{\tau}_1, \vec{u}_2) = -B^{\text{curl}}(\vec{\tau}_1, \vec{u}_2) & \forall \vec{\tau}_1 \in H(\text{curl}), \quad (4.8a) \\ (\vec{v}_2, \frac{\partial \vec{u}_2}{\partial t}) + (\vec{v}_2, \vec{\omega} \times \vec{u}_2) & \\ +\nu (\vec{v}_2, \text{curl} \vec{\omega}_1) - (\text{div} \vec{v}_2, p_3) = (\vec{v}_2, \vec{f}) - B^{\text{grad}}(\vec{v}_2, p_3) & \forall \vec{v}_2 \in H(\text{div}), \quad (4.8b) \\ (q_3, \text{div} \vec{u}_2) = 0 & \forall q_3 \in L^2. \quad (4.8c) \end{array} \right.$$

4.1.2 Curl conforming weak form

The second weak form comes from the choice to set $\vec{u} \in H(\text{curl})$. From $\vec{u} \in H(\text{curl})$ we note that the div operator in (4.1c) has to be applied weakly as div^* , while in (4.1a) the curl can be applied directly to \vec{u} , this gives $\vec{\omega} \in H(\text{div})$.

In the evolution equation (4.1b) we now see that $\nu \text{curl} \vec{\omega}$ cannot be computed and that we must use $\nu \text{curl}^* \vec{\omega}$, while $\text{grad} p$ needs not be changed. This results in the following weak form:

Find $\{\vec{\omega}_2 \in H(\text{div}), \vec{u}_1 \in H(\text{curl}), p_0 \in H^1\}$ such that

$$\left\{ \begin{array}{ll} (\vec{\tau}_2, \vec{\omega}_2) - (\vec{\tau}_2, \text{curl} \vec{u}_1) = 0 & \forall \vec{\tau}_2 \in H(\text{div}), \quad (4.9a) \\ (\vec{v}_1, \frac{\partial \vec{u}_1}{\partial t}) + (\vec{v}_1, \vec{\omega} \times \vec{u}_1) & \\ +\nu (\text{curl} \vec{v}_1, \vec{\omega}_2) + (\vec{v}_1, \text{grad} p_0) = (\vec{v}_1, \vec{f}) + \nu B^{\text{curl}}(\vec{v}_1, \vec{\omega}_2) & \forall \vec{v}_1 \in H(\text{curl}), \quad (4.9b) \\ (\text{grad} q_0, \vec{u}_1) = B^{\text{div}}(q_0, \vec{u}_1) & \forall q_0 \in H^1. \quad (4.9c) \end{array} \right.$$

This weak form will be referred to as the curl conforming weak form, as the curl of the velocity field can be applied directly.

¹The subscripts we use here are inspired by the differential forms the fields correspond to. In terms of vector calculus, a subscript 0 indicates member of H^1 , 1 a member of $H(\text{curl})$, 2 a member of $H(\text{div})$ and 3 a member of L^2 .

4.2 Three dimensional dual-field weak form

The function space of the vorticity in the nonlinear term has been purposefully left out in the above weak forms. In order to efficiently handle the nonlinear term in the numerical method, we will use a leap-frog time stepping scheme where the vorticity computed via one of the weak forms, will be used to linearize the nonlinear term in the other weak form. As such, the space of vorticity in a nonlinear term must match the space of vorticity in the other weak form. Combined, this gives the following dual-field weak form:

Find $\{\vec{\omega}_1 \in H(\text{curl}), \vec{u}_2 \in H(\text{div}), p_3 \in L^2, \vec{\omega}_2 \in H(\text{div}), \vec{u}_1 \in H(\text{curl}), p_0 \in H^1\}$ such that

$$\left\{ \begin{array}{ll} (\vec{\tau}_1, \vec{\omega}_1) - (\text{curl } \vec{\tau}_1, \vec{u}_2) = -B^{\text{curl}}(\vec{\tau}_1, \vec{u}_2) & \forall \vec{\tau}_1 \in H(\text{curl}), \quad (4.10a) \\ (\vec{v}_2, \frac{\partial \vec{u}_2}{\partial t}) + (\vec{v}_2, \vec{\omega}_2 \times \vec{u}_2) & \\ +\nu (\vec{v}_2, \text{curl } \vec{\omega}_1) - (\text{div } \vec{v}_2, p_3) = (\vec{v}_2, \vec{f}) - B^{\text{grad}}(\vec{v}_2, p_3) & \forall \vec{v}_2 \in H(\text{div}), \quad (4.10b) \\ (q_3, \text{div } \vec{u}_2) = 0 & \forall q_3 \in L^2, \quad (4.10c) \\ (\vec{\tau}_2, \vec{\omega}_2) - (\vec{\tau}_2, \text{curl } \vec{u}_1) = 0 & \forall \vec{\tau}_2 \in H(\text{div}), \quad (4.10d) \\ (\vec{v}_1, \frac{\partial \vec{u}_1}{\partial t}) + (\vec{v}_1, \vec{\omega}_1 \times \vec{u}_1) & \\ +\nu (\text{curl } \vec{v}_1, \vec{\omega}_2) + (\vec{v}_1, \text{grad } p_0) = (\vec{v}_1, \vec{f}) + \nu B^{\text{curl}}(\vec{v}_1, \vec{\omega}_2) & \forall \vec{v}_1 \in H(\text{curl}), \quad (4.10e) \\ (\text{grad } q_0, \vec{u}_1) = B^{\text{div}}(q_0, \vec{u}_1) & \forall q_0 \in H^1. \quad (4.10f) \end{array} \right.$$

We will not investigate the well posedness of the nonlinear weak forms. While we might not be able to show the nonlinear terms to be finite, this will be the case once we introduce discrete function spaces.

Remark (Helicity).

In order to prove helicity conservation of the numerical method, the integral $(\vec{\omega}, \vec{u})$ has to be obtainable in the discrete problem. When considering the divergence and curl conforming weak forms separately as in Section 4.1, such a statement would not be obtainable, as the sought after velocity and vorticity fields are in different function spaces.

In the dual-field weak form, however, we have expression for helicity either as $(\vec{\omega}_2, \vec{u}_2)$ or $(\vec{\omega}_1, \vec{u}_1)$. This connection between the two different weak forms to form an obtainable expression for helicity was the direct motivation in [1] to introduce the dual-field approach which this thesis will employ as well.

4.3 Two dimensional weak forms

As noted earlier, the 2D Navier-Stokes equations are given by

$$\left\{ \begin{array}{ll} \omega - \text{rot } \vec{u} = 0, & (4.11a) \\ \frac{\partial \vec{u}}{\partial t} + \omega \times \vec{u} + \nu \text{curl } \omega + \text{grad } p = \vec{f}, & (4.11b) \\ \text{div } \vec{u} = 0, & (4.11c) \end{array} \right.$$

and the 2D de Rham complexes are given by

$$H^1 \begin{array}{c} \xleftarrow{\text{curl}} \\ \xrightarrow{\text{rot}^*} \end{array} H(\text{div}) \begin{array}{c} \xrightarrow{\text{div}} \\ \xleftarrow{\text{grad}^*} \end{array} L^2, \quad (4.12)$$

and

$$H^1 \begin{array}{c} \xrightarrow{\text{grad}} \\ \xleftarrow{\text{div}^*} \end{array} H(\text{rot}) \begin{array}{c} \xrightarrow{\text{rot}} \\ \xleftarrow{\text{curl}^*} \end{array} L^2. \quad (4.13)$$

We again find that we can construct two weak forms, one starting from $\vec{u} \in H(\text{div})$, the divergence conforming weak form, and one starting from $\vec{u} \in H(\text{rot})$, the curl conforming weak form.

4.3.1 Divergence conforming weak form

We set $\vec{u} \in H(\text{div})$ and directly see that the rot operator has to be applied weakly in (4.11a), as $\text{rot}^* : H(\text{div}) \rightarrow H^1$ we also identify $\omega \in H^1$. Now from the evolution equation (4.11b) we see that curl can be directly applied to ω . Since $\text{curl} : H^1 \rightarrow H(\text{div})$, we must have apply the gradient operator weakly as $\text{grad}^* p \in H(\text{div})$. Again for now omitting the space of the vorticity in the nonlinear term, this results in the following weak form:

Find $\{\vec{u}_1 \in H(\text{div}), \omega_0 \in H^1, p_2 \in L^2\}^2$ such that

$$\left\{ \begin{array}{l} (\tau_0, \omega_0) - (\text{curl}_0 \tau_0, \vec{u}_1) = -B^{\text{curl}}(\tau_0, \vec{u}_1) \quad \forall \tau_0 \in H^1, \quad (4.14a) \\ (\vec{v}_1, \frac{\partial \vec{u}_1}{\partial t}) + (\vec{v}_1, \omega \times \vec{u}_1) \\ +\nu (\vec{v}_1, \text{curl } \omega_0) - (\text{grad } \vec{v}_1, p_2) = (\vec{v}_1, \vec{f}) - B^{\text{grad}}(\vec{v}_1, p_2) \quad \forall v_1 \in H(\text{div}), \quad (4.14b) \\ (q_2, \text{div } \vec{u}_1) = 0 \quad \forall q_2 \in L^2. \quad (4.14c) \end{array} \right.$$

4.3.2 Curl conforming weak form

When we start with $\vec{u} \in H(\text{rot})$ we find that the div in (4.11c) needs to weakly applied, while rot u can be computed as is. (4.11a) now shows that $\omega \in L^2$. In (4.11b) we now see that the curl needs to be weakly applied and that we can set $p \in H^1$ and apply grad directly. The second, curl (rot) conforming, weak form is now given by:

Find $\{\vec{u}_1 \in H(\text{rot}), \omega_2 \in L^2, p_0 \in H^1\}$ such that

$$\left\{ \begin{array}{l} (\tau_2, \omega_2) - (\tau_2, \text{rot } \vec{u}_1) = 0 \quad \forall \vec{v}_1 \in H(\text{rot}), \quad (4.15a) \\ (\vec{v}_1, \frac{\partial \vec{u}_1}{\partial t}) + (\vec{v}_1, \omega \times \vec{u}_1) \\ +\nu (\text{rot } \vec{v}_1, \omega_2) + (\vec{v}_1, \text{grad } p_0) = (\vec{v}_1, \vec{f}) - \nu B^{\text{curl}}(\vec{v}_1, \omega) \quad \forall \tau_2 \in L^2, \quad (4.15b) \\ (\text{grad } q_0, \vec{u}_1) = B^{\text{div}}(q_0, \vec{u}_1) \quad \forall q_0 \in H^1. \quad (4.15c) \end{array} \right.$$

²The subscripts we use here are again inspired by the differential forms the fields correspond to. The associated function spaces are slightly different in 2D. A subscript 0 indicates member of H^1 , 1 a member of $H(\text{div})$ or $H(\text{rot})$ depending on the used de Rham complex and 2 a member of L^2 .

4.4 Two dimensional dual-field weak form

The same motivation as in the three dimensional case applies. The 2D dual-field weak form is given by:

Find $\{\vec{u}_1 \in H(\text{div}), \omega_0 \in H^1, p_2 \in L^2, \vec{u}_1 \in H(\text{rot}), \omega_2 \in L^2, p_0 \in H^1\}$ such that

$$\left\{ \begin{array}{ll} (\tau_0, \omega_0) - (\text{curl}_0 \tau_0, \vec{u}_1) = -B^{\text{curl}}(\tau_0, \vec{u}_1) & \forall \tau_0 \in H^1, \quad (4.16a) \\ (\vec{v}_1, \frac{\partial \vec{u}_1}{\partial t}) + (\vec{v}_1, \omega_2 \times \vec{u}_1) & \\ +\nu (\vec{v}_1, \text{curl } \omega_0) - (\text{grad } \vec{v}_1, p_2) = (\vec{v}_1, \vec{f}) - B^{\text{grad}}(\vec{v}_1, p_2) & \forall v_1 \in H(\text{div}), \quad (4.16b) \\ (q_2, \text{div } \vec{u}_1) = 0 & \forall q_2 \in L^2, \quad (4.16c) \\ (\tau_2, \omega_2) - (\tau_2, \text{rot } \vec{u}_1) = 0 & \forall \vec{v}_1 \in H(\text{rot}), \quad (4.16d) \\ (\vec{v}_1, \frac{\partial \vec{u}_1}{\partial t}) + (\vec{v}_1, \omega_0 \times \vec{u}_1) & \\ +\nu (\text{rot } \vec{v}_1, \omega_2) + (\vec{v}_1, \text{grad } p_0) = (\vec{v}_1, \vec{f}) - \nu B^{\text{curl}}(\vec{v}_1, \omega) & \forall \tau_2 \in L^2, \quad (4.16e) \\ (\text{grad } q_0, \vec{u}_1) = B^{\text{div}}(q_0, \vec{u}_1) & \forall q_0 \in H^1. \quad (4.16f) \end{array} \right.$$

5 Discrete function spaces

In Sections 2 and 3 it was noted that the de Rham complex contains the structure necessary to prove energy, enstrophy and helicity conservation. To be able to prove conservation properties at the discrete level, we should start by constructing a de Rham complex of discrete function spaces. These spaces will then be used to spatially discretize the weak form of Section 4 such that discrete conservation properties can be proven in Section 6.

In this thesis we chose to work with tensor product B-spline basis functions for the discrete spaces as the subject matter is connected to isogeometric analysis, where B-splines are used to exactly reproduce geometries designed with CAD software. For usage of B-splines in mimetic methods and more on isogeometric analysis see [25]–[30]. However, we are only concerned with problems on rectangular domains in this thesis, and hence we will not discuss pull back operators. We will now first discuss some properties of B-spline basis functions, and then show how they can be used to form a discrete de Rham complex.

We will now first describe some relevant properties of B-spline basis functions, then, we will define basis functions for discrete spaces in a one dimensional de Rham complex. These are then extended to two and three dimensions using tensor products. Finally we a short discussion on incidence matrices is included, these matrices which will be use as discrete representation of differential operators.

5.1 B-spline basis functions

For an introduction to B-splines and their basis functions, see [38], [39]. Given a knot vector of non decreasing knots

$$\Xi = \{\xi_i\}_i, \quad \xi_i \leq \xi_{i+1}, \quad (5.1)$$

The i 'th B-spline basis function or order r , $B_{i,r}$, can be generated using the following recursive relation [38]

$$B_{i,1}(x) = \begin{cases} 1 & \text{if } x \in [\xi_i, \xi_{i+1}) \\ 0 & \text{otherwise} \end{cases} \quad (5.2a)$$

$$B_{i,r}(x) = \frac{x - \xi_i}{\xi_{i+r} - \xi_i} B_{i,r-1}(x) + \frac{\xi_{i+1} - x}{\xi_{i+1} - \xi_i} B_{i+1,r-1}(x), \quad (5.2b)$$

where we use the convention that division by zero yields zero. Note how the B-spline order is always one more than the polynomial degree. For our purposes, we require an expression for the derivative of a B-spline basis function. Using $\text{Supp}(B_{i,r})$ for the size of the support of $B_{i,r}$ and

$$\tilde{B}_{i,r} := \frac{(r-1)}{\text{Supp}(B_{i,r})} B_{i,r}, \quad (5.3)$$

we find the general expression for the derivative of a B-spline basis function [38]

$$\frac{d}{dx} B_{i,r} = \left(\tilde{B}_{i-1,r-1} - \tilde{B}_{i,r-1} \right), \quad (5.4)$$

where $B_{i,r}$ and $B_{i,r-1}$ are assumed to be generated from the same knot vector.

For open knot vector, that is knot vectors where the first and last knots are repeated r times, we find that when $B_{i,r}$ and $B_{i,r-1}$ are generated from the same knot vector, that the first and last basis function of $B_{i,r}$ are identically zero. To disregard these zero functions, we can instead consider $B_{i,r-1}$ to be generated from the same knot vector with the first and last knot removed. This gives

$$\frac{d}{dx}B_{i,r} = \begin{cases} -\tilde{B}_{1,r-1} & \text{if } i = 1 \\ \tilde{B}_{n-1,r-1} & \text{if } i = n \\ \left(\tilde{B}_{i-1,r-1} - \tilde{B}_{i,r-1}\right) & \text{otherwise} \end{cases} . \quad (5.5)$$

B-spline basis functions can also be derived for periodic domains. This is done by considering a periodic knot vector. Given a regular knot vector $\Xi = \{\xi_i\}_{i=1}^n$ $\xi_i \leq \xi_{i+1}$, a periodic knot vector Ξ^L with period $L = \xi_n - \xi_1$ can be defined as $\Xi^L = \{\xi_i + kL : K \in \mathbb{Z}\}_{i=1}^n$, ignoring additional multiplicities introduced for ξ_1 and ξ_n . From this periodic knot vector B-spline basis functions can be generated as before. Using this approach, basis functions that are smooth across the periodic boundary can be obtained.

At first glance, generating basis functions for a periodic knot vector as described above yields an infinite number of basis functions. However, due to the periodic nature of the knot vector, the basis functions will eventually repeat themselves, albeit translated. That is, there is some n such that

$$B_{i,r}(x) = B_{i+n,r}(x + L). \quad (5.6)$$

Let f be a periodic function with period L , given as a linear combination of periodic basis functions

$$f := \sum_{k \in \mathbb{Z}} \sum_{i=1}^n \bar{f}_{i+kn} B_{i+kn,r}, \quad (5.7)$$

then we can note that by (5.6) and by the periodicity of f we must have

$$\bar{f}_{i+kn} = \bar{f}_i \quad \forall k \in \mathbb{Z}. \quad (5.8)$$

Now f can be written as

$$f = \sum_{i=1}^n \bar{f}_i \sum_{k \in \mathbb{Z}} B_{i+kn,r}. \quad (5.9)$$

As we know that the periodic basis functions satisfy (5.6), n subsequent basis functions are sufficient to represent the whole set. Allowing for some abuse of notation, we can use $B_{i,r}$ as a representative of $B_{i+kn,r} \quad \forall k \in \mathbb{Z}$ to write

$$f = \sum_{i=1}^n \bar{f}_i B_{i,r}. \quad (5.10)$$

Again, the general expression for the derivative of a B-spline basis function (5.4) holds. In the case of periodic basis functions, there are no basis functions identically zero and so we can directly

use this expression. It should be noted, however, that the basis indexing for periodic bases is not necessarily obvious. Depending on what basis function is considered to be the first, the indices in (5.4) might shift. In the subsequent sections, we will assume that the indexing is chosen such that (5.4) holds as is.

With these expressions in place, we can derive basis functions for the discrete spaces.

5.2 One dimensional basis functions

Consider the one dimensional de Rham complex

$$H^1 \xrightarrow{\frac{d}{dx}} L^2, \quad (5.11)$$

We aim to construct basis functions for the discrete spaces $H_h^1 \subset H^1$ and $L_h^2 \subset L^2$ that adhere to a discrete version of this de Rham complex, i.e.

$$H_h^1 \xrightarrow{\frac{d}{dx}} L_h^2, \quad (5.12)$$

As we aim to use B-spline basis functions, let us define H_h^1 to be

$$H_h^1 := \text{span}\{B_{i,r}\}_{i=1}^n. \quad (5.13)$$

In the case of an aperiodic domain these basis functions will be generated from an open knot vector. This results in interpolating basis functions at the boundary, that is, writing ξ_1 and ξ_m for the first and last knot,

$$B_{1,r}(\xi_1) = 1 \quad \text{and} \quad B_{n,r}(\xi_m) = 1, \quad (5.14a)$$

$$B_{i,r}(\xi_1) = 0 \quad \forall i \neq 1 \quad \text{and} \quad B_{i,r}(\xi_m) = 0 \quad \forall i \neq n. \quad (5.14b)$$

This will allow for easy handling of the Dirichlet boundary conditions. In the case of a periodic domain the basis functions will be generated from a periodic knot vector.

Now we can construct a discrete space L_h^2 that adheres to (5.12). All that needs to hold for L_h^2 is that

$$f \in H_h^1 \implies \frac{d}{dx} f \in L_h^2. \quad (5.15)$$

As noted in the previous subsection, the derivative of a B-spline basis function depends on whether we consider periodic or aperiodic basis functions. We will first consider aperiodic basis functions and then consider periodic basis functions.

5.2.1 Aperiodic basis functions

Now to construct basis function for L_h^2 , let us first consider $f := \sum_{i=1}^n \bar{f}_i B_{i,r} \in H_h^1$, then

$$\frac{d}{dx} f = \sum_{i=1}^n \bar{f}_i \frac{d}{dx} B_{i,r} \quad (5.16a)$$

$$\stackrel{(5.5)}{=} -\bar{f}_1 \tilde{B}_{1,r-1} + \sum_{i=2}^{n-1} \bar{f}_i (\tilde{B}_{i-1,r-1} - \tilde{B}_{i,r-1}) + \bar{f}_n \tilde{B}_{n-1,r-1} \quad (5.16b)$$

$$= \sum_{i=1}^{n-1} (\bar{f}_{i+1} - \bar{f}_i) \tilde{B}_{i,r-1} \quad (5.16c)$$

$$\in \text{span}\{\tilde{B}_{i,r-1}\}_{i=1}^{n-1}. \quad (5.16d)$$

Now if we define

$$L_h^2 := \text{span}\{\tilde{B}_{i,r-1}\}_{i=1}^{n-1}, \quad (5.17)$$

we obtain the implication

$$f \in H_h^1 \implies \frac{d}{dx} f \in L_h^2, \quad (5.18)$$

and so the discrete spaces adhere to a discrete de Rham complex (5.12). In actuality, (5.16b) already suffices to conclude (5.16d). However, the remaining derivation will help us to express the action of a differential operator as a linear operation on the DoF's in Section 5.5. Note that $\tilde{B}_{i,r-1}$ are generated from the same knot vector as $B_{i,r}$ but with the first and last knot removed as assumed by (5.5).

5.2.2 Periodic basis functions

We follow a similar approach as taken for the aperiodic basis functions. Let f be a periodic function in H_h^1 , $f := \sum_{i=1}^n \bar{f}_i B_{i,r} \in H_h^1$, then

$$\frac{d}{dx} f = \sum_{i=1}^n \bar{f}_i \frac{d}{dx} B_{i,r} \quad (5.19a)$$

$$\stackrel{(5.4)}{=} \sum_{i=1}^n \bar{f}_i (\tilde{B}_{i-1,r-1} - \tilde{B}_{i,r-1}) \quad (5.19b)$$

$$= \sum_{i=1}^n (\bar{f}_{i+1} - \bar{f}_i) \tilde{B}_{i,r-1} \quad (5.19c)$$

$$\stackrel{(5.8)}{=} \sum_{i=1}^{n-1} (\bar{f}_{i+1} - \bar{f}_i) \tilde{B}_{i,r-1} + (\bar{f}_1 - \bar{f}_n) \tilde{B}_{n,r-1} \quad (5.19d)$$

$$\in \text{span}\{\tilde{B}_{i,r-1}\}_{i=1}^n. \quad (5.19e)$$

Now we can again define

$$L_h^2 := \text{span}\{\tilde{B}_{i,r-1}\}_{i=1}^n, \quad (5.20)$$

to obtain the implication

$$f \in H_h^1 \implies \frac{d}{dx} f \in L_h^2, \quad (5.21)$$

and so the discrete spaces adhere to a discrete de Rham complex (5.12).

Figures showing the periodic and a periodic basis functions are shown in Figures 1 and 2. We refer to the basis functions of H_h^1 as nodal functions, and to the basis functions of L_h^2 as edge functions in line with [40].

5.3 Two dimensional basis functions

In two dimensions we find two discrete de Rham complexes

$$H_h^1 \xrightarrow{\text{curl}} H_h(\text{div}) \xrightarrow{\text{div}} L_h^2, \quad (5.22)$$

and

$$H_h^1 \xrightarrow{\text{grad}} H_h(\text{rot}) \xrightarrow{\text{rot}} L_h^2, \quad (5.23)$$

from the two continuous de Rham complexes (3.13) and (3.14). The difference between these two complexes will be evident in the basis function of $H_h(\text{rot})$ and $H_h(\text{div})$. Let us first define the discrete spaces in (5.23).

5.3.1 Basis functions for the $H_h(\text{rot})$ complex

Using tensor products of the one dimensional basis functions, we define the two dimensional spaces by

$$H_h^1 := \text{span}\{B_{i,r} \otimes B_{j,r} \}_{i,j}, \quad (5.24a)$$

$$H_h(\text{rot}) := \text{span}\{\tilde{B}_{i,r-1} \otimes B_{j,r} \}_{i,j} \times \text{span}\{B_{i,r} \otimes \tilde{B}_{j,r-1}\}_{i,j}, \quad (5.24b)$$

$$L_h^2 := \text{span}\{\tilde{B}_{i,r-1} \otimes \tilde{B}_{j,r-1}\}_{i,j}. \quad (5.24c)$$

The exact ranges of the indices are omitted to allow for a general formulation that fits both periodic and aperiodic basis functions.

To show these functions constitute a discrete de Rham complex, we must show

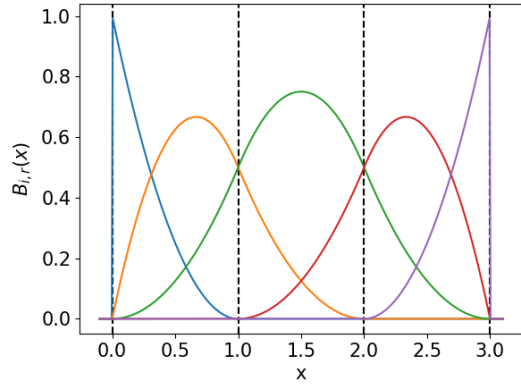
$$f \in H_h^1 \implies \text{grad } f \in H_h(\text{rot}) \quad (5.25)$$

and

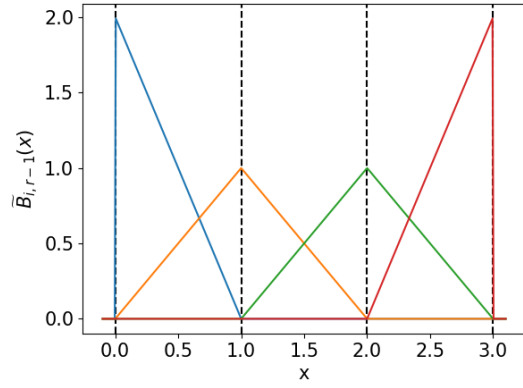
$$\vec{f} \in H_h(\text{rot}) \implies \text{rot } \vec{f} \in L_h^2. \quad (5.26)$$

Then, by (2.22), we also must have

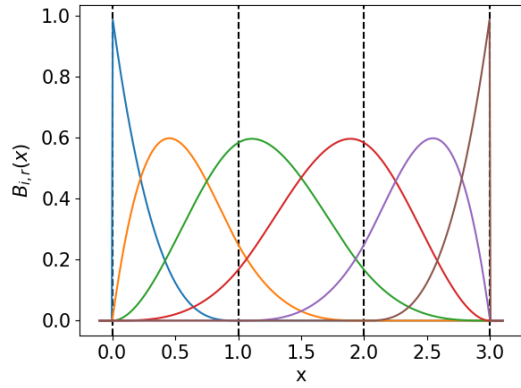
$$f \in H_h^1 \implies \text{rot grad } f \equiv 0. \quad (5.27)$$



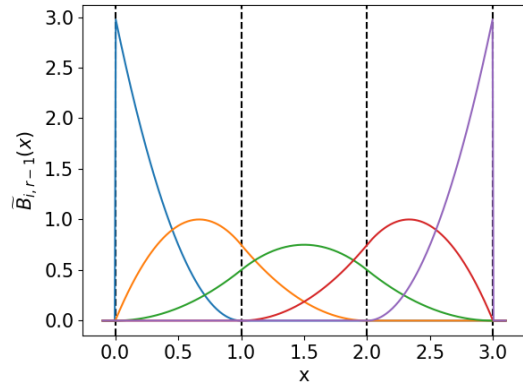
(a) Order 3 nodal functions



(b) Order 2 edge functions, computed from (a)



(c) Order 4 nodal functions



(d) Order 3 edge functions, computed from (c)

Figure 1: Aperiodic nodal functions generated from knot vector $\Xi = [0, \dots, 0, 1, 2, 3, \dots, 3]$ with associated edge functions.

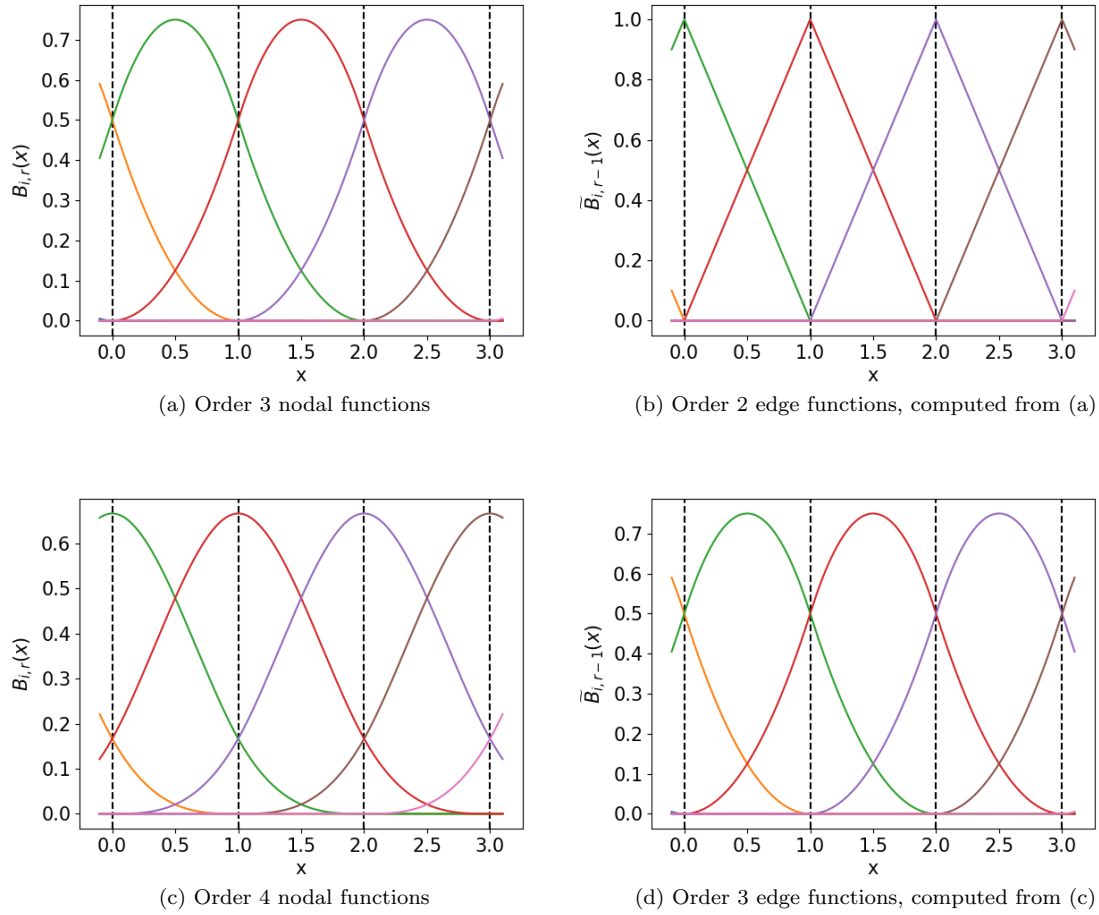


Figure 2: Periodic nodal functions generated from a periodic knot vector $\Xi^3 = [\dots, 0, 1, 2, 3, \dots]$ with associated edge functions.

We no longer treat the aperiodic and periodic basis functions separately. Instead we use the expressions in (5.16c) and (5.19c), which are identical for both types, in our derivations.

First we show (5.25). Let $f = \sum_j \sum_i \bar{f}_{i,j} B_{i,r}(x) B_{j,r}(y) \in H_h(\text{rot})$. We will show the spaces to which $\frac{\partial}{\partial x} f$ and $\frac{\partial}{\partial y} f$ belong, these are then combined to form the space of $\text{grad } f$. We find

$$\frac{\partial}{\partial x} f(x, y) = \frac{\partial}{\partial x} \sum_j \sum_i \bar{f}_{i,j} B_{i,r}(x) B_{j,r}(y) \quad (5.28a)$$

$$= \sum_j \left(\sum_i \bar{f}_{i,j} \frac{d}{dx} B_{i,r}(x) \right) B_{j,r}(y) \quad (5.28b)$$

Now we use (5.16c) in the case of aperiodic basis functions and (5.19c) in the case of periodic basis functions to, in both cases, obtain

$$\frac{\partial}{\partial x} f(x, y) = \sum_j \left(\sum_i (\bar{f}_{i+1,j} - \bar{f}_{i,j}) \tilde{B}_{i,r}(x) \right) B_{j,r}(y) \quad (5.28c)$$

$$\in \text{span}\{\tilde{B}_{i,r-1} \otimes B_{j,r}\}_{i,j}. \quad (5.28d)$$

Following a similar derivation for $\frac{\partial}{\partial y} f$ yields

$$\frac{\partial}{\partial y} f(x, y) \in \text{span}\{B_{j,r} \otimes \tilde{B}_{i,r-1}\}_{i,j}, \quad (5.29)$$

and so

$$\text{grad } f \in \text{span}\{\tilde{B}_{i,r-1} \otimes B_{j,r}\}_{i,j} \times \text{span}\{B_{j,r} \otimes \tilde{B}_{i,r-1}\}_{i,j} = H_h(\text{rot}) \quad (5.30)$$

as required.

Now to show (5.26) let $\vec{f} := [\vec{f}_1, \vec{f}_2]^\top \in H_h(\text{rot})$. We will show the spaces to which $\frac{d}{dy} \vec{f}_1$ and $\frac{d}{dx} \vec{f}_2$ belong, these results are then combined to find the space of $\text{rot } \vec{f}$. We find

$$\frac{d}{dy} \vec{f}_1(x, y) := \sum_i \sum_j \bar{f}_{1,i,j} \tilde{B}_{i,r-1}(x) \frac{d}{dy} B_{j,r-1} \quad (5.31)$$

$$= \sum_i \left(\sum_j \bar{f}_{1,i,j} \frac{d}{dy} B_{j,r-1} \right) \tilde{B}_{i,r-1}(x). \quad (5.32)$$

Now we can again use (5.16c) and (5.19c) to find

$$\frac{d}{dy} \vec{f}_1(x, y) = \sum_i \left(\sum_j (\bar{f}_{1,i+1,j} - \bar{f}_{1,i,j}) \tilde{B}_{j,r-1} \right) \tilde{B}_{i,r-1}(x) \quad (5.33)$$

$$\in \text{span}\{\tilde{B}_{i,r-1} \otimes \tilde{B}_{j,r-1}\}_{i,j}. \quad (5.34)$$

Following a similar derivation for $\frac{d}{dx}\vec{f}_2$ yields

$$\frac{d}{dy}\vec{f}_1(x, y) \in \text{span}\{\tilde{B}_{i,r-1} \otimes \tilde{B}_{j,r-1}\}_{i,j}, \quad (5.35)$$

and so

$$\text{rot } \vec{f} \in \text{span}\{\tilde{B}_{i,r-1} \otimes \tilde{B}_{j,r-1}\}_{i,j} = L_h^2 \quad (5.36)$$

as required.

Having shown (5.25) and (5.26) we conclude that the discrete spaces in (5.24) constitute a de Rham complex.

5.3.2 Basis functions for the $H_h(\text{div})$ complex

Following similar derivations used above, a suitable definition of discrete spaces of (5.22) can be found to be

$$H_h^1 := \text{span}\{B_{i,r} \otimes B_{j,r}\}_{i,j}, \quad (5.37a)$$

$$H_h(\text{div}) := \text{span}\{B_{i,r} \otimes \tilde{B}_{j,r-1}\}_{i,j} \times \text{span}\{-\tilde{B}_{i,r-1} \otimes B_{j,r}\}_{i,j}, \quad (5.37b)$$

$$L_h^2 := \text{span}\{\tilde{B}_{i,r-1} \otimes \tilde{B}_{j,r-1}\}_{i,j}. \quad (5.37c)$$

When compared to (5.24), the definitions of H_h^1 and L_h^2 are identical. Only the spaces of $H_h(\text{rot})$ and $H_h(\text{div})$ differ. However, using separate basis functions for $H_h(\text{div})$ and $H_h(\text{rot})$ is not strictly necessary.

To see this, note how the basis functions of $H_h(\text{div})$ are the basis functions for $H_h(\text{rot})$ but ‘rotated 90 degrees’. When we see $\vec{u} \in H_h(\text{div})$ not as specifying the tangential direction of a velocity field as usual, but as specifying the normal direction of the velocity field, its basis functions become exactly equal to those of $H_h(\text{rot})$, as in two dimensions the normal direction of velocity is a 90 degree rotation of the tangential direction.

As a consequence, we can use the basis functions of $H_h(\text{rot})$ to represent members of $H_h(\text{div})$, so long as we remember the ‘rotation’, i.e. so long as we remember that $\vec{u} \in H_h(\text{div})$ represents the normal direction of the velocity field, not the usual tangential direction. This simplifies the bookkeeping and relieves the memory requirements of codes utilizing both $H_h(\text{rot})$ and $H_h(\text{div})$. So long as the input data and results of a discrete problem are adequately transformed, all computations can be done using the basis functions presented in (5.24).

By the same logic, there is no need to make a distinction between $\text{curl} : H_h^1 \rightarrow H_h(\text{div})$ and $\text{grad} : H_h^1 \rightarrow H_h(\text{rot})$. Given $f \in H_h^1$, we find that

$$\text{grad } f = \left[\frac{d}{dx}f, \frac{d}{dy}f \right] \quad \text{and} \quad \text{curl } f = \left[\frac{d}{dy}f, -\frac{d}{dx}f \right], \quad (5.38)$$

these results show the same difference that (5.37) and (5.24) do. From this we can see that computing $\text{curl } f$ and interpreting the result as a regular vector field yields the same result as applying $\text{grad } f$ and interpreting the result as the normal direction of a vector field. A similar observation can be made to render the distinction between rot and div obsolete, so long as the results are correctly interpreted.

In differential geometry, the switch from interpreting \vec{u} as specifying the tangential direction to the normal direction, is described by the Hodge- \star operator, which maps inner-oriented forms to outer-oriented forms and vice versa. The observation that curl and grad (and rot and div) can be considered the same operator, only differing in the adequate perspective, is captured by the exterior derivative. As referenced before, more on the Hodge- \star and exterior derivative can be found in for example [13], [19], [36], [37].

5.4 Three dimensional basis functions

In three dimensions we find the discrete de Rham complex

$$H_h^1 \xrightarrow{\text{grad}} H_h(\text{curl}) \xrightarrow{\text{curl}} H_h(\text{div}) \xrightarrow{\text{div}} L_h^2. \quad (5.39)$$

Using derivations akin to those in Section 5.3.1, basis functions for these discrete spaces can be found to be

$$H_h^1 = \text{span}\{B_{i,r} \otimes B_{j,r} \otimes B_{k,r}\}_{i,j,k}, \quad (5.40a)$$

$$\begin{aligned} H_h(\text{curl}) &= \text{span}\{\tilde{B}_{i,r-1} \otimes B_{j,r} \otimes B_{k,r}\}_{i,j,k} \\ &\times \text{span}\{B_{i,r} \otimes \tilde{B}_{j,r-1} \otimes B_{k,r}\}_{i,j,k} \\ &\times \text{span}\{B_{i,r} \otimes B_{j,r} \otimes \tilde{B}_{k,r-1}\}_{i,j,k}, \end{aligned} \quad (5.40b)$$

$$\begin{aligned} H_h(\text{div}) &= \text{span}\{B_{i,r} \otimes \tilde{B}_{j,r-1} \otimes \tilde{B}_{k,r-1}\}_{i,j,k} \\ &\times \text{span}\{\tilde{B}_{i,r-1} \otimes B_{j,r} \otimes \tilde{B}_{k,r-1}\}_{i,j,k} \\ &\times \text{span}\{\tilde{B}_{i,r-1} \otimes \tilde{B}_{j,r-1} \otimes B_{k,r}\}_{i,j,k}, \end{aligned} \quad (5.40c)$$

$$L_h^2 = \text{span}\{\tilde{B}_{i,r-1} \otimes \tilde{B}_{j,r-1} \otimes \tilde{B}_{k,r-1}\}_{i,j,k}. \quad (5.40d)$$

5.5 Incidence matrices

In this thesis it has been chosen to take an axiomatic approach to introducing the discrete function spaces and their basis functions. A different approach could have been to introduce discrete differential operators as dual operators to a discrete boundary operator, as briefly touched upon for the continuous setting in Section 3. This then leads to more a geometrically motivated approach. This approach would be superfluous for the work at hand, but some of the geometric associations are worth noting. For more on this geometrically motivated approach, see for example [13] for an in depth overview of differential geometry and algebraic topology for mimetic methods, or [20] where is used in a mimetic method for Stokes flow.

Specifically we wish to introduce the incidence matrices, who's transpose can be used as discrete differential operators. Here, we simply briefly show that the introduced basis functions allow for the action of a differential operator to be represented by a matrix product with its degrees of freedom (DoF). These matrix products will be used in the presentation of the numerical method as a linear system. Similarly to the basis functions, we will introduce this for the one dimensional case, and

then extend it to higher dimensions. We will also briefly touch upon the relation between DoF's and integral values on geometric objects.

For a function f in some discrete function space, we will denote the vector containing its DoF's as $\bar{\mathbf{f}}$. Consider a one dimensional function $f = \sum_i \bar{f}_i B_{i,r} \in H_h^1$, with $\frac{d}{dx} f = g \in L_h^2$. We now seek a matrix $E_{0,1}$ ³, called an incidence matrix, such that the DoF's of g are given by

$$\bar{\mathbf{g}} = E_{0,1}^\top \bar{\mathbf{f}}. \quad (5.41)$$

By (5.16c) and (5.19c) we find

$$\frac{d}{dx} f = g \implies \bar{f}_{i+1} - \bar{f}_i = \bar{g}_i, \quad (5.42)$$

and so we define

$$[E^\top \bar{\mathbf{f}}]_i := \bar{f}_{i+1} - \bar{f}_i. \quad (5.43)$$

Now for higher dimension we will show the relations between the DoF's that hold as in (5.42). From these relations matrices can be setup. In two dimensions, we will only focus on the grad and rot operator as supported by Section 5.3.2.

Discrete grad operator (2D)

Let $f \in H_h^1$ and $\vec{g} = \text{grad } f \in H_h(\text{rot})$, then the DoF's of \vec{g} , denoted $\bar{g}_{d,i,j,k}$, where d is the component of the vector, are given by

$$\bar{g}_{1,i,j,k} = \bar{f}_{i+1,j,k} - \bar{f}_{i,j,k}, \quad (5.44a)$$

$$\bar{g}_{2,i,j,k} = \bar{f}_{i,j+1,k} - \bar{f}_{i,j,k}, \quad (5.44b)$$

These relations define the matrix $E_{0,1}$ such that $\bar{\mathbf{g}} = E_{0,1}^\top \bar{\mathbf{f}}$

Discrete rot operator (2D)

Let $\vec{f} \in H_h(\text{rot})$ and $g = \text{rot } \vec{f} \in L_h^2$, then the DoF's of g are given by

$$\bar{g}_{i,j,k} = (\bar{f}_{2,i+1,j,k} - \bar{f}_{2,i,j,k}) - (\bar{f}_{1,i,j+1,k} - \bar{f}_{1,i,j,k}). \quad (5.45a)$$

These relations define the matrix $E_{1,2}$ such that $\bar{\mathbf{g}} = E_{1,2}^\top \bar{\mathbf{f}}$

Discrete grad operator (3D)

Let $f \in H_h^1$ and $\vec{g} = \text{grad } f \in H_h(\text{curl})$, then the DoF's of \vec{g} are given by

$$\bar{g}_{1,i,j,k} = \bar{f}_{i+1,j,k} - \bar{f}_{i,j,k}, \quad (5.46a)$$

$$\bar{g}_{2,i,j,k} = \bar{f}_{i,j+1,k} - \bar{f}_{i,j,k}, \quad (5.46b)$$

$$\bar{g}_{3,i,j,k} = \bar{f}_{i,j,k+1} - \bar{f}_{i,j,k}. \quad (5.46c)$$

These relations define the matrix $E_{0,1}$ such that $\bar{\mathbf{g}} = E_{0,1}^\top \bar{\mathbf{f}}$

³The subscripts on these matrices are again inspired by the (discrete) differential forms the matrices act on. A matrix $E_{1,2}$ in 3D acts on $H_h(\text{curl})$ DoF's and returns $H_h(\text{div})$ DoF's. In 1D a matrix $E_{0,1}$ acts on H_h^1 DoF's and returns L_h^2 DoF's.

Discrete curl operator (3D)

Let $\vec{f} \in H_h(\text{curl})$ and $\vec{g} = \text{curl } \vec{f} \in H_h(\text{div})$, then the DoF's of \vec{g} are given by

$$\bar{g}_{1,i,j,k} = (\bar{f}_{3,i,j+1,k} - \bar{f}_{3,i,j,k}) - (\bar{f}_{2,i,j,k+1} - \bar{f}_{2,i,j,k}), \quad (5.47a)$$

$$\bar{g}_{2,i,j,k} = (\bar{f}_{1,i,j,k+1} - \bar{f}_{1,i,j,k}) - (\bar{f}_{3,i+1,j,k} - \bar{f}_{3,i,j,k}), \quad (5.47b)$$

$$\bar{g}_{3,i,j,k} = (\bar{f}_{2,i+1,j,k} - \bar{f}_{2,i,j,k}) - (\bar{f}_{1,i,j+1,k} - \bar{f}_{1,i,j,k}). \quad (5.47c)$$

These relations define the matrix $E_{1,2}$ such that $\bar{\mathbf{g}} = E_{1,2}^\top \bar{\mathbf{f}}$

Discrete div operator (3D)

Let $\vec{f} \in H_h(\text{div})$ and $g = \text{div } \vec{f} \in L_h^2$, then the DoF's of g are given by

$$\bar{g}_{i,j,k} = (\bar{f}_{1,i+1,j,k} - \bar{f}_{1,i,j,k}) + (\bar{f}_{2,i,j+1,k} - \bar{f}_{2,i,j,k}) + (\bar{f}_{3,i,j,k+1} - \bar{f}_{3,i,j,k}). \quad (5.48)$$

These relations define the matrix $E_{2,3}$ such that $\bar{g} = E_{2,3}^\top \bar{\mathbf{f}}$.

6 Discrete problem

First we will discretize the curl and divergence conforming weak forms derived in Section 4 in space. Then we will combine the two weak forms in a leapfrog time stepping scheme, the main motivation behind this is to obtain a valid discrete expression for helicity. We will later see that helicity is conserved by the numerical scheme. This scheme, based on these ideas, was initially proposed in [1] for periodic domains. In this section we present the numerical scheme for two and three dimensional problems, for both Dirichlet and periodic boundary conditions, and then present the conservation properties of the scheme. The scheme will first be described for three dimensional problems, this then readily generalizes to two dimensions.

6.1 Spatial discretization

The three dimensional weak form (4.10) is quickly discretized in space using the discrete function spaces.

The spatially discrete problem is given by:

Find $\{\vec{\omega}_1 \in H_h(\text{curl}), \vec{u}_2 \in H_h(\text{div}), p_3 \in L_h^2, \vec{\omega}_2 \in H_h(\text{div}), \vec{u}_1 \in H_h(\text{curl}), p_0 \in H_h^1\}$ such that

$$\left\{ \begin{array}{ll} (\vec{\tau}_1, \vec{\omega}_1) - (\text{curl } \vec{\tau}_1, \vec{u}_2) = -B^{\text{curl}}(\vec{\tau}_1, \vec{u}_2) & \forall \vec{\tau}_1 \in H_h(\text{curl}), \quad (6.1a) \\ (\vec{v}_2, \frac{\partial \vec{u}_2}{\partial t}) + (\vec{v}_2, \vec{\omega}_2 \times \vec{u}_2) \\ + \nu (\vec{v}_2, \text{curl } \vec{\omega}_1) - (\text{div } \vec{v}_2, p_3) = (\vec{v}_2, \vec{f}) - B^{\text{grad}}(\vec{v}_2, p_3) & \forall \vec{v}_2 \in H_h(\text{div}), \quad (6.1b) \\ (q_3, \text{div } \vec{u}_2) = 0 & \forall q_3 \in L_h^2, \quad (6.1c) \\ (\vec{\tau}_2, \vec{\omega}_2) - (\vec{\tau}_2, \text{curl } \vec{u}_1) = 0 & \forall \vec{\tau}_2 \in H_h(\text{div}), \quad (6.1d) \\ (\vec{v}_1, \frac{\partial \vec{u}_1}{\partial t}) + (\vec{v}_1, \vec{\omega}_1 \times \vec{u}_1) \\ + \nu (\text{curl } \vec{v}_1, \vec{\omega}_2) + (\vec{v}_1, \text{grad } p_0) = (\vec{v}_1, \vec{f}) + \nu B^{\text{curl}}(\vec{v}_1, \vec{\omega}_2) & \forall \vec{v}_1 \in H_h(\text{curl}), \quad (6.1e) \\ (\text{grad } q_0, \vec{u}_1) = B^{\text{div}}(q_0, \vec{u}_1) & \forall q_0 \in H_h^1. \quad (6.1f) \end{array} \right.$$

The boundary terms will be discussed in Section 6.3.

6.2 Temporal integration

First let us, given some Δt , introduce two time sequences, one at integer time steps $(\Delta t \cdot 0, \Delta t \cdot 1, \dots) = (t^0, t^1, \dots)$ and one at half integer time steps $(\Delta t \cdot 1/2, \Delta t \cdot (1 + 1/2), \dots) = (t^{1/2}, t^{1+1/2}, \dots)$. We write $f(\cdot, t^k) = f^k$. The time integration is done via a combination of the midpoint rule and the trapezoidal rule.

The numerical scheme now consists of two evolution steps, one obtained from (6.1b), using (6.1a) and (6.1c) as constraints, and one obtained from (6.1e), using (6.1d) and (6.1f) as constraints. The spatially discrete divergence conforming weak form, (6.1a- 6.1c), will be integrated over the half integer steps. The spatially discrete curl conforming weak form, (6.1d- 6.1f), will be integrated over the integer time steps.

The half integer time steps can be computed from the gradient conforming discrete problem:

Given $\{\vec{u}_2^{k-\frac{1}{2}} \in H_h(\text{div}), \vec{\omega}_1^{k+\frac{1}{2}} \in H_h(\text{curl}), \vec{\omega}_2^k \in H_h(\text{div})\}$, find $\{\vec{u}_2^{k+\frac{1}{2}} \in H_h(\text{div}), \vec{\omega}_1^{k+\frac{1}{2}} \in$

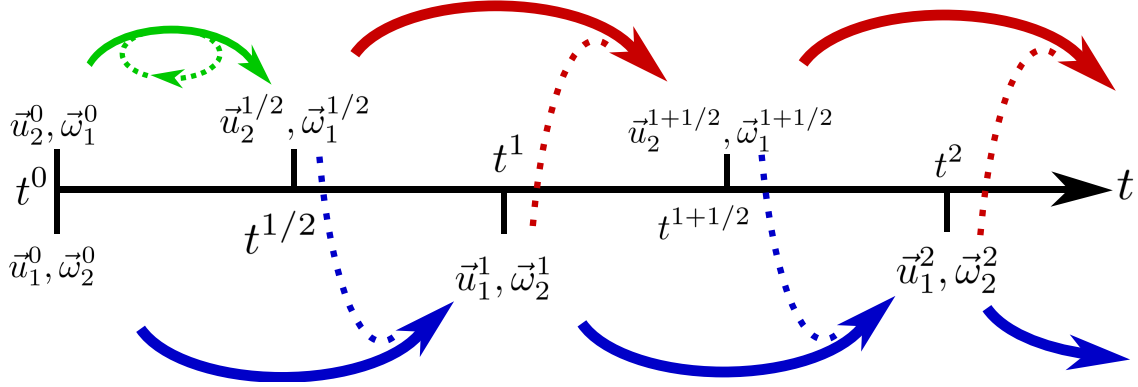


Figure 3: Visualization of the leapfrog time stepping. The handling of the nonlinearity is shown by the dotted lines, either via iterations or via the vorticity field of the other time sequence. The green step is computed using (6.20), the blue steps are computed using (6.19) and the red steps are computed using (6.18).

Given $\{\vec{u}_2^0 \in H_h(\text{div}), \vec{\omega}_1^0 \in H_h(\text{curl})\}$, find $\{\vec{u}_2^{\frac{1}{2}} \in H_h(\text{div}), \vec{\omega}_1^{\frac{1}{2}} \in H_h(\text{curl}), p_3^{\frac{1}{2}} \in L_h^2\}$ such that

$$\left\{ \begin{array}{ll} (\vec{\tau}_1, \vec{\omega}_1^{\frac{1}{2}}) - (\text{curl } \vec{\tau}_1, \vec{u}_2^{\frac{1}{2}}) = -B^{\text{curl}}(\vec{\tau}_1, \vec{u}_2^{\frac{1}{2}}) & \forall \vec{\tau}_1 \in H_h(\text{curl}), \quad (6.4a) \\ (\vec{v}_2, \frac{\vec{u}_2^{\frac{1}{2}} - \vec{u}_2^0}{\Delta t}) + (\vec{v}_2, \vec{\omega}_2^{\frac{1}{2}} \times \frac{\vec{u}_2^{\frac{1}{2}} + \vec{u}_2^0}{2}) \\ + \nu (\vec{v}_2, \text{curl } \frac{\vec{\omega}_1^{\frac{1}{2}} + \vec{\omega}_1^0}{2}) - (\text{div } \vec{v}_2, p_3^{\frac{1}{2}}) = (\vec{v}_2, \vec{f}^{\frac{1}{4}}) - B^{\text{grad}}(\vec{v}_2, p_3^{\frac{1}{2}}) & \forall \vec{v}_2 \in H_h(\text{div}), \quad (6.4b) \\ (q_3, \text{div } \vec{u}_2^{\frac{1}{2}}) = 0 & \forall p_3 \in L_h^2. \quad (6.4c) \end{array} \right.$$

Picard iteration are then used to find a solution to this problem, where the computed vorticity $\vec{\omega}_1^{\frac{1}{2}}$ in each iteration is used as approximation for $\vec{\omega}_2^{\frac{1}{2}}$. It should be noted that the computed vorticity is in a different function space than the vorticity that is being approximated. To resolve this $\vec{\omega}_1^{\frac{1}{2}} \in H_h(\text{curl})$ should be projected to $H_h(\text{div})$. With the fully discrete problem in place, we can write is as a linear system.

6.3 Boundary conditions

The boundary integrals B are, in three dimensions, given by:

$$B^{\text{div}}(f, \vec{g}) = \int_{\partial\Omega} f (\vec{g} \cdot \vec{n}) \, d\partial\Omega, \quad (6.5a)$$

$$B^{\text{curl}}(\vec{f}, \vec{g}) = \int_{\partial\Omega} \vec{f} \times \vec{g} \cdot d\partial\Omega, \quad (6.5b)$$

$$B^{\text{grad}}(\vec{f}, g) = \int_{\partial\Omega} g (\vec{f} \cdot \vec{n}) \, d\partial\Omega, \quad (6.5c)$$

and in two dimensions by:

$$B^{\text{rot}}(f, \vec{g}) = \int_{\partial\Omega} f \begin{bmatrix} \vec{g}_2 \\ -\vec{g}_1 \end{bmatrix} \cdot d\partial\Omega, \quad (6.5d)$$

$$B^{\text{div}}(f, \vec{g}) = \int_{\partial\Omega} f (\vec{g} \cdot n) d\partial\Omega, \quad (6.5e)$$

$$B^{\text{grad}}(\vec{f}, g) = \int_{\partial\Omega} g (\vec{f} \cdot n) d\partial\Omega, \quad (6.5f)$$

$$B^{\text{curl}}(\vec{f}, g) = \int_{\partial\Omega} g \begin{bmatrix} \vec{f}_2 \\ -\vec{f}_1 \end{bmatrix} \cdot d\partial\Omega. \quad (6.5g)$$

The boundary integrals (6.5a), (6.5c), (6.5e), (6.5f) measure flow out of the domain and integrals (6.5b), (6.5d), (6.5g) measure flow along the boundary.

6.3.1 Periodic boundary conditions

In the case of periodic boundary conditions all boundary terms B disappear. All flow out of the domain flows into the domain on the opposite side of the domain. All flow along the boundary, flows along the boundary in the same direction on the opposite side of the domain, however, the opposite side of the boundary is traversed in opposite direction in the integral. It can be concluded that all boundary integrals equal zero in this case.

6.3.2 Dirichlet boundary conditions

By the boundary integrals in the divergence conforming problem, we find that boundary conditions can be specified on

$$(\vec{u}_2 \times n \text{ or } \vec{\tau}_1 \times n) \quad \text{and} \quad (p_3 \text{ or } \vec{v}_2 \cdot n). \quad (6.6)$$

Assuming that boundary conditions on velocity are specified for the continuous problem, this shows us that the inflow into the boundary should be strongly enforced to specify $\vec{v}_2 \cdot n = 0$, and that the velocity tangential to the boundary can be enforced weakly to specify $\vec{u}_2 \cdot t$.

A different motivation could be to call upon differential geometry to note the association between \vec{u}_2 and fluxes through surfaces [19], [20].

The boundary integrals in the curl conforming problem show us that boundary conditions can be specified on

$$(\vec{v}_1 \times n \text{ or } \vec{\omega}_2 \times n) \quad \text{and} \quad (q_0 \text{ or } \vec{u}_1 \cdot n). \quad (6.7)$$

Assuming again that boundary conditions on the velocity are specified, this shows that now the inflow should be weakly enforced and that the tangential velocity should be strongly enforced. However, strongly enforcing the tangential velocity leads to an unstable problem, where the pressure computed by the curl conforming problem shows a checkerboard pattern. Instead we can assume to have boundary conditions specified on the inflow and on the tangential vorticity rather than the tangential velocity. Then, $\vec{\omega}_2 \times n$ can be weakly enforced. We will now first describe the boundary

integrals resulting from the choices above, then, the assumption that boundary conditions on both velocity and tangential vorticity are specified is relaxed.

Let \vec{u}_∂ and $\vec{\omega}_\partial$ denote the boundary conditions, then the boundary integrals can be computed from

$$B^{\text{div}}(q_0, \vec{u}_\partial^{k+1}) = \int_{\partial\Omega} q_0 (\vec{u}_\partial^{k+1} \cdot \vec{n}) \, d\partial\Omega, \quad (6.8a)$$

$$B^{\text{grad}}(\vec{v}_2, p_3^k) = \int_{\partial\Omega} p_3^k (\vec{v}_2 \cdot \vec{n}) \, d\partial\Omega = 0, \quad (6.8b)$$

$$B^{\text{curl}}(\vec{\tau}_1, \vec{u}_\partial^{k+\frac{1}{2}}) = \int_{\partial\Omega} \vec{\tau}_1 \times \vec{u}_\partial^{k+\frac{1}{2}} \cdot d\partial\Omega, \quad (6.8c)$$

$$B^{\text{curl}}(\vec{v}_1, \vec{\omega}_\partial^{k+\frac{1}{2}}) = \int_{\partial\Omega} \vec{v}_1 \times \vec{\omega}_\partial^{k+\frac{1}{2}} \cdot d\partial\Omega. \quad (6.8d)$$

To relieve ourselves of the restrictive assumption that boundary conditions on both velocity and tangential vorticity are specified, we could set $\vec{\omega}_\partial := \text{curl } \vec{u}_\partial$ to obtain vorticity boundary conditions from the velocity boundary conditions. However, for problems where \vec{u}_∂ is not smooth, such as in a lid-driven cavity problem, this approach breaks down.

We choose to resolve this instead by using a solution to the divergence conforming problem as boundary conditions for the curl conforming problem. Using the leapfrog scheme, the vorticity at time $t^{k+1/2}$ is approximated by $\vec{\omega}_1^{k+\frac{1}{2}}$. This field can be used in (6.8d) as an approximation of $\vec{\omega}_\partial$. We will see this approximation yields no degradation in convergence order when compared to periodic boundary conditions.

Using this replacement, the boundary term $B^{\text{curl}}(\vec{v}_1, \vec{\omega}_\partial^{k+\frac{1}{2}})$ in (6.3b) now becomes

$$B^{\text{curl}}(\vec{v}_1, \vec{\omega}_\partial^{k+\frac{1}{2}}) = \int_{\partial\Omega} \vec{v}_1 \times \vec{\omega}_1^{k+\frac{1}{2}} \cdot d\partial\Omega. \quad (6.9)$$

In two dimensions we similarly find:

$$B^{\text{div}}(\tau_0, \vec{u}_\partial^{k+\frac{1}{2}}) = \int_{\partial\Omega} \tau_0 (\vec{u}_\partial^{k+\frac{1}{2}} \cdot \vec{n}) \, d\partial\Omega, \quad (6.10a)$$

$$B^{\text{grad}}(\vec{v}_1, p_2^k) = \int_{\partial\Omega} p_2^k (\vec{v}_1 \cdot \vec{n}) \, d\partial\Omega = 0, \quad (6.10b)$$

$$B^{\text{rot}}(\tau_0, \vec{u}_\partial^{k+\frac{1}{2}}) = \int_{\partial\Omega} \tau_0 \begin{bmatrix} \vec{u}_{\partial,2}^{k+\frac{1}{2}} \\ -\vec{u}_{\partial,1}^{k+\frac{1}{2}} \end{bmatrix} \cdot d\partial\Omega, \quad (6.10c)$$

$$B^{\text{curl}}(\vec{v}_1, \omega_\partial^{k+\frac{1}{2}}) = \int_{\partial\Omega} \omega_1^{k+\frac{1}{2}} \begin{bmatrix} \vec{v}_{1,1} \\ -\vec{v}_{1,2} \end{bmatrix} \cdot d\partial\Omega. \quad (6.10d)$$

In the following sections we will omit the boundary terms

$$B^{\text{grad}}(\vec{v}_1, p_2^k) \quad \text{and} \quad B^{\text{grad}}(\vec{v}_2, p_3^k) \quad (6.11)$$

as they evaluate to zero regardless of boundary conditions.

Remark (Different Dirichlet boundary conditions).

In the above we assumed Dirichlet boundary conditions on velocity to be specified, but different boundary conditions should work as well. Given any admissible boundary condition for the divergence conforming problem, we can obtain boundary conditions for the curl conforming problem using the ‘trick’ described above. To see this note that by (6.6) any admissible boundary conditions for the divergence conforming problem must specify either $\vec{v}_2 \cdot n$ or p_3 . In either case, $\vec{u}_1 \cdot n$ or q_0 is specified by the same boundary condition. For admissible boundary conditions on the curl conforming problem then, only additional specifications on $\vec{\omega}_2 \times n$ are required, which can be obtained as previously described.

6.4 Fully discrete problem as linear systems

To write the fully discrete problems as linear systems, let us introduce some notation. We write M_0, M_1, M_2, M_3 for the mass matrices of $H_h^1, H_h(\text{curl}), H_h(\text{div}), L_h^2$ respectively. We write $N_2(\vec{\omega}_2)$ and $N_1(\vec{\omega}_1)$ for the matrices resulting from $(\vec{v}_2, \vec{\omega}_2 \times \vec{u}_2)$ and $(\vec{v}_1, \vec{\omega}_1 \times \vec{u}_1)$ respectively. The vectors resulting from $B^d(\cdot, \cdot)$ are written as $\mathbf{B}^d(\cdot, \cdot)$ and the vector resulting from (a_k, \vec{f}) is written as $M_k(\vec{f})$. Lastly, given a discrete function f_i at time t^k , f_i^k , we denote the vector containing all its degrees of freedom as \mathbf{f}_i^k . We will first show how to obtain the linear system for a toy problem, this then readily generalizes to the weak forms above. Consider the following two dimensional toy problem, find $\{\vec{u}_2 \in H_h(\text{div}), \vec{\omega}_1 \in H_h(\text{curl})\}$ such that

$$(q_3, \text{div } \vec{u}_2) = 0 \quad \forall q_3 \in H_h^1. \quad (6.12)$$

We can expand the fields in terms of basis functions to find

$$(\tilde{B}_{k,r-1}(x)\tilde{B}_{l,r-1}(y), \sum_{i,j} \tilde{B}_{i,r-1}(x)\tilde{B}_{j,r-1}(y) ((\bar{u}_{1,i+1,j} - \bar{u}_{1,i,j}) + (\bar{u}_{2,i,j+1} - \bar{u}_{2,i,j}))) = 0 \quad \forall k, l. \quad (6.13)$$

Using the definition of the incidence matrices (5.48) this gives

$$(\tilde{B}_{k,r-1}(x)\tilde{B}_{l,r-1}(y), \sum_{i,j} \tilde{B}_{i,r-1}(x)\tilde{B}_{j,r-1}(y) [E_{1,2}^\top \vec{u}_2]_{i,j}) = 0 \quad \forall k, l. \quad (6.14)$$

Now by the linearity of the inner product this gives

$$\sum_{i,j} (\tilde{B}_{k,r-1}(x)\tilde{B}_{l,r-1}(y), \tilde{B}_{i,r-1}(x)\tilde{B}_{j,r-1}(y)) [E_{1,2}^\top \vec{u}_2]_{i,j} = 0 \quad \forall k, l. \quad (6.15)$$

Denoting the mass matrix of L_h^2 as M_2 , i.e. using

$$[M_2]_{(k,l),(i,j)} = (\tilde{B}_{k,r-1}(x)\tilde{B}_{l,r-1}(y), \tilde{B}_{i,r-1}(x)\tilde{B}_{j,r-1}(y)), \quad (6.16)$$

we can write (6.15) compactly as the linear system

$$M_2 E_{1,2}^\top \vec{u}_2 = 0. \quad (6.17)$$

The divergence conforming fully discrete problem can now be written as:

$$\begin{aligned} & \begin{bmatrix} -M_1 & E_{2,1}M_2 & 0 \\ \nu M_1 E_{2,1}^\top \frac{1}{2} & M_2 \frac{1}{\Delta t} + N_2(\bar{\omega}_2^k) \frac{1}{2} & E_{2,3}M_3 \\ 0 & M_3 E_{2,3}^\top & 0 \end{bmatrix} \begin{bmatrix} \bar{\mathbf{w}}_1^{k+\frac{1}{2}} \\ \bar{\mathbf{u}}_2^{k+\frac{1}{2}} \\ \bar{\mathbf{p}}_3^{k+\frac{1}{2}} \end{bmatrix} \\ & = \begin{bmatrix} \mathbf{B}^{\text{curl}}(\bar{\tau}_1, \bar{u}_\partial^{k+\frac{1}{2}}) \\ M_2(\bar{f}^k) + \left(M_2 \frac{1}{\Delta t} - N_2(\bar{\omega}_2^k) \frac{1}{2} \right) \bar{\mathbf{u}}_2^{k-\frac{1}{2}} - \nu M_1 E_{2,1}^\top \frac{1}{2} \bar{\mathbf{w}}_1^{k-\frac{1}{2}} \\ 0 \end{bmatrix}, \end{aligned} \quad (6.18)$$

and similarly the curl conforming time integrated problem can be written as:

$$\begin{aligned} & \begin{bmatrix} -M_2 & M_2 E_{2,1}^\top & 0 \\ \nu E_{2,1} M_2 \frac{1}{2} & M_1 \frac{1}{\Delta t} + N_1(\bar{\omega}_1^{k+\frac{1}{2}}) \frac{1}{2} & -M_1 E_{0,1}^\top \\ 0 & -E_{0,1} M_1 & 0 \end{bmatrix} \begin{bmatrix} \bar{\mathbf{w}}_2^{k+1} \\ \bar{\mathbf{u}}_1^{k+1} \\ \bar{\mathbf{p}}_0^{k+1} \end{bmatrix} \\ & = \begin{bmatrix} 0 \\ M_1(\bar{f}^k) + \nu \mathbf{B}^{\text{curl}}(\bar{v}_1, \bar{\omega}_1^{k+\frac{1}{2}}) + \left(M_1 \frac{1}{\Delta t} - N_1(\bar{\omega}_1^{k+\frac{1}{2}}) \frac{1}{2} \right) \bar{\mathbf{u}}_1^k - \nu M_1 E_{2,1}^\top \frac{1}{2} \bar{\mathbf{w}}_2^k \\ \mathbf{B}^{\text{div}}(q_0, \bar{u}_\partial^{k+1}) \end{bmatrix}. \end{aligned} \quad (6.19)$$

Finally the solution at $t^{\frac{1}{2}}$ can be computed from the following system by Picard iterations

$$\begin{aligned} & \begin{bmatrix} -M_1 & E_{2,1}M_2 & 0 \\ \nu M_1 E_{2,1}^\top \frac{1}{2} & M_2 \frac{1}{\Delta t} + N_2(\bar{\omega}_2^{\frac{1}{2}}) \frac{1}{2} & -E_{2,3}M_3 \\ 0 & -M_3 E_{2,3}^\top & 0 \end{bmatrix} \begin{bmatrix} \bar{\mathbf{w}}_1^{\frac{1}{2}} \\ \bar{\mathbf{u}}_2^{\frac{1}{2}} \\ \bar{\mathbf{p}}_3^{\frac{1}{2}} \end{bmatrix} \\ & = \begin{bmatrix} \mathbf{B}^{\text{curl}}(\bar{\tau}_1, \bar{u}_\partial^{\frac{1}{2}}) \\ M_2(\bar{f}^{\frac{1}{2}}) + \left(M_2 \frac{1}{\Delta t} - N_2(\bar{\omega}_2^{\frac{1}{2}}) \frac{1}{2} \right) \bar{\mathbf{u}}_2^0 - \nu M_1 E_{2,1}^\top \frac{1}{2} \bar{\mathbf{w}}_1^0 \\ 0 \end{bmatrix}. \end{aligned} \quad (6.20)$$

6.5 Two dimensional linear systems

Using notation introduced above, the linear system for the divergence conforming problem is given by

$$\begin{aligned} & \begin{bmatrix} -M_0 & E_{1,0}M_1 & 0 \\ \nu M_0 E_{1,0}^\top \frac{1}{2} & M_1 \frac{1}{\Delta t} + N_2(w_2^k) \frac{1}{2} & -E_{1,2}M_2 \\ 0 & -M_2 E_{1,2}^\top & 0 \end{bmatrix} \begin{bmatrix} \bar{\mathbf{w}}_0^{k+\frac{1}{2}} \\ \bar{\mathbf{u}}_1^{k+\frac{1}{2}} \\ \bar{\mathbf{p}}_2^{k+\frac{1}{2}} \end{bmatrix} \\ & = \begin{bmatrix} \mathbf{B}^{\text{rot}}(\tau_0, \bar{u}_\partial^{k+\frac{1}{2}}) \\ M_1(\bar{f}^k) + \left(M_1 \frac{1}{\Delta t} - N_2(w_2^k) \frac{1}{2} \right) \bar{\mathbf{u}}_1^{k-\frac{1}{2}} - \nu M_0 E_{1,0}^\top \frac{1}{2} \bar{\mathbf{w}}_0^{k-\frac{1}{2}} \\ 0 \end{bmatrix}, \end{aligned} \quad (6.21)$$

and similarly the curl conforming problem is given by

$$\begin{aligned}
& \begin{bmatrix} -M_2 & M_2 E_{2,1}^\top & 0 \\ \nu E_{2,1} M_2 \frac{1}{2} & M_1 \frac{1}{\Delta t} + N_0(w_0^{k+\frac{1}{2}}) \frac{1}{2} & M_1 E_{0,1}^\top \\ 0 & E_{0,1} M_1 & 0 \end{bmatrix} \begin{bmatrix} \bar{\mathbf{w}}_2^{k+1} \\ \bar{\mathbf{u}}_1^{k+1} \\ \bar{\mathbf{p}}_0^{k+1} \end{bmatrix} \\
& = \begin{bmatrix} 0 \\ M_1(\vec{f}^k) + \nu \mathbf{B}^{\text{curl}}(\vec{v}_1, \bar{\omega}_1^{k+\frac{1}{2}}) + \left(M_1 \frac{1}{\Delta t} - N_0(w_0^{k+\frac{1}{2}}) \frac{1}{2} \right) \bar{\mathbf{u}}_1^k - \nu M_1 E_{2,1}^\top \frac{1}{2} \bar{\mathbf{w}}_2^k \\ \mathbf{B}^{\text{div}}(q_0, \bar{u}_\partial^{k+1}) \end{bmatrix}. \tag{6.22}
\end{aligned}$$

Finally the solution at $t^{\frac{1}{2}}$ can be computed from the following system with Picard iterations:

$$\begin{aligned}
& \begin{bmatrix} -M_0 & E_{1,0} M_1 & 0 \\ \nu M_0 E_{1,0}^\top \frac{1}{2} & M_1 \frac{1}{\Delta t} + N_2(w_2^{\frac{1}{2}}) \frac{1}{2} & -E_{1,2} M_2 \\ 0 & -M_2 E_{1,2}^\top & 0 \end{bmatrix} \begin{bmatrix} \bar{\mathbf{w}}_0^{\frac{1}{2}} \\ \bar{\mathbf{u}}_1^{\frac{1}{2}} \\ \bar{\mathbf{p}}_2^{\frac{1}{2}} \end{bmatrix} \\
& = \begin{bmatrix} \mathbf{B}^{\text{curl}}(\tau_0, \bar{u}_\partial^{\frac{1}{2}}) \\ M_1(\vec{f}^{\frac{1}{4}}) + \left(M_1 \frac{1}{\Delta t} - N_2(w_2^{\frac{1}{2}}) \frac{1}{2} \right) \bar{\mathbf{u}}_1^0 - \nu M_0 E_{1,0}^\top \frac{1}{2} \bar{\mathbf{w}}_0^0 \\ 0 \end{bmatrix}. \tag{6.23}
\end{aligned}$$

6.6 Conservation properties of the numerical method

We will show mass conservation, and present derivations for the discrete rate of change of helicity and kinetic energy. Under the same conditions under which the continuous problem conserves these quantities (inviscid limit $\nu \rightarrow 0$, conservative source function $\vec{f} = \text{grad } \phi$, absence of boundary contributions) the discrete problem will also exactly conserve these quantities. Enstrophy is not conserved. For problems where the quantities are not exactly conserved, we identify different behaviors in the cases of periodic and Dirichlet boundary conditions.

We will find in the case of periodic boundary conditions, that the derived expressions approximate the true rate of change without nonphysical contributions. For problems with Dirichlet boundary conditions, we find, for problem with inflow or normal vorticity at the boundary, additional terms contributing to the rates. These additional terms represent the rate of change of energy or helicity at the boundary, but we cannot meaningfully describe them any further. In the absence of boundary conditions these contributions are not present and as such exact energy and helicity conservation can still be attained.

Finally it should be noted that the derived rates are for discrete representations of the physical quantities which resemble their continuous counterparts. While they are integrals of the same physical fields, they must contain approximations. Naturally in the fields themselves, but also in the use of the midpoint rule when combining fields computed at different time instances. The value of these discrete quantities is in their approximation of their continuous counterparts, while showing conservation under similar conditions.

6.6.1 Mass conservation

Mass conservation, i.e. a pointwise divergence free velocity field, is obtained in solutions to the divergence conforming problem (6.18). Consider the following problem:

Given $f_3 \in L_h^2$, find $\vec{u}_2 \in H_h(\text{div})$ such that for all $q_3 \in L_h^2$ it holds that

$$(q_3, \text{div } \vec{u}_2) = (q_3, f_3). \quad (6.24)$$

As a linear problem this becomes

$$M_3 E_{2,3}^\top \vec{u}_2 = M_3 \vec{f}_3, \quad (6.25)$$

which implies

$$E_{2,3}^\top \vec{u}_2 = \vec{f}_3. \quad (6.26)$$

By the construction of the basis functions in the previous section, specifically equation (5.48), this gives

$$\text{div } \vec{u}_2 = f_3. \quad (6.27)$$

This situation is identical to the bottom equation of (6.18) with $f_3 = 0$. We conclude that $u_2^{k+\frac{1}{2}}$ is pointwise divergence free for all k .

Similarly, it can be seen that

$$\text{curl } \vec{u}_1 = \vec{\omega}_2, \quad (6.28)$$

in the curl conforming problem is exactly satisfied.

6.6.2 Kinetic energy conservation

As mentioned in the beginning of Section 6.6, we will take discrete representations of kinetic energy, and show the rate of change of these representations approximate the rate of change of the continuous kinetic energy. Then, we will show that the discrete kinetic energy is conserved under the same conditions for which the continuous kinetic energy is conserved.

For the continuous Navier-Stokes problem, with no inflow boundary condition, we found that

$$\frac{d\mathcal{K}}{dt} = -\nu (\text{curl } \vec{\omega}, \vec{u}) + (\vec{f}, \vec{u}) - \int_{\partial\Omega} p(\vec{u} \cdot \vec{n}) \, d\partial\Omega. \quad (6.29)$$

In the discrete problem we find two representations of kinetic energy,

$$\mathcal{K}_1^k := \frac{1}{2}(\vec{u}_1^k, \vec{u}_1^k) \quad \text{and} \quad \mathcal{K}_2^{k+\frac{1}{2}} := \frac{1}{2}(\vec{u}_2^{k+\frac{1}{2}}, \vec{u}_2^{k+\frac{1}{2}}). \quad (6.30)$$

Their discrete time derivatives are given by

$$\frac{\mathcal{K}_1^{k+1} - \mathcal{K}_1^k}{\Delta t} = \left(\frac{\vec{u}_1^{k+1} + \vec{u}_1^k}{2}, \frac{\vec{u}_1^{k+1} - \vec{u}_1^k}{\Delta t} \right), \quad (6.31)$$

and

$$\frac{\mathcal{K}_2^{k+\frac{1}{2}} - \mathcal{K}_2^{k-\frac{1}{2}}}{\Delta t} = \left(\frac{\vec{u}_2^{k+\frac{1}{2}} + \vec{u}_2^{k-\frac{1}{2}}}{2}, \frac{\vec{u}_2^{k+\frac{1}{2}} - \vec{u}_2^{k-\frac{1}{2}}}{\Delta t} \right). \quad (6.32)$$

Let us first consider \mathcal{K}_2 . The discrete solution satisfies (6.2b) for any $\vec{v}_2 \in H_h(\text{div})$. When considering periodic boundary conditions we note that there are no strongly enforced boundary conditions on \vec{v}_2 and as a result we can set $\vec{v}_2 = \frac{\vec{u}_2^{k+\frac{1}{2}} + \vec{u}_2^{k-\frac{1}{2}}}{2}$. When considering Dirichlet boundary conditions, this approach is invalid, as the normal component of \vec{v}_2 is zero at the boundary, while that of \vec{u}_2 is not in general. In the following derivation of the rate of change of \mathcal{K}_2 we will assume that the normal component of \vec{u}_2 is zero at the boundary as well, as in a problem with no inflow. Note that in a problem where this assumption does not hold, there will be an additional contribution to the rate of change of kinetic energy. This contribution can be quantified by splitting the velocity in a part containing all the degrees of freedom related to the normal component at the boundary, $\vec{u}_{\perp\partial}$, and a remaining part which has no inflow, \vec{u}'_2 , as $\vec{u}_2 = \vec{u}_{\perp\partial} + \vec{u}'_2$. The additional term is then given by

$$\left(\frac{\vec{u}_{\perp\partial}^{k+\frac{1}{2}} + \vec{u}_{\perp\partial}^{k-\frac{1}{2}}}{2}, \frac{\vec{u}_2^{k+\frac{1}{2}} - \vec{u}_2^{k-\frac{1}{2}}}{\Delta t} \right). \quad (6.33)$$

It should be noted that for energy conservation in (6.29) one must ensure that

$$\int_{\partial\Omega} p(\vec{u} \cdot n) d\partial\Omega \quad (6.34)$$

does not break the conservation. In this sense, assuming $\vec{u}|_{\partial\Omega} \cdot n = 0$ to obtain energy conservation in a problem with Dirichlet boundary conditions is a reasonable assumption to avoid boundary contributions. In this case energy conservation can still be attained by the numerical method. We continue the following derivation assuming no inflow at the boundary for problems with Dirichlet boundary conditions. Using (6.2b) with $\vec{v}_2 = \frac{\vec{u}_2^{k+\frac{1}{2}} + \vec{u}_2^{k-\frac{1}{2}}}{2}$ we can now rewrite the time derivative as

$$\begin{aligned} \left(\frac{\vec{u}_2^{k+\frac{1}{2}} + \vec{u}_2^{k-\frac{1}{2}}}{2}, \frac{\vec{u}_2^{k+\frac{1}{2}} - \vec{u}_2^{k-\frac{1}{2}}}{\Delta t} \right) &= - \left(\frac{\vec{u}_2^{k+\frac{1}{2}} + \vec{u}_2^{k-\frac{1}{2}}}{2}, \vec{\omega}_2^k \times \frac{\vec{u}_2^{k+\frac{1}{2}} + \vec{u}_2^{k-\frac{1}{2}}}{2} \right) \\ &\quad - \nu \left(\frac{\vec{u}_2^{k+\frac{1}{2}} + \vec{u}_2^{k-\frac{1}{2}}}{2}, \text{curl} \frac{\vec{\omega}_1^{k+\frac{1}{2}} + \vec{\omega}_1^{k-\frac{1}{2}}}{2} \right) \\ &\quad + \left(\text{div} \frac{\vec{u}_2^{k+\frac{1}{2}} + \vec{u}_2^{k-\frac{1}{2}}}{2}, p_3^k \right) + \left(\frac{\vec{u}_2^{k+\frac{1}{2}} + \vec{u}_2^{k-\frac{1}{2}}}{2}, \vec{f}^k \right). \end{aligned} \quad (6.35a)$$

Note how the nonlinear term is zero by orthogonality. Furthermore, we find by (6.2c) with $q_3 = p_3^k$, that the third term equates to zero as well,

$$\begin{aligned} \left(\frac{\vec{u}_2^{k+\frac{1}{2}} + \vec{u}_2^{k-\frac{1}{2}}}{2}, \frac{\vec{u}_2^{k+\frac{1}{2}} - \vec{u}_2^{k-\frac{1}{2}}}{\Delta t} \right) &= -\nu \left(\frac{\vec{u}_2^{k+\frac{1}{2}} + \vec{u}_2^{k-\frac{1}{2}}}{2}, \text{curl} \frac{\vec{\omega}_1^{k+\frac{1}{2}} + \vec{\omega}_1^{k-\frac{1}{2}}}{2} \right) + \left(\frac{\vec{u}_2^{k+\frac{1}{2}} + \vec{u}_2^{k-\frac{1}{2}}}{2}, \vec{f}^k \right) \\ &=: \mathcal{D}_{\mathcal{K}_2}^k. \end{aligned} \quad (6.35b)$$

This expression is an approximation of the continuous rate of change 6.29 in the case of no inflow. We will now show that in the inviscid limit, $\nu \rightarrow 0$, and with conservative source function, $\vec{f} =$

grad ϕ , this expression reduces to zero in the absence of boundary contributions, giving exact energy conservation. In the inviscid limit (6.35b) becomes

$$\left(\frac{\vec{u}_2^{k+\frac{1}{2}} + \vec{u}_2^{k-\frac{1}{2}}}{2}, \frac{\vec{u}_2^{k+\frac{1}{2}} - \vec{u}_2^{k-\frac{1}{2}}}{\Delta t} \right) = \left(\frac{\vec{u}_2^{k+\frac{1}{2}} + \vec{u}_2^{k-\frac{1}{2}}}{2}, \vec{f}^k \right). \quad (6.36)$$

To continue the analysis for a conservative source function $\vec{f}^k = \text{grad } \phi^k$, consider the following: In order for $\left(\frac{\vec{u}_2^{k+1} + \vec{u}_2^k}{2}, \vec{f}^k \right)$ to be well defined, we require $\vec{f}^k \in H(\text{div})$. Since $\text{grad} : H^1 \rightarrow H(\text{curl})$, we cannot set $\vec{f}^k = \text{grad } \phi^k$ directly. Instead, we use the adjoint operator $\text{grad}^* : L^2 \rightarrow H(\text{div})$. This gives

$$\left(\frac{\vec{u}_2^{k+\frac{1}{2}} + \vec{u}_2^{k-\frac{1}{2}}}{2}, \frac{\vec{u}_2^{k+\frac{1}{2}} - \vec{u}_2^{k-\frac{1}{2}}}{\Delta t} \right) = \left(\frac{\vec{u}_2^{k+\frac{1}{2}} + \vec{u}_2^{k-\frac{1}{2}}}{2}, \text{grad}^* \phi^k \right) \quad (6.37a)$$

$$= -(\text{div } \frac{\vec{u}_2^{k+\frac{1}{2}} + \vec{u}_2^{k-\frac{1}{2}}}{2}, \phi^k) + B^{\text{grad}} \left(\frac{\vec{u}_2^{k+\frac{1}{2}} + \vec{u}_2^{k-\frac{1}{2}}}{2}, \phi^k \right). \quad (6.37b)$$

Now we can use (6.2c) again with $q_3 = \phi^k$ to cancel the first term giving

$$\left(\frac{\vec{u}_2^{k+\frac{1}{2}} + \vec{u}_2^{k-\frac{1}{2}}}{2}, \frac{\vec{u}_2^{k+\frac{1}{2}} - \vec{u}_2^{k-\frac{1}{2}}}{\Delta t} \right) = B^{\text{grad}} \left(\frac{\vec{u}_2^{k+\frac{1}{2}} + \vec{u}_2^{k-\frac{1}{2}}}{2}, \phi^k \right). \quad (6.37c)$$

In the above we substituted $q_3 = \phi^k$, where ϕ^k is not necessarily a discrete field. However, as ϕ^k only occurs in an inner product with $\text{div } \frac{\vec{u}_2^{k+\frac{1}{2}} + \vec{u}_2^{k-\frac{1}{2}}}{2} \in L_h^2$, correctly projecting ϕ^k to this same space does not change the inner product, and we can safely substitute $q_3 = \phi^k$. This same logic will be used repeatedly to show conservation from conservative source functions.

Using again the assumption of no inflow at the boundary, or simply assuming the absence of boundary contributions, gives the final result of energy conservation:

$$\left(\frac{\vec{u}_2^{k+\frac{1}{2}} + \vec{u}_2^{k-\frac{1}{2}}}{2}, \frac{\vec{u}_2^{k+\frac{1}{2}} - \vec{u}_2^{k-\frac{1}{2}}}{\Delta t} \right) = 0. \quad (6.38)$$

For the first half integer time step we can perform a similar derivation. When the initial condition satisfies the constraints of (6.2a) and (6.2c) we find

$$\left(\frac{\vec{u}_2^{\frac{1}{2}} + \vec{u}_2^0}{2}, \frac{\vec{u}_2^{\frac{1}{2}} - \vec{u}_2^0}{\Delta t} \right) = -\nu \left(\frac{\vec{u}_2^{\frac{1}{2}} + \vec{u}_2^0}{2}, \text{curl } \frac{\vec{\omega}_1^{\frac{1}{2}} + \vec{\omega}_1^0}{2} \right) + \left(\frac{\vec{u}_2^{\frac{1}{2}} + \vec{u}_2^0}{2}, \vec{f}_1^{\frac{1}{4}} \right), \quad (6.39)$$

which, in the inviscid limit with no inflow at the boundary and conservative source function, becomes

$$\left(\frac{\vec{u}_2^{\frac{1}{2}} + \vec{u}_2^0}{2}, \frac{\vec{u}_2^{\frac{1}{2}} - \vec{u}_2^0}{\Delta t} \right) = 0. \quad (6.40)$$

Now we follow a similar derivation for \mathcal{K}_1 . The discrete solution satisfies (6.3b) for each $\vec{v}_1 \in$

$H_h(\text{curl})$. Since there are no strongly enforced boundary conditions in the curl conforming problem regardless of boundary conditions considered, we can use $\vec{v}_1 = \frac{\vec{u}_1^{k+1} + \vec{u}_1^k}{2}$ to rewrite the time derivative as

$$\begin{aligned} \left(\frac{\vec{u}_1^{k+1} + \vec{u}_1^k}{2}, \frac{\vec{u}_1^{k+1} - \vec{u}_1^k}{\Delta t} \right) &= - \left(\frac{\vec{u}_1^{k+1} + \vec{u}_1^k}{2}, \vec{\omega}_1^{k+\frac{1}{2}} \times \frac{\vec{u}_1^{k+1} + \vec{u}_1^k}{2} \right) \\ &\quad - \nu \left(\text{curl} \frac{\vec{u}_1^{k+1} + \vec{u}_1^k}{2}, \frac{\vec{\omega}_2^{k+1} + \vec{\omega}_2^k}{2} \right) - \left(\frac{\vec{u}_1^{k+1} + \vec{u}_1^k}{2}, \text{grad } p_0^{k+\frac{1}{2}} \right) \\ &\quad + \left(\frac{\vec{u}_1^{k+1} + \vec{u}_1^k}{2}, \vec{f}^{k+\frac{1}{2}} \right) + \nu B^{\text{curl}} \left(\frac{\vec{u}_1^{k+1} + \vec{u}_1^k}{2}, \vec{\omega}_1^{k+\frac{1}{2}} \right). \end{aligned} \quad (6.41a)$$

The nonlinear term is again zero due to orthogonality. Additionally, (6.3c) can be used with $q_0 = p_0^{k+\frac{1}{2}}$ to rewrite the third term, giving

$$\begin{aligned} \left(\frac{\vec{u}_1^{k+1} + \vec{u}_1^k}{2}, \frac{\vec{u}_1^{k+1} - \vec{u}_1^k}{\Delta t} \right) &= -\nu \left(\text{curl} \frac{\vec{u}_1^{k+1} + \vec{u}_1^k}{2}, \frac{\vec{\omega}_2^{k+1} + \vec{\omega}_2^k}{2} \right) - B^{\text{div}} \left(p_0^{k+\frac{1}{2}}, \frac{\vec{u}_\partial^{k+1} + \vec{u}_\partial^k}{2} \right) \\ &\quad + \left(\frac{\vec{u}_1^{k+1} + \vec{u}_1^k}{2}, \vec{f}^{k+\frac{1}{2}} \right) + \nu B^{\text{curl}} \left(\frac{\vec{u}_1^{k+1} + \vec{u}_1^k}{2}, \vec{\omega}_1^{k+\frac{1}{2}} \right) \\ &=: \mathcal{D}_{\mathcal{K}_1}^{k+\frac{1}{2}}. \end{aligned} \quad (6.41b)$$

This expression is an approximation of the continuous rate of change 6.29. We will now show that in the inviscid limit, $\nu \rightarrow 0$, with conservative source function, $\vec{f} = \text{grad } \phi$, this expression reduces to zero in the absence of boundary conditions, giving exact energy conservation. In the inviscid limit this expression reduces to

$$\left(\frac{\vec{u}_1^{k+1} + \vec{u}_1^k}{2}, \frac{\vec{u}_1^{k+1} - \vec{u}_1^k}{\Delta t} \right) = -B^{\text{div}} \left(p_0^{k+\frac{1}{2}}, \frac{\vec{u}_\partial^{k+1} + \vec{u}_\partial^k}{2} \right) + \left(\frac{\vec{u}_1^{k+1} + \vec{u}_1^k}{2}, \vec{f}^{k+\frac{1}{2}} \right). \quad (6.41c)$$

Considering a conservative source function, we now have $\vec{f}^{k+\frac{1}{2}} \in H(\text{curl})$, and as such we can set $\vec{f}^{k+\frac{1}{2}} = \text{grad } \phi^{k+\frac{1}{2}}$ directly. This results in

$$\left(\frac{\vec{u}_1^{k+1} + \vec{u}_1^k}{2}, \frac{\vec{u}_1^{k+1} - \vec{u}_1^k}{\Delta t} \right) = -B^{\text{div}} \left(p_0^{k+\frac{1}{2}}, \frac{\vec{u}_\partial^{k+1} + \vec{u}_\partial^k}{2} \right) + \left(\frac{\vec{u}_1^{k+1} + \vec{u}_1^k}{2}, \text{grad } \phi^{k+\frac{1}{2}} \right). \quad (6.42)$$

Now, (6.3c) with $q_0 = \phi^{k+\frac{1}{2}}$ can be used to rewrite the second term

$$\left(\frac{\vec{u}_1^{k+1} + \vec{u}_1^k}{2}, \frac{\vec{u}_1^{k+1} - \vec{u}_1^k}{\Delta t} \right) = -B^{\text{div}} \left(p_0^{k+\frac{1}{2}}, \frac{\vec{u}_\partial^{k+1} + \vec{u}_\partial^k}{2} \right) + B^{\text{div}} \left(\phi^{k+\frac{1}{2}}, \frac{\vec{u}_\partial^{k+1} + \vec{u}_\partial^k}{2} \right). \quad (6.43)$$

Finally, when we consider a problem with no inflow at the boundary, or if we simply assume the absence of boundary contributions, this results in energy conservation:

$$\left(\frac{\vec{u}_1^{k+1} + \vec{u}_1^k}{2}, \frac{\vec{u}_1^{k+1} - \vec{u}_1^k}{\Delta t} \right) = 0. \quad (6.44)$$

For the discrete rate of change of \mathcal{K}_1 we found an expression, (6.41b) that approximates the true rate of energy dissipation (6.29) with no nonphysical contributions. For the rate of change of \mathcal{K}_2 we found, in the case of no inflow at the boundary, a similar result in (6.35b). In the case of nonzero inflow at the boundary there is a contribution to the energy dissipation, (6.33), which we at this point cannot meaningfully quantify.

In the case of energy conservation, i.e. in the inviscid limit, $\nu \rightarrow 0$, with no inflow at the boundary, $\vec{v}|_{\partial\Omega} \cdot n = 0$ and with conservative source function $\vec{f} = \text{grad } \phi$, we find that the solutions on both time sequences show exact energy conservation.

6.6.3 Helicity conservation

As mentioned in the beginning of Section 6.6, we will take discrete representations of helicity, and show the rate of change of these representations approximate the rate of change of the continuous helicity. Then, we will show that the discrete helicity is conserved under the same conditions for which the continuous helicity is conserved.

For the continuous Navier-Stokes problem we found (2.9h):

$$\begin{aligned} \frac{d\mathcal{H}}{dt} = & -\nu \left((\text{curl } \vec{\omega}, \vec{\omega}) + (\vec{u}, \text{curl curl } \vec{\omega}) \right) + (\vec{f}, \vec{\omega}) + (\vec{u}, \text{curl } \vec{f}) \\ & + \int_{\partial\Omega} \vec{u} \times (\vec{\omega} \times \vec{u}) \cdot d\partial\Omega - \int_{\partial\Omega} p(\vec{\omega} \cdot n) d\partial\Omega. \end{aligned} \quad (6.45)$$

From this we will first derive an expression that will be more clearly related to the discrete helicity rate of change. To this end we first do integration by parts on $(\vec{u}, \text{curl } \vec{f})$:

$$\begin{aligned} \frac{d\mathcal{H}}{dt} = & -\nu \left((\text{curl } \vec{\omega}, \vec{\omega}) + (\vec{u}, \text{curl curl } \vec{\omega}) \right) + 2(\vec{f}, \vec{\omega}) \\ & + \int_{\partial\Omega} \vec{u} \times (\vec{\omega} \times \vec{u}) \cdot d\partial\Omega - \int_{\partial\Omega} p(\vec{\omega} \cdot n) d\partial\Omega - \int_{\partial\Omega} \vec{u} \times \vec{f} \cdot d\partial\Omega. \end{aligned} \quad (6.46a)$$

Now we can expand \vec{f} using (2.1b) to find

$$\begin{aligned} \frac{d\mathcal{H}}{dt} = & -\nu \left((\text{curl } \vec{\omega}, \vec{\omega}) + (\vec{u}, \text{curl curl } \vec{\omega}) \right) + 2(\vec{f}, \vec{\omega}) \\ & - \int_{\partial\Omega} p(\vec{\omega} \cdot n) d\partial\Omega - \int_{\partial\Omega} \vec{u} \times \left(\frac{\partial \vec{u}}{\partial t} + \nu \text{curl } \vec{\omega} + \text{grad } p \right) \cdot d\partial\Omega. \end{aligned} \quad (6.46b)$$

Finally, consider integration by parts on $-\nu (\vec{u}, \text{curl curl } \vec{\omega})$, this gives

$$\frac{d\mathcal{H}}{dt} = -\nu \left((\text{curl } \vec{\omega}, \vec{\omega}) + (\text{curl } \vec{u}, \text{curl } \vec{\omega}) \right) + 2(\vec{f}, \vec{\omega}) + \int_{\partial\Omega} \nu \vec{u} \times \text{curl } \vec{\omega} \cdot d\partial\Omega \quad (6.46c)$$

$$\begin{aligned} & - \int_{\partial\Omega} p(\vec{\omega} \cdot n) d\partial\Omega - \int_{\partial\Omega} \vec{u} \times \left(\frac{\partial \vec{u}}{\partial t} + \nu \text{curl } \vec{\omega} + \text{grad } p \right) \cdot d\partial\Omega \\ & = -\nu \left((\text{curl } \vec{\omega}, \vec{\omega}) + (\text{curl } \vec{u}, \text{curl } \vec{\omega}) \right) + 2(\vec{f}, \vec{\omega}) \\ & - \int_{\partial\Omega} p(\vec{\omega} \cdot n) d\partial\Omega - \int_{\partial\Omega} \vec{u} \times \left(\frac{\partial \vec{u}}{\partial t} + \text{grad } p \right) \cdot d\partial\Omega. \end{aligned} \quad (6.46d)$$

$$\begin{aligned} & \stackrel{(2.1a)}{=} -2\nu(\text{curl } \vec{\omega}, \vec{\omega}) + 2(\vec{f}, \vec{\omega}) \\ & - \int_{\partial\Omega} p(\vec{\omega} \cdot n) d\partial\Omega - \int_{\partial\Omega} \vec{u} \times \left(\frac{\partial \vec{u}}{\partial t} + \text{grad } p \right) \cdot d\partial\Omega. \end{aligned} \quad (6.46e)$$

This expression can be easily compared and contrasted with its discrete counterpart which will be derived after introducing the discrete counterparts of helicity itself.

In the discrete problem we find four representations of helicities, two on integer time steps,

$$\mathcal{H}_1^k := (\vec{u}_1^k, \frac{\vec{\omega}_1^{k+\frac{1}{2}} + \vec{\omega}_1^{k-\frac{1}{2}}}{2}) \quad \text{and} \quad \mathcal{H}_2^k := (\frac{\vec{u}_2^{k+\frac{1}{2}} + \vec{u}_2^{k-\frac{1}{2}}}{2}, \vec{\omega}_2^k), \quad (6.47)$$

and two on the half integer time steps,

$$\mathcal{H}_1^{k+\frac{1}{2}} := (\frac{\vec{u}_1^{k+1} + \vec{u}_1^k}{2}, \vec{\omega}_1^{k+\frac{1}{2}}) \quad \text{and} \quad \mathcal{H}_2^{k+\frac{1}{2}} := (\vec{u}_2^{k+\frac{1}{2}}, \frac{\vec{\omega}_2^{k+1} + \vec{\omega}_2^k}{2}). \quad (6.48)$$

It can be noted, as in [41], that the computed vorticity field is not necessarily exactly equal to the curl of the velocity field. By (6.28) we know $\vec{\omega}_2 = \text{curl } \vec{u}_1$, but no such relation holds for $\vec{\omega}_1$, and as such representations of helicity utilizing $\vec{\omega}_1$ may be seen as an altered representation of helicity. In the following derivations we will show that the same conservation properties hold for all representations above, and that the difference in dissipation rates between those utilizing $\vec{\omega}_2$ and those utilizing $\vec{\omega}_1$ is minor.

We will first discuss the integer time helicities, and then the half integer helicities.

Half integer time helicities

In line with Section 3.2.3 of [1], we will first derive expressions for

$$\left(\frac{\vec{u}_1^{k+1} - \vec{u}_1^k}{\Delta t}, \vec{\omega}_1^{k+\frac{1}{2}} \right) \quad \text{and} \quad \left(\frac{\vec{\omega}_1^{k+\frac{1}{2}} - \vec{\omega}_1^{k-\frac{1}{2}}}{\Delta t}, \vec{u}_1^k \right), \quad (6.49)$$

and then combine this in such a way as to form an expression for

$$\frac{\mathcal{H}_1^{k+\frac{1}{2}} - \mathcal{H}_1^{k-\frac{1}{2}}}{\Delta t} = \frac{\left((\vec{u}_1^{k+1} + \vec{u}_1^k, \vec{\omega}_1^{k+\frac{1}{2}}) - (\vec{u}_1^k + \vec{u}_1^{k-1}, \vec{\omega}_1^{k-\frac{1}{2}}) \right)}{2\Delta t}. \quad (6.50)$$

Finally $\mathcal{H}_1^{k+\frac{1}{2}}$ is used to derive an expression for $\mathcal{H}_2^{k+\frac{1}{2}}$.

To derive an expression for

$$\left(\frac{\vec{u}_1^{k+1} - \vec{u}_1^k}{\Delta t}, \vec{\omega}_1^{k+\frac{1}{2}}\right) \quad (6.51)$$

we first use (6.3b) with $\vec{v}_1 = \vec{\omega}_1^{k+\frac{1}{2}}$ to expand the time derivative. Recall how there are no strongly enforced boundary conditions in the curl conforming problem, regardless of boundary conditions and as such this is valid. We find

$$\begin{aligned} \left(\frac{\vec{u}_1^{k+1} - \vec{u}_1^k}{\Delta t}, \vec{\omega}_1^{k+\frac{1}{2}}\right) &= -(\vec{\omega}_1^{k+\frac{1}{2}}, \vec{\omega}_1^{k+\frac{1}{2}} \times \frac{\vec{u}_1^{k+1} + \vec{u}_1^k}{2}) - \nu (\text{curl } \vec{\omega}_1^{k+\frac{1}{2}}, \frac{\vec{\omega}_2^{k+1} + \vec{\omega}_2^k}{2}) \\ &\quad - (\vec{\omega}_1^{k+\frac{1}{2}}, \text{grad } p_0^{k+\frac{1}{2}}) + (\vec{\omega}_1^{k+\frac{1}{2}}, \vec{f}^{k+\frac{1}{2}}) + \nu B^{\text{curl}}(\vec{\omega}_1^{k+\frac{1}{2}}, \vec{\omega}_1^{k+\frac{1}{2}}). \end{aligned} \quad (6.52a)$$

By orthogonality the nonlinear term equals zero:

$$\begin{aligned} \left(\frac{\vec{u}_1^{k+1} - \vec{u}_1^k}{\Delta t}, \vec{\omega}_1^{k+\frac{1}{2}}\right) &= -\nu \left((\text{curl } \vec{\omega}_1^{k+\frac{1}{2}}, \frac{\vec{\omega}_2^{k+1} + \vec{\omega}_2^k}{2}) - B^{\text{curl}}(\vec{\omega}_1^{k+\frac{1}{2}}, \vec{\omega}_1^{k+\frac{1}{2}}) \right) \\ &\quad - (\vec{\omega}_1^{k+\frac{1}{2}}, \text{grad } p_0^{k+\frac{1}{2}}) + (\vec{\omega}_1^{k+\frac{1}{2}}, \vec{f}^{k+\frac{1}{2}}). \end{aligned} \quad (6.52b)$$

And by $\vec{a} \times \vec{a} = 0$ the boundary term equals zero:

$$\left(\frac{\vec{u}_1^{k+1} - \vec{u}_1^k}{\Delta t}, \vec{\omega}_1^{k+\frac{1}{2}}\right) = -\nu (\text{curl } \vec{\omega}_1^{k+\frac{1}{2}}, \frac{\vec{\omega}_2^{k+1} + \vec{\omega}_2^k}{2}) - (\vec{\omega}_1^{k+\frac{1}{2}}, \text{grad } p_0^{k+\frac{1}{2}}) + (\vec{\omega}_1^{k+\frac{1}{2}}, \vec{f}^{k+\frac{1}{2}}). \quad (6.52c)$$

Using (6.2a) with $\vec{\tau}_1 = \text{grad } p_0^{k+\frac{1}{2}}$ we can rewrite the second term to find

$$\begin{aligned} \left(\frac{\vec{u}_1^{k+1} - \vec{u}_1^k}{\Delta t}, \vec{\omega}_1^{k+\frac{1}{2}}\right) &= -\nu (\text{curl } \vec{\omega}_1^{k+\frac{1}{2}}, \frac{\vec{\omega}_2^{k+1} + \vec{\omega}_2^k}{2}) + (\vec{u}_2^{k+\frac{1}{2}}, \text{curl grad } p_0^{k+\frac{1}{2}}) \\ &\quad + B^{\text{curl}}(\text{grad } p_0^{k+\frac{1}{2}}, \vec{u}_\partial^{k+\frac{1}{2}}) + (\vec{\omega}_1^{k+\frac{1}{2}}, \vec{f}^{k+\frac{1}{2}}), \end{aligned} \quad (6.52d)$$

from which we can use the identity $\text{curl grad } a = 0$ to obtain

$$\begin{aligned} \left(\frac{\vec{u}_1^{k+1} - \vec{u}_1^k}{\Delta t}, \vec{\omega}_1^{k+\frac{1}{2}}\right) &= -\nu (\text{curl } \vec{\omega}_1^{k+\frac{1}{2}}, \frac{\vec{\omega}_2^{k+1} + \vec{\omega}_2^k}{2}) + B^{\text{curl}}(\text{grad } p_0^{k+\frac{1}{2}}, \vec{u}_\partial^{k+\frac{1}{2}}) \\ &\quad + (\vec{\omega}_1^{k+\frac{1}{2}}, \vec{f}^{k+\frac{1}{2}}). \end{aligned} \quad (6.52e)$$

Now we will find an expression for $\left(\frac{\vec{\omega}_1^{k+\frac{1}{2}} - \vec{\omega}_1^{k-\frac{1}{2}}}{\Delta t}, \vec{u}_1^k\right)$. First the time derivative of vorticity will be rewritten to a time derivative of velocity, which can then be expanded using the evolution equation again. By (6.2a) with $\vec{\tau}_1 = \vec{u}_1^k$ we can rewrite the expression in terms of a time derivative of velocity as

$$\left(\frac{\vec{\omega}_1^{k+\frac{1}{2}} - \vec{\omega}_1^{k-\frac{1}{2}}}{\Delta t}, \vec{u}_1^k\right) = \left(\frac{\vec{u}_2^{k+\frac{1}{2}} - \vec{u}_2^{k-\frac{1}{2}}}{\Delta t}, \text{curl } \vec{u}_1^k\right) + B^{\text{curl}}(\vec{u}_1^k, \frac{\vec{u}_\partial^{k+\frac{1}{2}} - \vec{u}_\partial^{k-\frac{1}{2}}}{\Delta t}). \quad (6.53)$$

Now wish to use (6.2b) with $\vec{v}_2 = \text{curl } \vec{u}_1^k$. However, strongly enforces boundary conditions again raise problems here. In the case of Dirichlet boundary conditions, the normal component of \vec{v}_2 at the boundary is zero. As such, this step is only valid when $\text{curl } \vec{u}_1^k \cdot n \stackrel{(6.28)}{=} \vec{\omega}_2^k \cdot n = 0$ as well, otherwise there will be an additional term contributing to the helicity dissipation. This term can again be found by splitting the $\vec{\omega}_2^k$ in a part with degrees of freedom related to the normal component at the boundary $\vec{\omega}_{\perp\partial}^k$, and a remaining part which would satisfy $\vec{\omega}_2^{k'}|_{\partial\Omega} \cdot n = 0$ as $\vec{\omega}_2^k = \vec{\omega}_{\perp\partial}^k + \vec{\omega}_2^{k'}$. The additional term is then given by

$$\left(\frac{\vec{u}_2^{k+\frac{1}{2}} - \vec{u}_2^{k-\frac{1}{2}}}{\Delta t}, \vec{\omega}_{\perp\partial}^k\right). \quad (6.54)$$

This term resembles the change of helicity introduced at the boundary. It should be noted that, in order for (6.46e) to yield helicity conservation, one must ensure that

$$\int_{\partial\Omega} p(\vec{\omega} \cdot n) d\partial\Omega \quad (6.55)$$

does not break the conservation. In this sense, assuming $\vec{\omega} \cdot n = 0$ to obtain helicity conservation in a problem with Dirichlet boundary conditions is a reasonable assumption to avoid boundary contributions. In this case helicity conservation can still be attained by the numerical method. With this in mind, using (6.2b) with $\vec{v}_2 = \text{curl } \vec{u}_1^k$ to expand the time derivative gives

$$\begin{aligned} \left(\frac{\vec{\omega}_1^{k+\frac{1}{2}} - \vec{\omega}_1^{k-\frac{1}{2}}}{\Delta t}, \vec{u}_1^k\right) &= -(\text{curl } \vec{u}_1^k, \vec{\omega}_2^k \times \frac{\vec{u}_2^{k+\frac{1}{2}} + \vec{u}_2^{k-\frac{1}{2}}}{2}) - \nu (\text{curl } \vec{u}_1^k, \text{curl } \frac{\vec{\omega}_1^{k+\frac{1}{2}} + \vec{\omega}_1^{k-\frac{1}{2}}}{2}) \\ &\quad + (\text{div curl } \vec{u}_1^k, p_3^k) + (\text{curl } \vec{u}_1^k, \vec{f}^k) \\ &\quad - B^{\text{curl}}(\vec{u}_1^k, \frac{\vec{u}_\partial^{k+\frac{1}{2}} - \vec{u}_\partial^{k-\frac{1}{2}}}{\Delta t}). \end{aligned} \quad (6.56a)$$

The third term equates to zero by $\text{div curl } \vec{a} = 0$, and by (6.28) we can use $\text{curl } \vec{u}_1^k = \vec{\omega}_2^k$ to write the above as

$$\begin{aligned} \left(\frac{\vec{\omega}_1^{k+\frac{1}{2}} - \vec{\omega}_1^{k-\frac{1}{2}}}{\Delta t}, \vec{u}_1^k\right) &= -(\vec{\omega}_2^k, \vec{\omega}_2^k \times \frac{\vec{u}_2^{k+\frac{1}{2}} + \vec{u}_2^{k-\frac{1}{2}}}{2}) - \nu (\vec{\omega}_2^k, \text{curl } \frac{\vec{\omega}_1^{k+\frac{1}{2}} + \vec{\omega}_1^{k-\frac{1}{2}}}{2}) \\ &\quad + (\vec{\omega}_2^k, \vec{f}^k) - B^{\text{curl}}(\vec{u}_1^k, \frac{\vec{u}_\partial^{k+\frac{1}{2}} - \vec{u}_\partial^{k-\frac{1}{2}}}{\Delta t}). \end{aligned} \quad (6.56b)$$

Now we can observe orthogonality in the nonlinear term to get the result

$$\begin{aligned} \left(\frac{\vec{\omega}_1^{k+\frac{1}{2}} - \vec{\omega}_1^{k-\frac{1}{2}}}{\Delta t}, \vec{u}_1^k\right) &= -\nu (\vec{\omega}_2^k, \text{curl } \frac{\vec{\omega}_1^{k+\frac{1}{2}} + \vec{\omega}_1^{k-\frac{1}{2}}}{2}) + (\vec{\omega}_2^k, \vec{f}^k) \\ &\quad - B^{\text{curl}}(\vec{u}_1^k, \frac{\vec{u}_\partial^{k+\frac{1}{2}} - \vec{u}_\partial^{k-\frac{1}{2}}}{\Delta t}). \end{aligned} \quad (6.56c)$$

So far we have found:

$$\begin{aligned} \left(\frac{\vec{u}_1^{k+1} - \vec{u}_1^k}{\Delta t}, \vec{\omega}_1^{k+\frac{1}{2}} \right) &= -\nu(\text{curl } \vec{\omega}_1^{k+\frac{1}{2}}, \frac{\vec{\omega}_2^{k+1} + \vec{\omega}_2^k}{2}) + B^{\text{curl}}(\text{grad } p_0^{k+\frac{1}{2}}, \vec{u}_\partial^{k+\frac{1}{2}}) \\ &\quad + (\vec{\omega}_1^{k+\frac{1}{2}}, \vec{f}^{k+\frac{1}{2}}), \end{aligned} \quad (6.57)$$

and

$$\left(\frac{\vec{\omega}_1^{k+\frac{1}{2}} - \vec{\omega}_1^{k-\frac{1}{2}}}{\Delta t}, \vec{u}_1^k \right) = -\nu(\vec{\omega}_2^k, \text{curl } \frac{\vec{\omega}_1^{k+\frac{1}{2}} + \vec{\omega}_1^{k-\frac{1}{2}}}{2}) + (\vec{\omega}_2^k, \vec{f}^k) - B^{\text{curl}}(\vec{u}_1^k, \frac{\vec{u}_\partial^{k+\frac{1}{2}} - \vec{u}_\partial^{k-\frac{1}{2}}}{\Delta t}). \quad (6.58)$$

Summing (6.57) and (6.58) now gives

$$\begin{aligned} \frac{1}{\Delta t} \left((\vec{u}_1^{k+1}, \vec{\omega}_1^{k+\frac{1}{2}}) - (\vec{u}_1^k, \vec{\omega}_1^{k-\frac{1}{2}}) \right) &= -\nu(\text{curl } \vec{\omega}_1^{k+\frac{1}{2}}, \frac{\vec{\omega}_2^{k+1} + \vec{\omega}_2^k}{2}) \\ &\quad + B^{\text{curl}}(\text{grad } p_0^{k+\frac{1}{2}}, \vec{u}_\partial^{k+\frac{1}{2}}) + (\vec{\omega}_1^{k+\frac{1}{2}}, \vec{f}^{k+\frac{1}{2}}) \\ &\quad - \nu(\vec{\omega}_2^k, \text{curl } \frac{\vec{\omega}_1^{k+\frac{1}{2}} + \vec{\omega}_1^{k-\frac{1}{2}}}{2}) + (\vec{\omega}_2^k, \vec{f}^k) \\ &\quad - B^{\text{curl}}(\vec{u}_1^k, \frac{\vec{u}_\partial^{k+\frac{1}{2}} - \vec{u}_\partial^{k-\frac{1}{2}}}{\Delta t}). \end{aligned} \quad (6.59)$$

Assuming sufficient time steps, we can lower the time step by one in (6.57) to get:

$$\begin{aligned} \left(\frac{\vec{u}_1^k - \vec{u}_1^{k-1}}{\Delta t}, \vec{\omega}_1^{k-\frac{1}{2}} \right) &= -\nu(\text{curl } \vec{\omega}_1^{k-\frac{1}{2}}, \frac{\vec{\omega}_2^k + \vec{\omega}_2^{k-1}}{2}) \\ &\quad + B^{\text{curl}}(\text{grad } p_0^{k-\frac{1}{2}}, \vec{u}_\partial^{k-\frac{1}{2}}) + (\vec{\omega}_1^{k-\frac{1}{2}}, \vec{f}^{k-\frac{1}{2}}). \end{aligned} \quad (6.60)$$

Now summing (6.60) and (6.58) gives:

$$\begin{aligned} \frac{1}{\Delta t} \left((\vec{u}_1^k, \vec{\omega}_1^{k+\frac{1}{2}}) - (\vec{u}_1^{k-1}, \vec{\omega}_1^{k-\frac{1}{2}}) \right) &= -\nu(\text{curl } \vec{\omega}_1^{k-\frac{1}{2}}, \frac{\vec{\omega}_2^k + \vec{\omega}_2^{k-1}}{2}) \\ &\quad + B^{\text{curl}}(\text{grad } p_0^{k-\frac{1}{2}}, \vec{u}_\partial^{k-\frac{1}{2}}) + (\vec{\omega}_1^{k-\frac{1}{2}}, \vec{f}^{k-\frac{1}{2}}) \\ &\quad - \nu(\vec{\omega}_2^k, \text{curl } \frac{\vec{\omega}_1^{k+\frac{1}{2}} + \vec{\omega}_1^{k-\frac{1}{2}}}{2}) + (\vec{\omega}_2^k, \vec{f}^k) \\ &\quad - B^{\text{curl}}(\vec{u}_1^k, \frac{\vec{u}_\partial^{k+\frac{1}{2}} - \vec{u}_\partial^{k-\frac{1}{2}}}{\Delta t}). \end{aligned} \quad (6.61)$$

Summing (6.59) and (6.61) now gives on the left hand side:

$$\frac{1}{\Delta t} \left((\vec{u}_1^{k+1} + \vec{u}_1^k, \vec{\omega}_1^{k+\frac{1}{2}}) - (\vec{u}_1^k + \vec{u}_1^{k-1}, \vec{\omega}_1^{k-\frac{1}{2}}) \right) = \frac{2}{\Delta t} \left(\mathcal{H}_1^{k+\frac{1}{2}} - \mathcal{H}_1^{k-\frac{1}{2}} \right), \quad (6.62)$$

and on the right hand side it gives:

$$\begin{aligned}
\frac{2}{\Delta t} \left(\mathcal{H}_1^{k+\frac{1}{2}} - \mathcal{H}_1^{k-\frac{1}{2}} \right) &= 2 \left[-\nu \left(\vec{\omega}_2^k, \operatorname{curl} \frac{\vec{\omega}_1^{k+\frac{1}{2}} + \vec{\omega}_1^{k-\frac{1}{2}}}{2} \right) \right. \\
&\quad \left. + \left(\vec{\omega}_2^k, \vec{f}^k \right) - B^{\operatorname{curl}} \left(\vec{u}_1^k, \frac{\vec{u}_\partial^{k+\frac{1}{2}} - \vec{u}_\partial^{k-\frac{1}{2}}}{\Delta t} \right) \right] \\
&\quad - \nu \left(\operatorname{curl} \vec{\omega}_1^{k-\frac{1}{2}}, \frac{\vec{\omega}_2^k + \vec{\omega}_2^{k-1}}{2} \right) \\
&\quad + B^{\operatorname{curl}} \left(\operatorname{grad} p_0^{k-\frac{1}{2}}, \vec{u}_\partial^{k-\frac{1}{2}} \right) + \left(\vec{\omega}_1^{k-\frac{1}{2}}, \vec{f}^{k-\frac{1}{2}} \right) \\
&\quad - \nu \left(\operatorname{curl} \vec{\omega}_1^{k+\frac{1}{2}}, \frac{\vec{\omega}_2^{k+1} + \vec{\omega}_2^k}{2} \right) \\
&\quad + B^{\operatorname{curl}} \left(\operatorname{grad} p_0^{k+\frac{1}{2}}, \vec{u}_\partial^{k+\frac{1}{2}} \right) + \left(\vec{\omega}_1^{k+\frac{1}{2}}, \vec{f}^{k+\frac{1}{2}} \right).
\end{aligned} \tag{6.63}$$

Collecting terms this becomes:

$$\begin{aligned}
\frac{1}{\Delta t} \left(\mathcal{H}_1^{k+\frac{1}{2}} - \mathcal{H}_1^{k-\frac{1}{2}} \right) &= -\nu \left[\left(\vec{\omega}_2^k, \operatorname{curl} \frac{\vec{\omega}_1^{k+\frac{1}{2}} + \vec{\omega}_1^{k-\frac{1}{2}}}{2} \right) \right. \\
&\quad \left. + \frac{1}{2} \left(\operatorname{curl} \vec{\omega}_1^{k-\frac{1}{2}}, \frac{\vec{\omega}_2^k + \vec{\omega}_2^{k-1}}{2} \right) + \frac{1}{2} \left(\operatorname{curl} \vec{\omega}_1^{k+\frac{1}{2}}, \frac{\vec{\omega}_2^{k+1} + \vec{\omega}_2^k}{2} \right) \right] \\
&\quad + \left(\vec{\omega}_2^k, \vec{f}^k \right) + \frac{1}{2} \left(\vec{\omega}_1^{k-\frac{1}{2}}, \vec{f}^{k-\frac{1}{2}} \right) + \frac{1}{2} \left(\vec{\omega}_1^{k+\frac{1}{2}}, \vec{f}^{k+\frac{1}{2}} \right) \\
&\quad - B^{\operatorname{curl}} \left(\vec{u}_1^k, \frac{\vec{u}_\partial^{k+\frac{1}{2}} - \vec{u}_\partial^{k-\frac{1}{2}}}{\Delta t} \right) \\
&\quad + \frac{1}{2} B^{\operatorname{curl}} \left(\operatorname{grad} p_0^{k-\frac{1}{2}}, \vec{u}_\partial^{k-\frac{1}{2}} \right) + \frac{1}{2} B^{\operatorname{curl}} \left(\operatorname{grad} p_0^{k+\frac{1}{2}}, \vec{u}_\partial^{k+\frac{1}{2}} \right) \\
&=: \mathcal{D}_{\mathcal{H}_1}^k.
\end{aligned} \tag{6.64}$$

In the case of periodic boundary conditions, or in the case where there the normal component of vorticity is zero at the boundary, this expression approximates the true helicity rate of change (6.46e) without nonphysical contributions. Otherwise, there will be an additional term, (6.54), contributing to the rate of change as noted earlier.

To show helicity conservation, consider $\nu \rightarrow 0$, the expression now reduces to

$$\begin{aligned}
\frac{1}{\Delta t} \left(\mathcal{H}_1^{k+\frac{1}{2}} - \mathcal{H}_1^{k-\frac{1}{2}} \right) &= \left(\vec{\omega}_2^k, \vec{f}^k \right) + \frac{1}{2} \left(\vec{\omega}_1^{k-\frac{1}{2}}, \vec{f}^{k-\frac{1}{2}} \right) + \frac{1}{2} \left(\vec{\omega}_1^{k+\frac{1}{2}}, \vec{f}^{k+\frac{1}{2}} \right) \\
&\quad - B^{\operatorname{curl}} \left(\vec{u}_1^k, \frac{\vec{u}_\partial^{k+\frac{1}{2}} - \vec{u}_\partial^{k-\frac{1}{2}}}{\Delta t} \right) \\
&\quad + \frac{1}{2} B^{\operatorname{curl}} \left(\operatorname{grad} p_0^{k-\frac{1}{2}}, \vec{u}_\partial^{k-\frac{1}{2}} \right) + \frac{1}{2} B^{\operatorname{curl}} \left(\operatorname{grad} p_0^{k+\frac{1}{2}}, \vec{u}_\partial^{k+\frac{1}{2}} \right).
\end{aligned} \tag{6.65a}$$

Similarly to the continuous case, we must assume the absence of boundary contributions in order to obtain helicity conservation. With this assumption we find

$$\frac{1}{\Delta t} \left(\mathcal{H}_1^{k+\frac{1}{2}} - \mathcal{H}_1^{k-\frac{1}{2}} \right) = (\vec{\omega}_2^k, \vec{f}^k) + \frac{1}{2}(\vec{\omega}_1^{k-\frac{1}{2}}, \vec{f}^{k-\frac{1}{2}}) + \frac{1}{2}(\vec{\omega}_1^{k+\frac{1}{2}}, \vec{f}^{k+\frac{1}{2}}). \quad (6.65b)$$

Finally, consider a conservative source function. In $(\vec{\omega}_2^k, \vec{f}^k)$ we identify $\vec{f} \in H(\text{div})$, and so we set $\vec{f} = \text{grad}^* \phi$, this gives

$$\frac{1}{\Delta t} \left(\mathcal{H}_1^{k+\frac{1}{2}} - \mathcal{H}_1^{k-\frac{1}{2}} \right) = (\vec{\omega}_2^k, \text{grad}^* \phi^k) + \frac{1}{2}(\vec{\omega}_1^{k-\frac{1}{2}}, \vec{f}^{k-\frac{1}{2}}) + \frac{1}{2}(\vec{\omega}_1^{k+\frac{1}{2}}, \vec{f}^{k+\frac{1}{2}}) \quad (6.65c)$$

$$= -(\text{div } \vec{\omega}_2^k, \phi^k) + \frac{1}{2}(\vec{\omega}_1^{k-\frac{1}{2}}, \vec{f}^{k-\frac{1}{2}}) + \frac{1}{2}(\vec{\omega}_1^{k+\frac{1}{2}}, \vec{f}^{k+\frac{1}{2}}) + B^{\text{grad}}(\vec{\omega}_2^k, \phi^k). \quad (6.65d)$$

The first term equates zero by (6.28) and $\text{div } \text{curl } \vec{a} = 0$, and the boundary term equates to zero by assumption. This results in

$$\frac{1}{\Delta t} \left(\mathcal{H}_1^{k+\frac{1}{2}} - \mathcal{H}_1^{k-\frac{1}{2}} \right) = \frac{1}{2}(\vec{\omega}_1^{k-\frac{1}{2}}, \vec{f}^{k-\frac{1}{2}}) + \frac{1}{2}(\vec{\omega}_1^{k+\frac{1}{2}}, \vec{f}^{k+\frac{1}{2}}) \quad (6.65e)$$

Now In $(\vec{\omega}_1^{k-\frac{1}{2}}, \vec{f}^{k-\frac{1}{2}})$ we identify $\vec{f} \in H(\text{curl})$, and so we can set $\vec{f} = \text{grad } \phi$,

$$\frac{1}{\Delta t} \left(\mathcal{H}_1^{k+\frac{1}{2}} - \mathcal{H}_1^{k-\frac{1}{2}} \right) = \frac{1}{2}(\vec{\omega}_1^{k-\frac{1}{2}}, \text{grad } \phi^{k-\frac{1}{2}}) + \frac{1}{2}(\vec{\omega}_1^{k+\frac{1}{2}}, \text{grad } \phi^{k+\frac{1}{2}}). \quad (6.65f)$$

By (6.2a) with $\vec{\tau}_1 = \text{grad } \phi$ with $\text{curl } \text{grad } a = 0$ we find

$$\frac{1}{\Delta t} \left(\mathcal{H}_1^{k+\frac{1}{2}} - \mathcal{H}_1^{k-\frac{1}{2}} \right) = \frac{1}{2}B^{\text{curl}}(\text{grad } \phi^{k-\frac{1}{2}}, \vec{u}_\partial^{k-\frac{1}{2}}) + \frac{1}{2}B^{\text{curl}}(\text{grad } \phi^{k+\frac{1}{2}}, \vec{u}_\partial^{k+\frac{1}{2}}). \quad (6.65g)$$

Again, by the assumption of the absence of boundary contributions, we now arrive at helicity conservation

$$\frac{1}{\Delta t} \left(\mathcal{H}_1^{k+\frac{1}{2}} - \mathcal{H}_1^{k-\frac{1}{2}} \right) = 0. \quad (6.65h)$$

To derive an expression for

$$\mathcal{H}_2^{k+\frac{1}{2}} = (\vec{u}_2^{k+\frac{1}{2}}, \frac{\vec{\omega}_2^{k+1} + \vec{\omega}_2^k}{2}) \quad (6.66)$$

from

$$\mathcal{H}_1^{k+\frac{1}{2}} = \left(\frac{\vec{u}_1^{k+1} + \vec{u}_1^k}{2}, \vec{\omega}_1^{k+\frac{1}{2}} \right), \quad (6.67)$$

consider (6.2a) with $\vec{\tau}_1 = \frac{\vec{u}_1^{k+1} + \vec{u}_1^k}{2}$ followed by (6.3a) with $\vec{\tau}_2 = \vec{u}_2^{k+\frac{1}{2}}$. Together they give:

$$\mathcal{H}_1^{k+\frac{1}{2}} = \left(\frac{\vec{u}_1^{k+1} + \vec{u}_1^k}{2}, \vec{\omega}_1^{k+\frac{1}{2}} \right) \quad (6.68a)$$

$$= \left(\text{curl} \frac{\vec{u}_1^{k+1} + \vec{u}_1^k}{2}, \vec{u}_2^{k+\frac{1}{2}} \right) - B^{\text{curl} \left(\frac{\vec{u}_1^{k+1} + \vec{u}_1^k}{2}, \vec{u}_\partial^{k+\frac{1}{2}} \right)} \quad (6.68b)$$

$$= \left(\frac{\vec{\omega}_2^{k+1} + \vec{\omega}_2^k}{2}, \vec{u}_2^{k+\frac{1}{2}} \right) - B^{\text{curl} \left(\frac{\vec{u}_1^{k+1} + \vec{u}_1^k}{2}, \vec{u}_\partial^{k+\frac{1}{2}} \right)} \quad (6.68c)$$

$$= \mathcal{H}_2^{k+\frac{1}{2}} - B^{\text{curl} \left(\frac{\vec{u}_1^{k+1} + \vec{u}_1^k}{2}, \vec{u}_\partial^{k+\frac{1}{2}} \right)}. \quad (6.68d)$$

And so

$$\frac{1}{\Delta t} \left(\mathcal{H}_2^{k+\frac{1}{2}} - \mathcal{K}_2^{k-\frac{1}{2}} \right) = \frac{1}{\Delta t} \left(\mathcal{H}_1^{k+\frac{1}{2}} + B^{\text{curl} \left(\frac{\vec{u}_1^{k+1} + \vec{u}_1^k}{2}, \vec{u}_\partial^{k+\frac{1}{2}} \right)} \right. \quad (6.69a)$$

$$\left. - \mathcal{K}_2^{k-\frac{1}{2}} - B^{\text{curl} \left(\frac{\vec{u}_1^k + \vec{u}_1^{k-1}}{2}, \vec{u}_\partial^{k-\frac{1}{2}} \right)} \right) \\ = \frac{1}{\Delta t} \left(\mathcal{H}_1^{k+\frac{1}{2}} - \mathcal{K}_2^{1-\frac{1}{2}} \right) \\ + \frac{1}{\Delta t} \left(B^{\text{curl} \left(\frac{\vec{u}_1^{k+1} + \vec{u}_1^k}{2}, \vec{u}_\partial^{k+\frac{1}{2}} \right)} - B^{\text{curl} \left(\frac{\vec{u}_1^k + \vec{u}_1^{k-1}}{2}, \vec{u}_\partial^{k-\frac{1}{2}} \right)} \right) \quad (6.69b) \\ =: \mathcal{D}_{\mathcal{H}_2}^k.$$

In general $\mathcal{H}_2^{k+\frac{1}{2}} = \mathcal{H}_1^{k+\frac{1}{2}}$ holds approximately. This is a result of both $\frac{\vec{u}_1^{k+1} + \vec{u}_1^k}{2}$ and $\vec{u}_2^{k+\frac{1}{2}}$ approximating the same velocity field at $t^{k+\frac{1}{2}}$. On periodic domains the relation is exact.

Integer time helicities

A similar approach taken for the half integer time steps also works for the integer time helicities. (6.57) and (6.58) give expressions for

$$\left(\frac{\vec{u}_1^{k+1} - \vec{u}_1^k}{\Delta t}, \vec{\omega}_1^{k+\frac{1}{2}} \right), \quad \text{and} \quad \left(\vec{u}_1^k, \frac{\vec{\omega}_1^{k+\frac{1}{2}} - \vec{\omega}_1^{k-\frac{1}{2}}}{\Delta t} \right). \quad (6.70)$$

Using the second term twice, once as is, and once for the next time step, these terms can be combined to form an expression for

$$\frac{\mathcal{H}_1^{k+1} - \mathcal{H}_1^k}{\Delta t} = \frac{\left((\vec{u}_1^{k+1}, \vec{\omega}_1^{k+\frac{1}{2}} + \vec{\omega}_1^{k+\frac{1}{2}}) - (\vec{u}_1^k, \vec{\omega}_1^{k+\frac{1}{2}} + \vec{\omega}_1^{k-\frac{1}{2}}) \right)}{2\Delta t}, \quad (6.71)$$

as desired. Then, to show $\mathcal{H}_1^k = \mathcal{H}_2^k$, (6.3a) and (6.2a) can be used again.

6.6.4 Enstrophy conservation

The numerical method does not conserve enstrophy, neither in 3D nor 2D. Deriving an expression for enstrophy using the two dimensional discrete weak form will result in a nonlinear term that does not cancel like the nonlinear terms that occur in the derivations above. In [8] a nonlinear term that incorporates the derivation in (2.24) is used to construct a enstrophy conserving scheme. The nonlinear term presented in [35] shows promising results as well.

7 Numerical results

We show temporal and spatial convergence results using manufactured solutions. We find optimal spatial convergence rates and second order temporal convergence as expected. We will also demonstrate the conservation properties and dissipation rates on both manufactured and non-manufactured solutions. For each case we show results using both Dirichlet and periodic boundary conditions.

7.1 Details on implementation

The code for running the problems below is open source Julia code [42], which makes use of the BSplineKit.jl library [43] to generate the nodal functions. The systems in Sections 6.4 and 6.5 can be implemented quite directly. However, one should take note of the following.

First, pressure is only determined up to addition by a constant. To resolve this we fix the first degree of freedom of pressure to be 0. When comparing computed solution with manufactured solutions, it should be taken into account that they may differ by a constant.

As a result of the ideas presented in Section 5.3.2, we must make sure that the input source function of the two dimensional curl conforming problem also specifies the normal component of the vector field. This means that the rotation to be applied to the computed velocity field has to be applied in reverse to the source function.

We generate nodal functions from equidistant knot vectors, with h denoting the distance between subsequent knots. The spatial discretization is then fully specified by h and the B-spline order of the nodal functions, denoted by r . The edge functions are then one order lower. The optimal spatial convergence order for a field is limited by its lowest order basis function. For nodal functions of B-spline order r , this means that fields in H_h^1 have optimal convergence order r , and fields in any other discrete space have optimal convergence order $r - 1$.

As a result of the tensor product structure of the basis functions, the mass and incidence matrices can be efficiently implemented using Kronecker products. Additionally, the incidence matrices can be efficiently stored as integer matrices since their entries are limited to -1, 0, and 1.

7.2 Convergence results

To obtain convergence results, manufactured solutions are used. Spatial and temporal convergence orders are presented, for two and three dimensional problems with periodic and Dirichlet boundary conditions. In all cases optimal convergence orders are observed.

7.2.1 Two dimensional problems

Consider a Taylor-Green Vortex (TGV) problem on $\Omega = [0, 2]^2$ with solution given by

$$\vec{u}_{ex}(x, y, t) = \begin{bmatrix} -\sin(\pi x) \cos(\pi y) \exp(-2\pi^2 \nu t) \\ \cos(\pi x) \sin(\pi y) \exp(-2\pi^2 \nu t) \end{bmatrix} \quad (7.1)$$

$$\omega_{ex}(x, y, t) = -2\pi \sin(\pi x) \sin(\pi y) \exp(-2\pi^2 \nu t) \quad (7.2)$$

$$p_{ex}(x, y, t) = -\frac{1}{4} (\cos(2\pi x) + \cos(2\pi y)) \exp(-2\pi^2 \nu t). \quad (7.3)$$

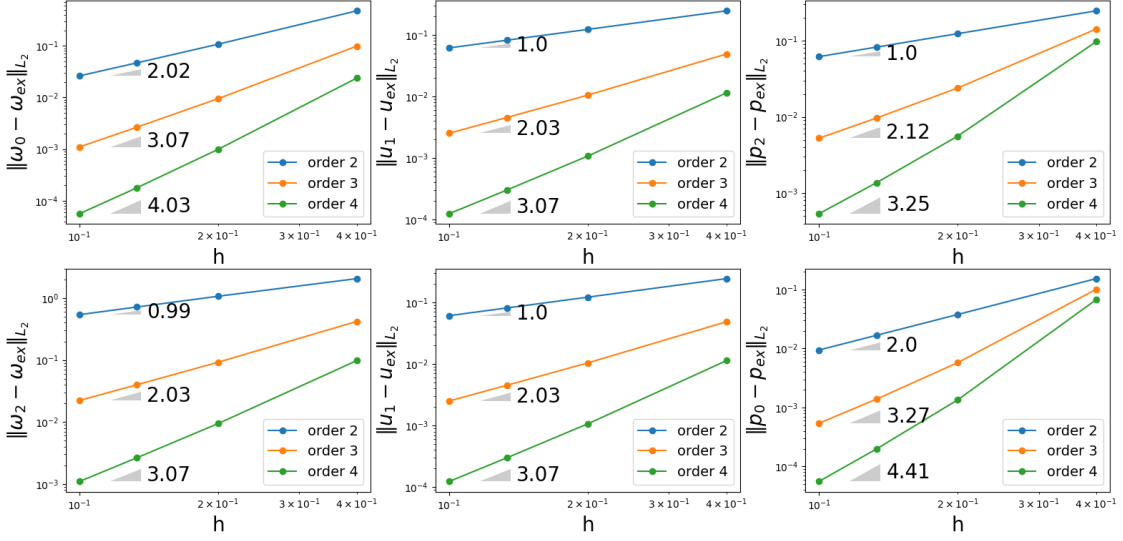


Figure 4: Spatial convergence results for the periodic two dimensional TGV problem. The order refers the B-spline order of the nodal functions used.

The problem is specified with either periodic boundary conditions or with Dirichlet boundary conditions $\vec{u}_\partial = \vec{u}_{ex}|_{\partial\Omega}$. Plugging in this solution into the Navier-Stokes equations gives the following source function

$$\vec{f} = \begin{bmatrix} \frac{1}{2}\pi \sin(2\pi x) \exp(-2\pi^2 \nu t) + 2\pi \sin(\pi x) \cos(\pi x) \sin(\pi y)^2 \exp(-4\pi^2 \nu t) \\ \frac{1}{2}\pi \sin(2\pi y) \exp(-2\pi^2 \nu t) + 2\pi \sin(\pi x)^2 \sin(\pi y) \cos(\pi y) \exp(-4\pi^2 \nu t) \end{bmatrix}. \quad (7.4)$$

In the results below we will always use $\nu = 0.1$.

Spatial convergence periodic domain

To compute the spatial convergence order we compute the error at $t_{\text{end}} = 0.2$ using $\Delta t = 0.005$ with increasingly refined periodic nodal functions of order 2 to 4. We use $h = 2/5, 2/10, 2/15, 2/20$.

In Figure 4 the resulting errors in the L_2 norm are shown in a log log plot, together with the convergence orders of the various nodal function orders. We observe optimal convergence rates for all fields.

Spatial convergence Dirichlet boundary conditions

We repeat the same test, but with the Dirichlet boundary conditions and aperiodic basis functions. The results are presented in Figure 5. We again observe optimal convergence rates for all fields.

Temporal convergence periodic domain

Using basis functions of order 4 and $h = 2/20$, we compute the error at $t_{\text{end}} = 0.5$ using increasingly refined time steps $\Delta t = t_{\text{end}}/2, t_{\text{end}}/4, t_{\text{end}}/6, t_{\text{end}}/8$.

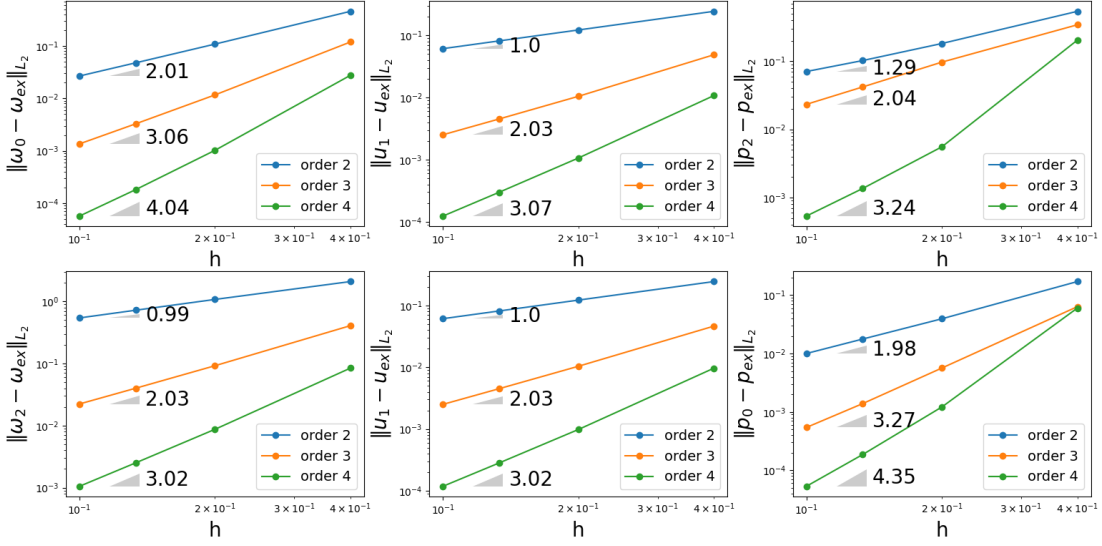


Figure 5: Spatial convergence results for the aperiodic two dimensional TGV problem. The order refers the B-spline order of the nodal functions used.

Note that running the numerical scheme until $t_{\text{end}} = k\Delta t$ yields approximations for ω_2 and \vec{u}_1 and p_3 at t_{end} , for ω_1 , \vec{u}_2 and p_0 at $t_{\text{end}} - \frac{\Delta t}{2}$ and for p_3 at $t_{\text{end}} - \Delta t$. Since only ω_2 and \vec{u}_1 are computed at $t_{\text{end}} = 0.5$, we present error statistics on these fields. Errors are computed in the L_2 norm and results are presented on their convergence order in Figure 6. We observe second convergence as is to be expected for a time integration scheme using the midpoint and trapezoidal rule.

Temporal convergence Dirichlet boundary conditions

We repeat the same test, but with the Dirichlet boundary conditions. The results are presented in Figure 7. We find second convergence for the tested fields as is optimal for midpoint and trapezoidal schemes for time integration.

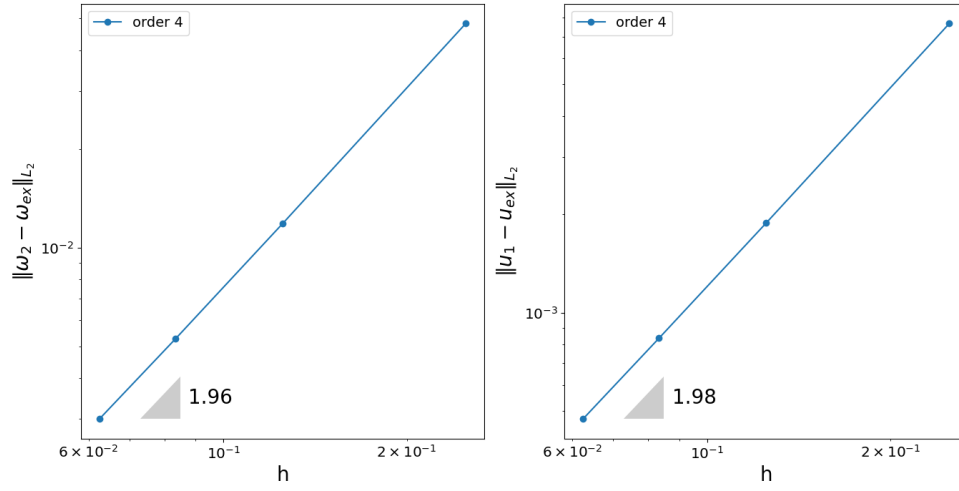


Figure 6: Temporal convergence results for the periodic two dimensional TGV problem. The order refers the B-spline order of the nodal functions used.

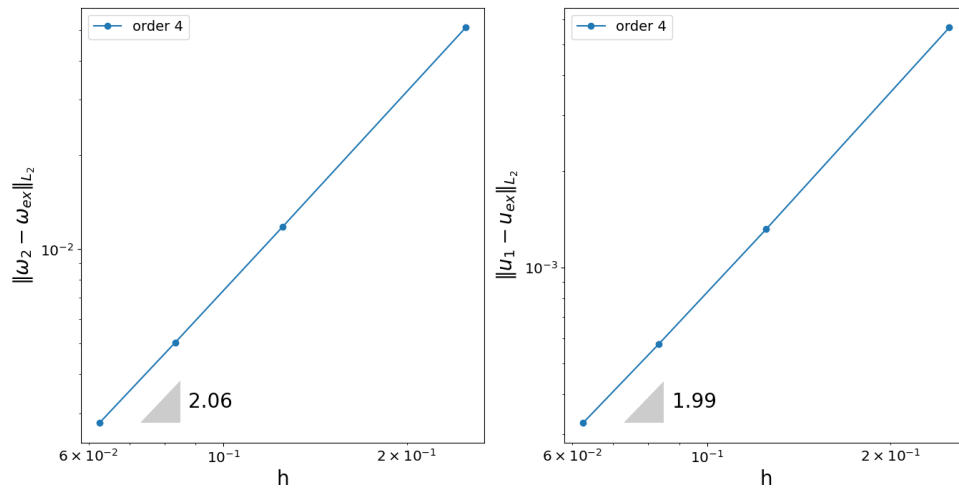


Figure 7: Temporal convergence results for the aperiodic two dimensional TGV problem. The order refers the B-spline order of the nodal functions used.

7.2.2 Three dimensional problems

Consider a Taylor-Green Vortex (TGV) problem on $\Omega = [0, 2]^3$ with solution given by

$$\vec{u}_{ex}(x, y, t) = \begin{bmatrix} -\sin(\pi x) \cos(\pi y) \cos(\pi z) \exp(-2\pi^2 \nu t) \\ \frac{1}{2} \cos(\pi x) \sin(\pi y) \cos(\pi z) \exp(-2\pi^2 \nu t) \\ \frac{1}{2} \cos(\pi x) \cos(\pi y) \sin(\pi z) \exp(-2\pi^2 \nu t) \end{bmatrix} \quad (7.5a)$$

$$\omega_{ex}(x, y, t) = \begin{bmatrix} 0 \\ \frac{3\pi}{2} \sin(\pi x) \cos(\pi y) \sin(\pi z) \exp(-2\pi^2 \nu t) \\ -\frac{3\pi}{2} \sin(\pi x) \sin(\pi y) \cos(\pi z) \exp(-2\pi^2 \nu t) \end{bmatrix} \quad (7.5b)$$

$$p_{ex}(x, y, t) = -\frac{1}{4} (\cos(2\pi x) + \cos(2\pi y) + \cos(2\pi z)) \exp(-2\pi^2 \nu t). \quad (7.5c)$$

The problem is specified with either periodic boundary conditions or with Dirichlet boundary conditions $\vec{u}_\partial = \vec{u}_{ex}|_{\partial\Omega}$. The source function can again be found by plugging in this solution into the Navier-Stokes equations. Again, in the results below we will always use $\nu = 0.1$.

Spatial convergence periodic domain

To compute the spatial convergence order we compute the error at $t_{\text{end}} = 0.2$ using $\Delta t = 0.01$ with increasingly refined periodic nodal functions of order 2 to 4. We use $h = 2/4, 2/6, 2/8$.

In Figure 8 the resulting errors in the L_2 norm are shown in a log log plot, together with the convergence orders of the various basis function orders. We observe optimal convergence rates for all fields.

Spatial convergence Dirichlet boundary conditions

We repeat the same test, but with the Dirichlet boundary conditions and aperiodic basis functions. The results are presented in Figure 9. We again observe optimal convergence rates for all fields.

Temporal convergence periodic domain

Using basis functions of order 4 and $h = 2/10$, we compute the error at $t_{\text{end}} = 0.5$ using increasingly refined time steps $\Delta t = t_{\text{end}}/1, t_{\text{end}}/2, t_{\text{end}}/3, t_{\text{end}}/4$. Since only ω_2 and \vec{u}_1 are computed at $t_{\text{end}} = 0.5$, we present error statistics on these fields. Errors are computed in the L_2 norm and results are presented on their convergence order in Figure 10. We observe second convergence as is to be expected for a time integration scheme using the midpoint and trapezoidal rule.

Temporal convergence Dirichlet boundary conditions

We repeat the same test, but with Dirichlet boundary conditions. The results are presented in Figure 11. We again find second convergence for the tested fields as is optimal for midpoint and trapezoidal schemes for time integration.

7.3 Conservation properties

We show results on energy conservation and dissipation rates using a lid-driven cavity problem. For this problem we additionally show that the divergence of velocity is pointwise zero. We will

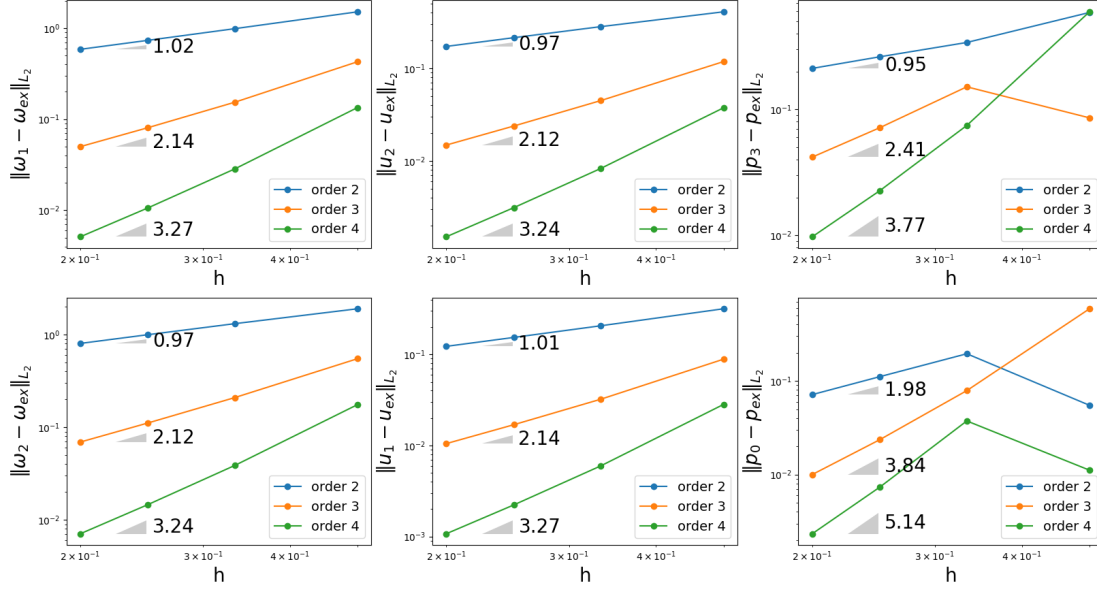


Figure 8: Spatial convergence results for the periodic three dimensional TGV problem. The order refers the B-spline order of the nodal functions used.

show helicity conservation using manufactured solution to ensure the condition $\vec{\omega} \cdot \vec{n} = 0$ is valid and results on helicity dissipation using a problem on a periodic domain. Further results on energy and helicity conservation on periodic domains are shown in [1].

Energy conservation

Let us first consider a modification of the lid-driven cavity problem on a domain $\Omega = [0, 1]^3$. The boundary conditions are given by

$$\vec{u}_{\partial}(x, y, z, t) = \begin{cases} [\sin(t), 0, \sin(2t)]^{\top} & \text{if } y = 1, \\ [0, 0, 0]^{\top} & \text{otherwise.} \end{cases} \quad (7.6)$$

All fields are initially zero,

$$\vec{u}|_{t=0} = [0, 0, 0]^{\top}, \quad (7.7)$$

$$\vec{v}|_{t=0} = [0, 0, 0]^{\top}, \quad (7.8)$$

$$p|_{t=0} = 0, \quad (7.9)$$

and we use $\vec{f} = 0$. The solution is computed using order 2 nodal functions with $h = 1/3$, until $t_{\text{end}} = 10$ with time step $\Delta t = 0.1$. Results on

$$\frac{\mathcal{K}_1^{k+1} - \mathcal{K}_1^k}{\Delta t} \quad \text{and} \quad \frac{\mathcal{K}_2^{k+\frac{1}{2}} - \mathcal{K}_1^{k-\frac{1}{2}}}{\Delta t} \quad (7.10)$$

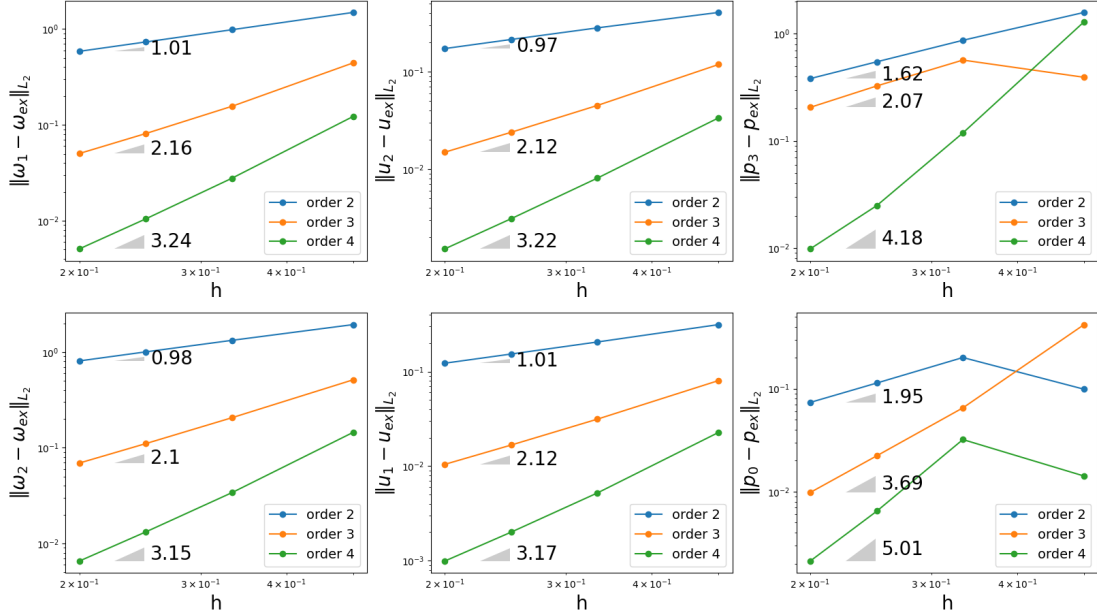


Figure 9: Spatial convergence results for the aperiodic three dimensional TGV problem. The order refers the B-spline order of the nodal functions used.

for $\nu = 0$ are presented in Figure 12. Results on the difference between these rates of change and the rates computed in (6.41b) and (6.35b) are presented in Figure 13 using $\nu = 0.1$. Note how the differences are in the order of 10^{-29} and 10^{-15} respectively. For $\nu = 0$ the solution to the curl conforming problem is always identically zero, as the boundary condition disappears for $\nu = 0$, and the nonlinear term with borrowed vorticity also yields zero, as the velocity solution is identically zero. The solution to the divergence conforming problem is not identically zero, but the velocity solution is. This is a result of the initial solution containing no kinetic energy combined with kinetic energy conservation.

Mass conservation

We consider the same modified lid-driven cavity problem. We use $\nu = 0.1$ and compute the solution until $t_{\text{end}} = 10$ with $\Delta t = 0.1$ using order 2 nodal functions with $h = 1/3$. Results on the L^∞ norm of $\text{div } \vec{u}_2$ are presented in Figure 14. Note how the results are in the order of 10^{-17} .

Helicity conservation

Now let us consider the manufactured solution problem of (7.5) on a domain $\Omega = [0, 1]^3$ with $\nu = 0.1$ and Dirichlet boundary conditions. The solution is computed using order 2 nodal functions with $h = 1/3$ until $t_{\text{end}} = 1$ with $\Delta t = 0.01$. Although the usual assumptions for helicity conservation do not hold, we do find that the manufactured solution does conserve helicity. We present results on

$$\frac{\mathcal{H}_1^{k+\frac{1}{2}} - \mathcal{H}_1^{k-\frac{1}{2}}}{\Delta t} \quad \text{and} \quad \frac{\mathcal{H}_2^{k+\frac{1}{2}} - \mathcal{H}_2^{k-\frac{1}{2}}}{\Delta t} \quad (7.11)$$

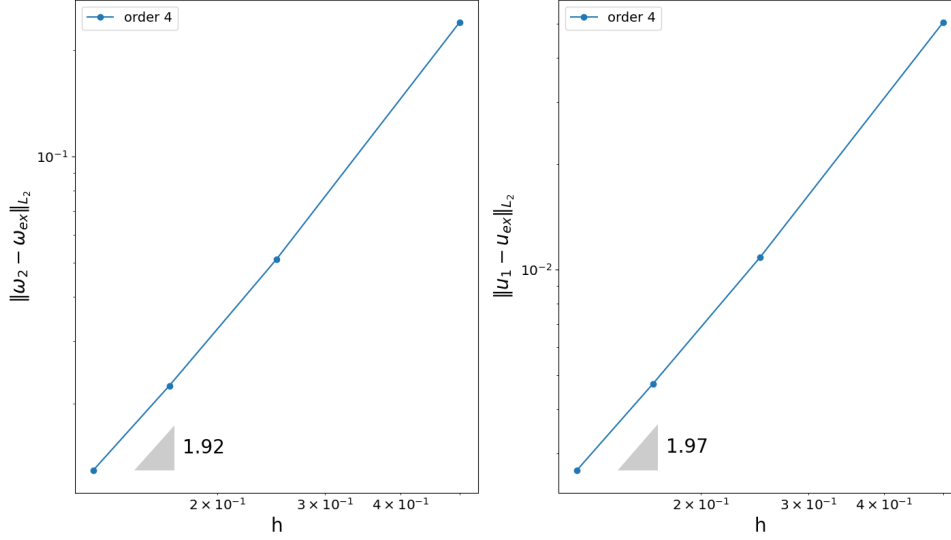


Figure 10: Temporal convergence results for the periodic three dimensional TGV problem. The order refers the B-spline order of the nodal functions used.

in Figure 15. Note how the values are in the order of 10^{-15} . This shows how the discrete solution adheres to the helicity conservation of the continuous problem, even though this is not immediately obvious from the derived rates (6.64) and (6.69).

To show results on helicity dissipation we reproduce a test case from [1]. Consider a periodic domain $\Omega = [0, 1]^3$ with initial condition

$$\vec{u}|_{t=0} = [\cos(2\pi z), \sin(2\pi z), \sin(2\pi x)]^\top, \quad (7.12)$$

$$p|_{t=0} = \frac{1}{4} (\cos(2\pi x) + \cos(2\pi y) + \cos(2\pi z)), \quad (7.13)$$

and $\nu = 0.01$. Results on

$$\frac{\mathcal{H}_1^{k+\frac{1}{2}} - \mathcal{H}_1^{k-\frac{1}{2}}}{\Delta t} - \mathcal{D}_{\mathcal{H}_1^k} \quad \text{and} \quad \frac{\mathcal{H}_2^{k+\frac{1}{2}} - \mathcal{H}_2^{k-\frac{1}{2}}}{\Delta t} - \mathcal{D}_{\mathcal{H}_2^k} \quad (7.14)$$

with $\vec{f} \equiv 0$ are shown in Figure 16 for and results with $\vec{f} = [\sin(2\pi x), \sin(2\pi x), \sin(2\pi x)]^\top$ are shown in Figure 17. Second order nodal functions are used with $h = 1/3$ and the solution is computed until $t_{\text{end}} = 10$ with $\Delta t = 0.1$. Note how all values are in the order of 10^{-13} .

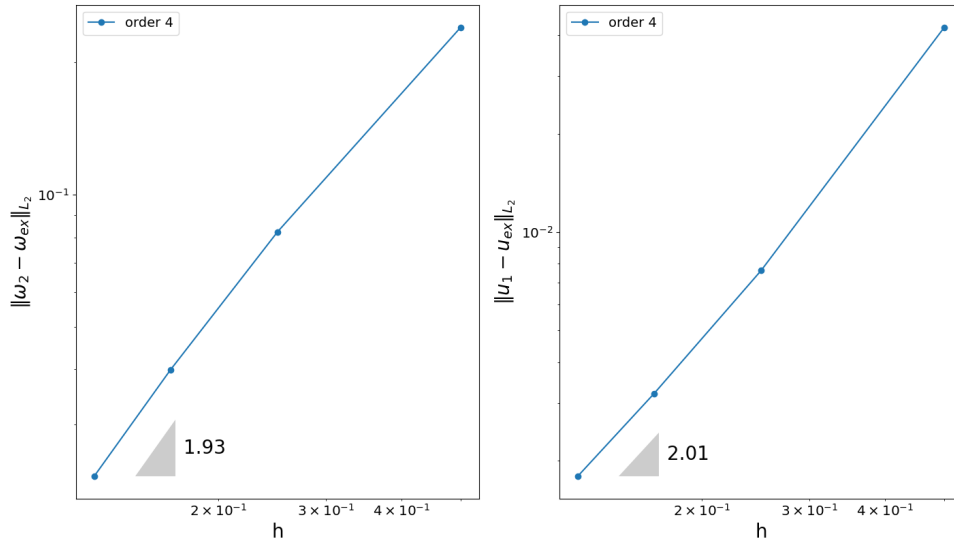


Figure 11: Temporal convergence results for the aperiodic three dimensional TGV problem. The order refers the B-spline order of the nodal functions used.

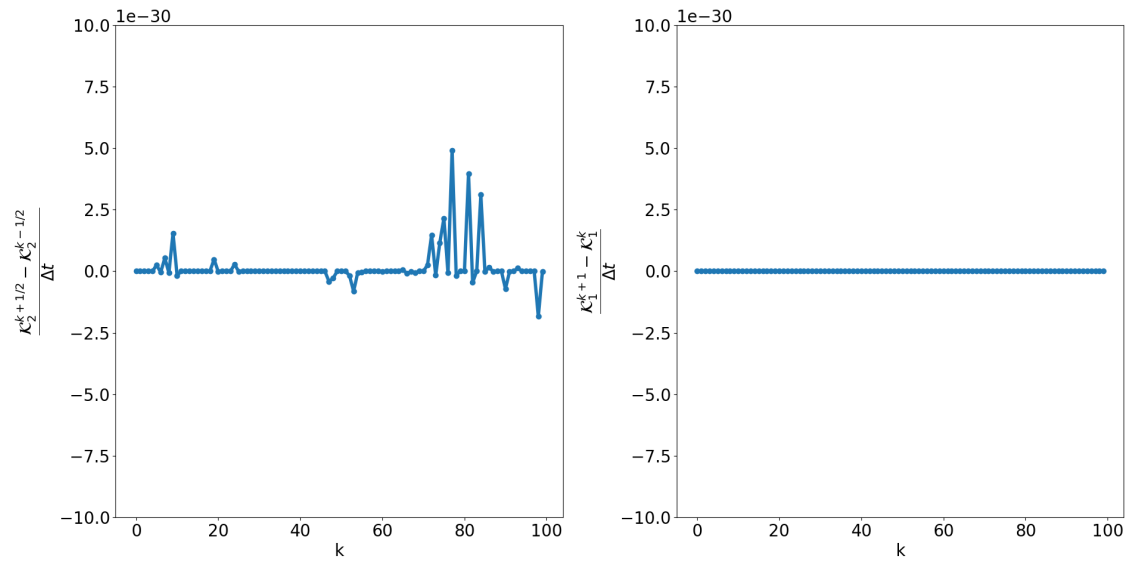


Figure 12: Results on energy conservation in a lid-driven cavity problem with $\nu = 0$, $h = 1/3$, $r = 2$.

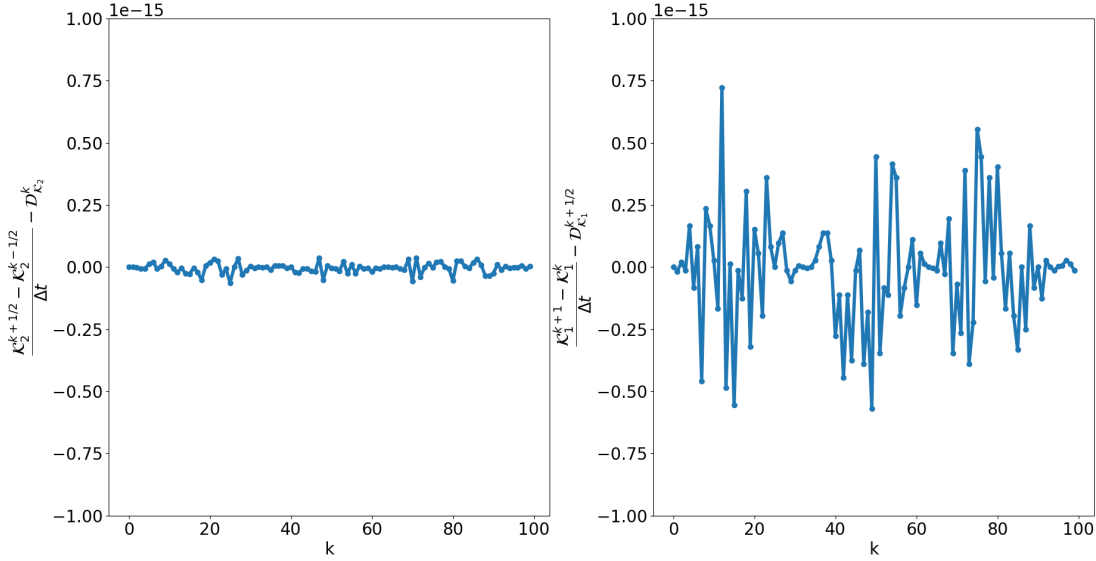


Figure 13: Results on energy dissipation in a lid-driven cavity problem with $\nu = 0.1$, $h = 1/3$, $r = 2$.

7.4 Lid-driven cavity

Let us revisit the lid-driven cavity problem, now in 2D and with the usual boundary conditions

$$\vec{u}_\partial(x, y, t) = \begin{cases} [1, 0, 0]^\top & \text{if } y = 1, \\ [0, 0, 0]^\top & \text{otherwise.} \end{cases} \quad (7.15)$$

The initial condition is selected to be the solution to the steady state Stokes problem with the same boundary conditions. The lid-driven cavity problem is perhaps the most common benchmark problem in computation fluid dynamics and is well studied, see for example [44], [45]. Important characteristics of the lid-driven cavity flow are the singularities in the corners of the domain and the corner vortices forming for smaller values of ν . We compute the solution for $\nu = 0.01$ using order 4 nodal functions, with $h = 1/30$, at $t_{\text{end}} = 1$, with $\Delta t = 0.01$.

Do note that usually a steady state solution is sought and here we simply iterate for a number of time steps. The goal here is to show how the numerical method handles the singularities and gives rise to the counter rotating eddies in the bottom corners, not to compare the numerical method to benchmark results. Do note that the methodology in this thesis can be extended to obtain steady state solutions by regarding time independent variables and iterating towards a solution using the divergence and curl conforming problems alternatingly, akin to Figure 3.

In Figure 18 a contour plot of the stream function is shown, colored according to the magnitude of velocity, red implying high a velocity, blue implying a low velocity. No additional treatment has been given to the singularities. Some potential artifacts of the singularities can be seen in the top left corner, where two small eddies are formed where there are be none for $\nu = 0.01$ in the steady state problem [44].

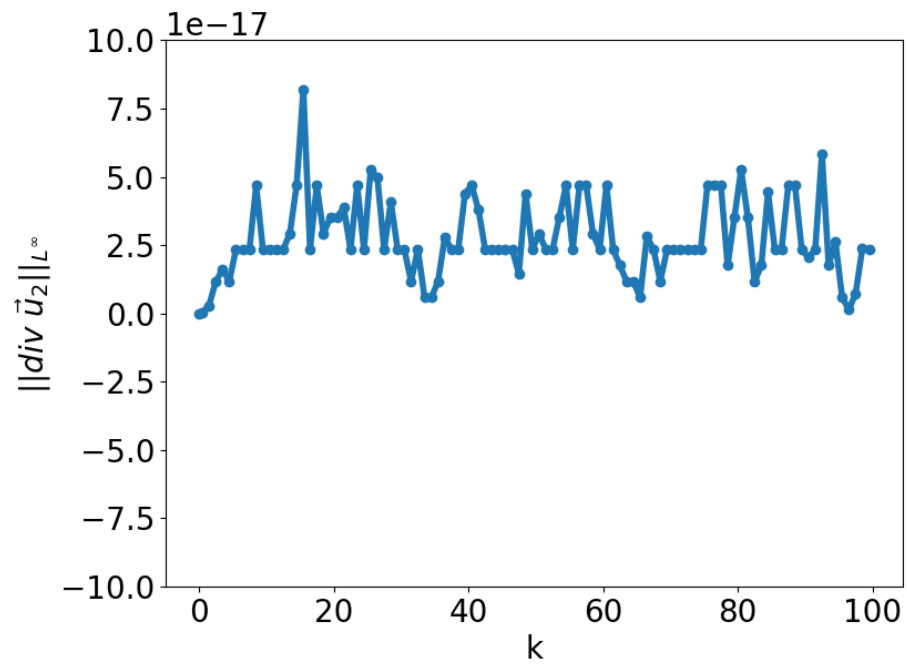


Figure 14: Results on mass conservation in a lid-driven cavity problem with $\nu = 0.1, h = 1/3, r = 2$.

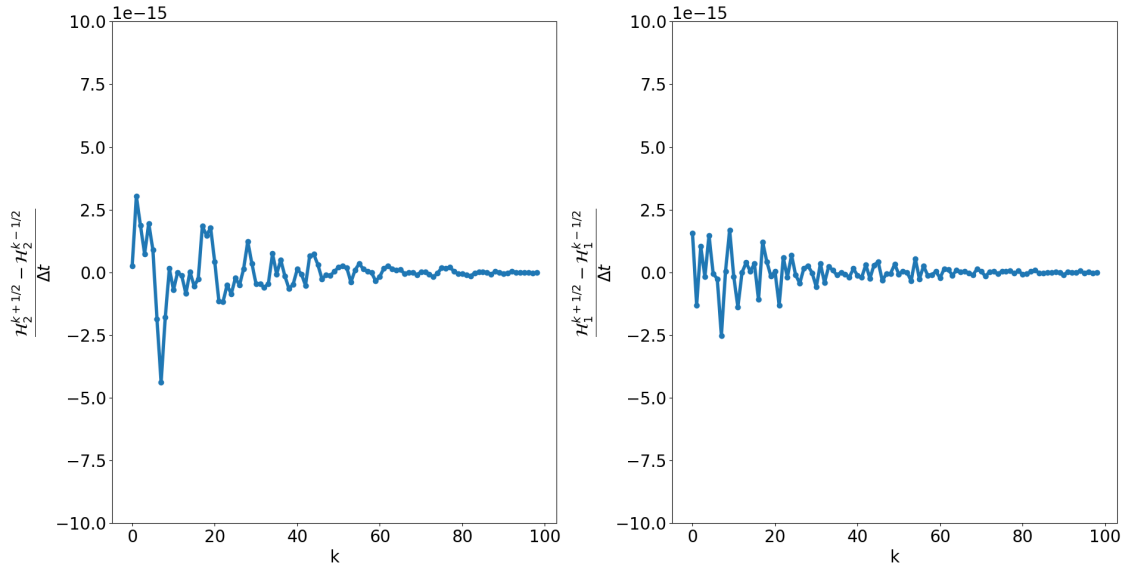


Figure 15: Results on helicity conservation in a manufactured solution problem with Dirichlet boundary conditions where the continuous solution has constant zero helicity (7.5). Computed using $\nu = 0.1$, $h = 1/3$, $r = 2$.

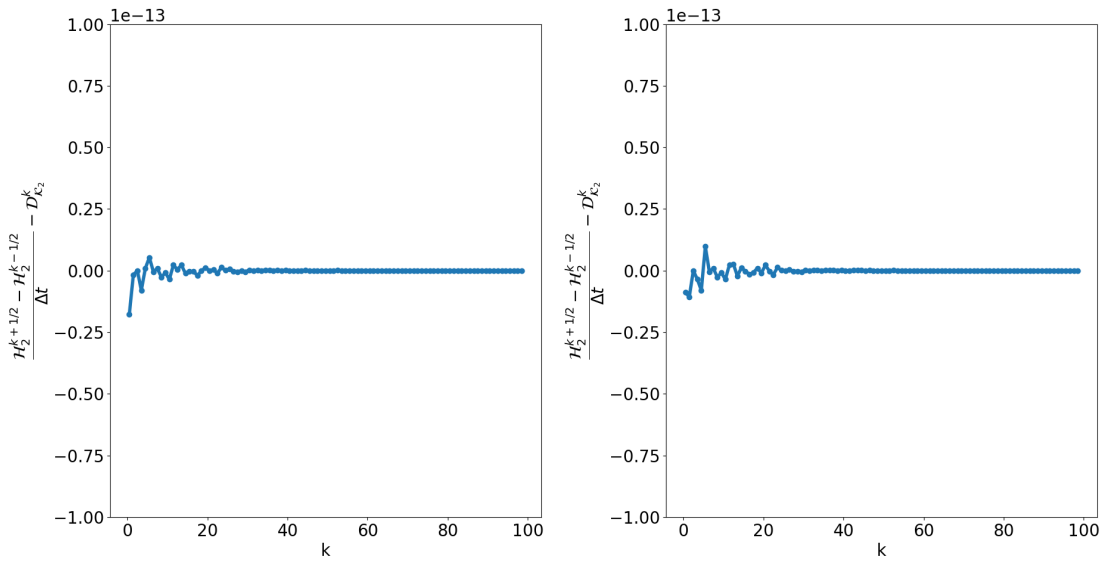


Figure 16: Results on helicity dissipation for a problem on a periodic domain with $\nu = 0.01$, $\vec{f} \equiv 0$, $h = 1/3$ and $r = 2$.

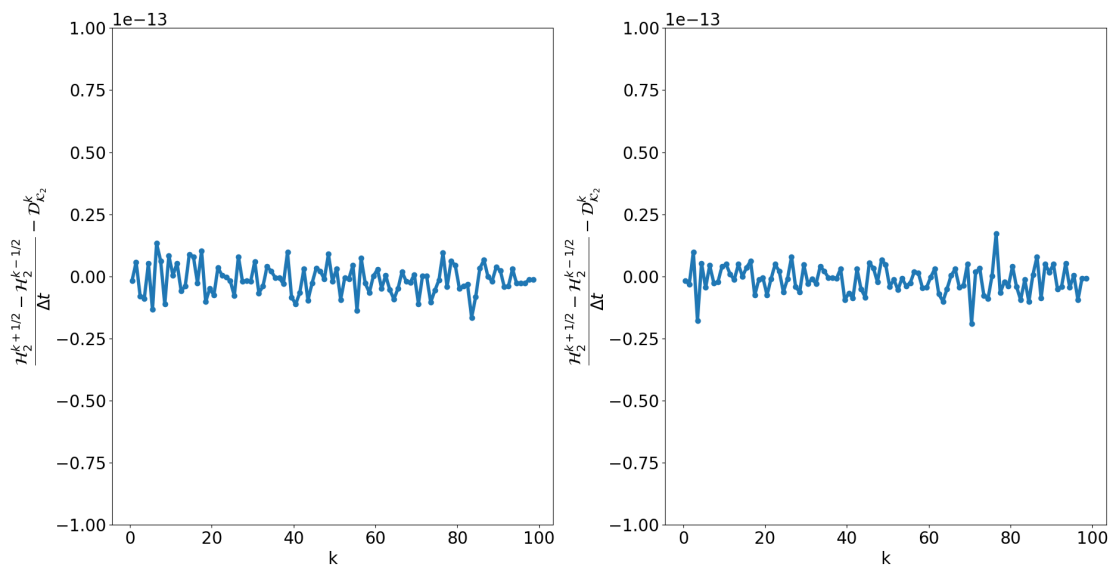


Figure 17: Results on helicity dissipation for a problem on a periodic domain with $\nu = 0.01$, $\vec{f} = [\sin(2\pi x), \sin(2\pi x), \sin(2\pi x)]^\top$, $h = 1/3$ and $r = 2$.

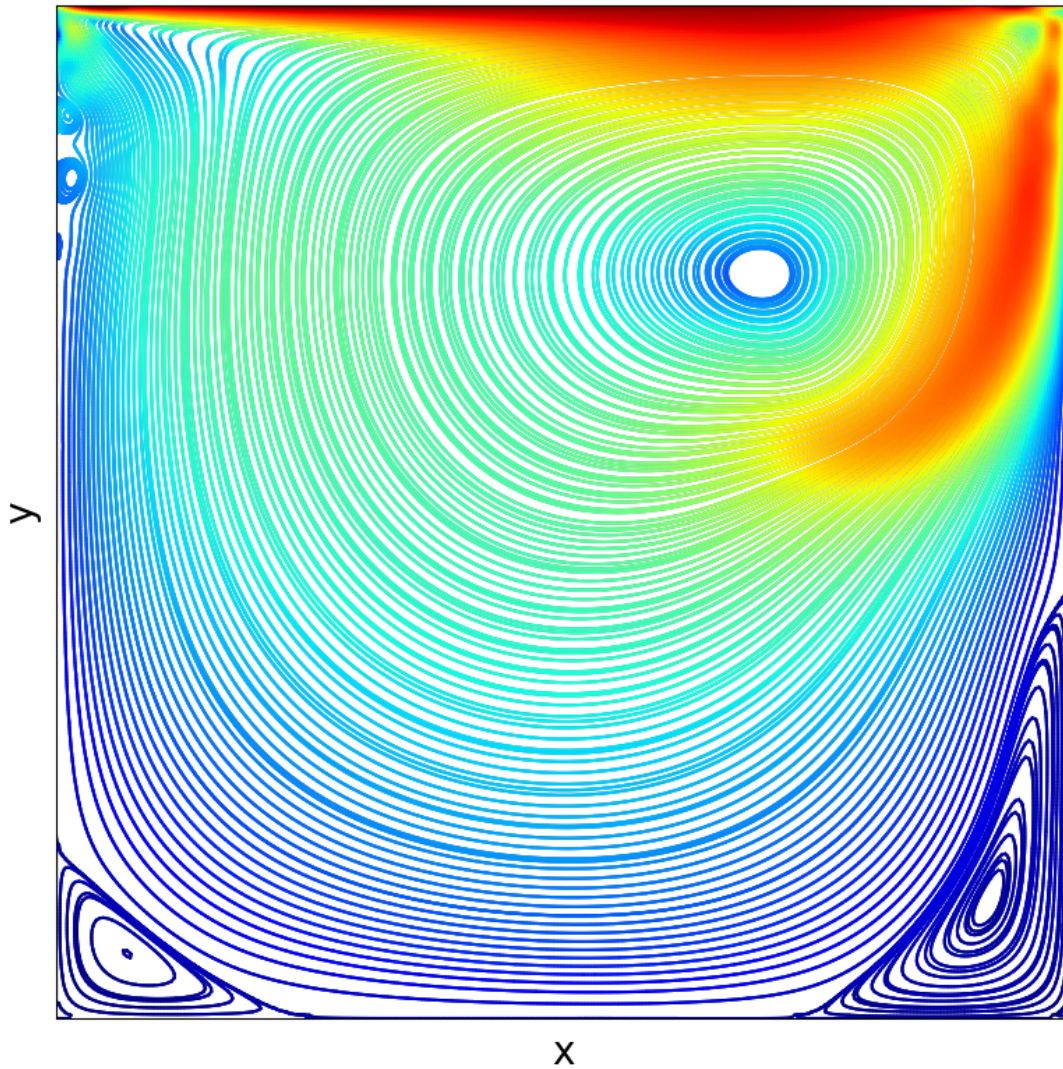


Figure 18: Stream function of a 2D lid-driven cavity problem, colored according to the magnitude of the velocity. Computed with $r = 4$, $h = 1/30$, $t_{\text{end}} = 1$, $\Delta t = 0.01$.

8 Conclusions and future research

Conclusions

In this thesis, we extend the work done in [1] to handle Dirichlet boundary conditions. We use a mimetic B-spline discretization to construct a weak form that adheres to a discrete de Rham complex, leading to a naturally stable discretization. As in [1], we are motivated by the dual nature of the physical field variables in the Navier-Stokes equations to use a dual-field discretization, where each continuous field is approximated by two different discrete representations. This leads to two different weak forms, which are solved alternatingly on staggered time sequences to propagate the solution in time. By sharing the computed vorticity fields between the two weak forms, the nonlinear term in the equations can be efficiently handled. Since the used discrete fields constitute a discrete exact de Rham complex, it is possible to derive valid conservation properties and dissipation rates at the discrete level.

For problems on periodic domains, the numerical method conserves kinetic energy and helicity when the Navier-Stokes equations do so too. When the Navier-Stokes equations allow for energy or helicity dissipation, the dissipation rates of the numerical mimic their continuous counterpart. For problems with Dirichlet boundary conditions, the same results are found with some notable additional assumptions on the problem at hand. When the problem allows for inflow into the domain, there is an additional term contributing to the energy dissipation. Similarly, when the problem allows for nonzero normal vorticity at the boundary, there is an additional term contributing to the helicity dissipation.

These additional contributions cannot be meaningfully quantified within the employed approach, and are a result of strongly enforced boundary conditions.

Furthermore, we observe optimal convergence properties. Mimetic discretizations allow for high order spatial approximations of the fields, and for all tested orders optimal convergence orders were found. The temporal discretization is done using a combination of the midpoint and trapezoidal rule, this leads to second order temporal convergence, which is verified numerically.

Future research

Specific to the current extension to Dirichlet boundary conditions, future research could investigate weak forms that do not use strong enforcement of boundary conditions. This would avoid the additional contributions to energy and helicity dissipation noted earlier. This is already attainable when considering boundary conditions on pressure and tangential velocity, but not for boundary conditions on tangential and normal velocity.

A possible route to attaining this for velocity boundary conditions could be to use the pressure solution of the curl conforming problem as a boundary condition in the divergence conforming problem. The strongly enforced boundary condition on normal velocity in the divergence conforming problem can then be replaced by a weakly enforced boundary condition on pressure. The initial half time step would still have to use the strongly enforced boundary condition. As both the normal and tangential component are enforced in one of the problems, and there is a two way linking between the problem, the velocity boundary conditions are not necessarily ‘lost’.

Furthermore, different formulations of the Navier-Stokes equations, specifically different formulations of the nonlinear term, can be investigated to potentially conserve more quantities such as

enstrophy or (angular) momentum. The nonlinear term introduced in [35] shows promising results. As currently presented however, it requires $\vec{u} \in H_h^1$, which is incompatible with the methodology presented in this work.

In [1] it was noted that the method accurately predicts the energy cascade up to scales where the solution is not sufficiently resolved, where it over estimates the kinetic energy. The current work has not addressed this, and the recommendation of using a sub-grid scale method to address this issue still stands.

As also noted in [1], future research could investigate mesh adaptivity using hierarchical B-splines, see for example [46]–[48]. Since the scheme approximates each physical field using two different discrete representations, the difference between these two approximation of the same field can be used as an indication of local accuracy.

References

- [1] Y. Zhang, A. Palha, M. Gerritsma, and L. G. Rebholz, “A mass-, kinetic energy- and helicity-conserving mimetic dual-field discretization for three-dimensional incompressible navier-stokes equations, part i: Periodic domains,” *Journal of Computational Physics*, vol. 451, p. 110868, 2022.
- [2] A. N. Kolmogorov, “The local structure of turbulence in incompressible viscous fluid for very large reynolds,” *Numbers. In Dokl. Akad. Nauk SSSR*, vol. 30, p. 301, 1941.
- [3] R. H. Kraichnan, “Inertial ranges in two-dimensional turbulence,” *The Physics of Fluids*, vol. 10, no. 7, pp. 1417–1423, 1967.
- [4] H. K. Moffatt, “The degree of knottedness of tangled vortex lines,” *Journal of Fluid Mechanics*, vol. 35, no. 1, pp. 117–129, 1969.
- [5] H. K. Moffatt and A. Tsinober, “Helicity in laminar and turbulent flow,” *Annual review of fluid mechanics*, vol. 24, no. 1, pp. 281–312, 1992.
- [6] A. Brissaud, U. Frisch, J. Léorat, M. Lesieur, and A. Mazure, “Helicity cascades in fully developed isotropic turbulence,” *Physics of Fluids*, vol. 16, no. 8, pp. 1366–1367, 1973.
- [7] Q. Chen, S. Chen, and G. L. Eyink, “The joint cascade of energy and helicity in three-dimensional turbulence,” *Physics of Fluids*, vol. 15, no. 2, pp. 361–374, 2003.
- [8] A. Palha and M. Gerritsma, “A mass, energy, enstrophy and vorticity conserving (meevc) mimetic spectral element discretization for the 2d incompressible navier-stokes equations,” *Journal of Computational Physics*, vol. 328, pp. 200–220, 2017.
- [9] E. Tonti, “The formal structure of physical theories,” Jan. 1975.
- [10] W. L. Burke, *Applied Differential Geometry*. Cambridge: Cambridge University Press, 1985.
- [11] J. M. Hyman and J. C. Scovel, “Deriving mimetic difference approximations to differential operators using algebraic topology,” *Los Alamos National Laboratory*, 1988.
- [12] P. B. Bochev and J. M. Hyman, “Principles of mimetic discretizations of differential operators,” in *Compatible spatial discretizations*, Springer, 2006, pp. 89–119.
- [13] J. Kreeft, A. Palha, and M. Gerritsma, “Mimetic framework on curvilinear quadrilaterals of arbitrary order,” *arXiv preprint arXiv:1111.4304*, 2011.
- [14] C. Mattiussi, “An analysis of finite volume, finite element, and finite difference methods using some concepts from algebraic topology,” *Journal of Computational Physics*, vol. 133, no. 2, pp. 289–309, 1997.
- [15] C. Mattiussi, “A reference discretization strategy for the numerical solution of physical field problems,” in *Advances in imaging and electron physics*, vol. 121, Elsevier, 2002, pp. 143–279.
- [16] D. Pavlov, P. Mullen, Y. Tong, E. Kanso, J. E. Marsden, and M. Desbrun, “Structure-preserving discretization of incompressible fluids,” *Physica D: Nonlinear Phenomena*, vol. 240, no. 6, pp. 443–458, 2011.
- [17] A. Bossavit, “On the geometry of electromagnetism,” *J. Japan Soc. Appl. Electromagn. & Mech*, vol. 6, pp. 17–28, 1998.
- [18] A. Bossavit, “Computational electromagnetism and geometry: Building a finite-dimensional “maxwell’s house,”” *J Japan Soc Appl Electromagn & Mech*, vol. 7, Jan. 1999.

- [19] J. Kreeft and M. Gerritsma, “Mixed mimetic spectral element method for stokes flow: A pointwise divergence-free solution,” *Journal of Computational Physics*, vol. 240, pp. 284–309, 2013.
- [20] R. R. Hiemstra, D. Toshniwal, R. Huijsmans, and M. I. Gerritsma, “High order geometric methods with exact conservation properties,” *Journal of Computational Physics*, vol. 257, pp. 1444–1471, 2014.
- [21] J. Kreeft and M. Gerritsma, “A priori error estimates for compatible spectral discretization of the stokes problem for all admissible boundary conditions,” *arXiv preprint arXiv:1206.2812*, 2012.
- [22] F. Laakmann, P. E. Farrell, and K. Hu, “Structure-preserving and helicity-conserving finite element approximations and preconditioning for the hall mhd equations,” *arXiv preprint arXiv:2202.11586*, 2022.
- [23] J. B. Perot, “Discrete conservation properties of unstructured mesh schemes,” *Annual review of fluid mechanics*, vol. 43, pp. 299–318, 2011.
- [24] P. Bochev, “A discourse on variational and geometric aspects of stability of discretizations,” *33rd Computational Fluid Dynamics Lecture Series, VKI LS*, vol. 5, 2003.
- [25] T. J. Hughes, J. A. Cottrell, and Y. Bazilevs, “Isogeometric analysis: Cad, finite elements, nurbs, exact geometry and mesh refinement,” *Computer methods in applied mechanics and engineering*, vol. 194, no. 39-41, pp. 4135–4195, 2005.
- [26] R. Hiemstra, R. Huijsmans, and M. Gerritsma, “High order gradient, curl and divergence conforming spaces, with an application to compatible nurbs-based isogeometric analysis,” *arXiv preprint arXiv:1209.1793*, 2012.
- [27] Y. Bazilevs, L. Beirao da Veiga, J. A. Cottrell, T. J. Hughes, and G. Sangalli, “Isogeometric analysis: Approximation, stability and error estimates for h-refined meshes,” *Mathematical Models and Methods in Applied Sciences*, vol. 16, no. 07, pp. 1031–1090, 2006.
- [28] A. Buffa, J. Rivas, G. Sangalli, and R. Vázquez, “Isogeometric discrete differential forms in three dimensions,” *SIAM Journal on Numerical Analysis*, vol. 49, no. 2, pp. 818–844, 2011.
- [29] J. A. Evans and T. J. Hughes, “Isogeometric divergence-conforming b-splines for the unsteady navier–stokes equations,” *Journal of Computational Physics*, vol. 241, pp. 141–167, 2013.
- [30] A. Ratnani and E. Sonnendrücker, “Isogeometric analysis in reduced magnetohydrodynamics,” *Computational Science & Discovery*, vol. 5, no. 1, p. 014007, 2012.
- [31] L. G. Rebholz, “An energy-and helicity-conserving finite element scheme for the navier–stokes equations,” *SIAM Journal on Numerical Analysis*, vol. 45, no. 4, pp. 1622–1638, 2007.
- [32] J.-G. Liu and W.-C. Wang, “Energy and helicity preserving schemes for hydro-and magnetohydrodynamics flows with symmetry,” *Journal of Computational Physics*, vol. 200, no. 1, pp. 8–33, 2004.
- [33] M. Case, V. J. Ervin, A. Linke, L. G. Rebholz, and N. E. Wilson, “Stable computing with an enhanced physics based scheme for the 3d navier-stokes equations,” Berlin: Weierstraß-Institut für Angewandte Analysis und Stochastik, Tech. Rep., 2010.
- [34] B. R. Cousins, L. G. Rebholz, and N. E. Wilson, “Enforcing energy, helicity and strong mass conservation in finite element computations for incompressible navier–stokes simulations,” *Applied Mathematics and Computation*, vol. 218, no. 4, pp. 1208–1221, 2011.

- [35] S. Charnyi, T. Heister, M. A. Olshanskii, and L. G. Rebholz, “On conservation laws of navier–stokes galerkin discretizations,” *Journal of Computational Physics*, vol. 337, pp. 289–308, 2017.
- [36] R. Abraham, J. E. Marsden, and T. Ratiu, *Manifolds, tensor analysis, and applications*. Springer Science & Business Media, 2012, vol. 75.
- [37] H. Flanders, *Differential forms with applications to the physical sciences*. Courier Corporation, 1963, vol. 11.
- [38] C. De Boor, “On calculating with b-splines,” *Journal of Approximation theory*, vol. 6, no. 1, pp. 50–62, 1972.
- [39] C. De Boor and C. De Boor, *A practical guide to splines*. springer-verlag New York, 1978, vol. 27.
- [40] M. Gerritsma, “Edge functions for spectral element methods,” in *Spectral and High Order Methods for Partial Differential Equations: Selected papers from the ICOSAHOM’09 conference, June 22-26, Trondheim, Norway*, Springer, 2010, pp. 199–207.
- [41] M. Olshanskii and L. G. Rebholz, “Note on helicity balance of the galerkin method for the 3d navier–stokes equations,” *Computer Methods in Applied Mechanics and Engineering*, vol. 199, no. 17-20, pp. 1032–1035, 2010.
- [42] W. Nederpel, *Isogeometricmimeticsolvers.jl*, <https://gitlab.com/wnederpel/IsogeometricMimeticSolvers.jl>, 2023.
- [43] J. I. Polanco, *BSplineKit.jl: B-spline based galerkin and collocation methods in julia*, <https://jipolanco.github.io/BSplineKit.jl/dev/>.
- [44] O. Botella and R. Peyret, “Benchmark spectral results on the lid-driven cavity flow,” *Computers & Fluids*, vol. 27, no. 4, pp. 421–433, 1998.
- [45] C.-H. Bruneau and M. Saad, “The 2d lid-driven cavity problem revisited,” *Computers & fluids*, vol. 35, no. 3, pp. 326–348, 2006.
- [46] C. Bracco, A. Buffa, C. Giannelli, and R. Vázquez, “Adaptive isogeometric methods with hierarchical splines: An overview,” *Discrete And Continuous Dynamical Systems*, vol. 39, no. ARTICLE, pp. 241–261, 2019.
- [47] J. A. Evans, M. A. Scott, K. M. Shepherd, D. C. Thomas, and R. Vázquez Hernández, “Hierarchical b-spline complexes of discrete differential forms,” *IMA Journal of Numerical Analysis*, vol. 40, no. 1, pp. 422–473, 2020.
- [48] K. M. Shepherd, “Hierarchical b-spline complexes of discrete differential forms,” 2018.